Deliverable Power Characteristics in Low-Voltage DC Distribution System Based on Voltage Stability

By

Doaa Mokhtar Yehia Ali Mustafa

A Thesis Submitted for the Degree of

Doctor of Engineering

Department of Electrical Engineering and Computer Science

Nagoya University

Japan

Abstract

With the fast growth of distributed generators, DC distribution system has been proposed as an efficient alternative for the conventional AC system. Consequently, understanding the deliverable power capabilities in the DC distribution system would be helpful for the application of such systems. In DC system, voltage instability proved to occur at the receiving ends for certain types of loads. Accordingly, this thesis investigates the deliverable power characteristics for low-voltage DC distribution system based on voltage stability.

First, the electrical loads in DC distribution system are modeled as a preliminary stage for the analysis of voltage stability and deliverable power characteristics. The DC load model is constructed from steady state unit and transient unit. Both units are derived from experimental measurements of the load power in the steady state and transient state. Then, the voltage instability phenomenon in DC distribution system is analyzed using Hurwitz stability criterion. Based on this analysis, the upper limitation of deliverable power P_{lim} is evaluated. The influence of load types, as expressed by the voltage sensitivity parameter, on the voltage instability and P_{lim} is discussed.

Since the distribution line parameters are important factors in voltage instability and determining P_{lim}, the influence of these parameters is clarified. Distribution line parameters include line cross-section, line length and inductance per meter. The effect of each parameter is evaluated, and then, improving the deliverable power characteristics is investigated by adding capacitor at the load terminals. Experimental measurements are carried out in order to confirm the validity of the theoretically calculated P_{lim}.

Finally, the influence of load model parameters is studied in order to specify the dominant parameter that affecting the deliverable power characteristics. In addition, P_{lim} for several loads is determined using an equivalent representation of multiple loads connected to the DC distribution system. The effect of power sharing between loads is also considered.

The obtained results in this thesis would be helpful in the design and operation of DC distribution systems.

Contents

List of figures

Chapter 1
Introduction

1.1 Overview

Today, in all countries in the world, the electricity is considered the most essential energy source in residential, commercial and industrial systems. This caused a continuous increase of world electricity demand [1]. Since the distribution system is one of the largest infrastructures in an electrical power system, there was a continuous attention given to improving and enhancing the efficiency of such systems [2]. Regarding this aspect, the Direct Current (DC) distribution system was proposed as a prospective way to replace or be apart of the conventional Alternating Current (AC) distribution system [3–6].

The concept of DC systems was used in the early developments of electricity by Thomas Edison who initiated the first large scale distribution network with 110 DC voltage. At that time there had been a lot of debate on the merits of DC and AC distribution systems. But, with the invention of transformer and induction motor, the AC distribution systems developed and became the main distribution systems allover the world.

However, recently, the interest in DC distribution system appeared once again as a result of fast growth of renewable energy sources [7]. This is because some of these sources like photovoltaic (PV) systems and fuel cells inherently produce DC output. The other renewable energy sources like hydro plants and wind turbines produce AC output with a different frequency than the grid, and are connected to the grid through an AC/DC/AC converter. So, the connection of these sources to a DC distribution system would eliminate the use of two sets of converters for each DC load [8]. In addition, the growth of renewable energy sources was coincided with a large progress in power electronics devices which enabled to make the DC voltage magnitude controllable like the AC voltage [9]. Figure 1.1 shows an example of renewable energy sources connected to a low-voltage DC distribution system [10].

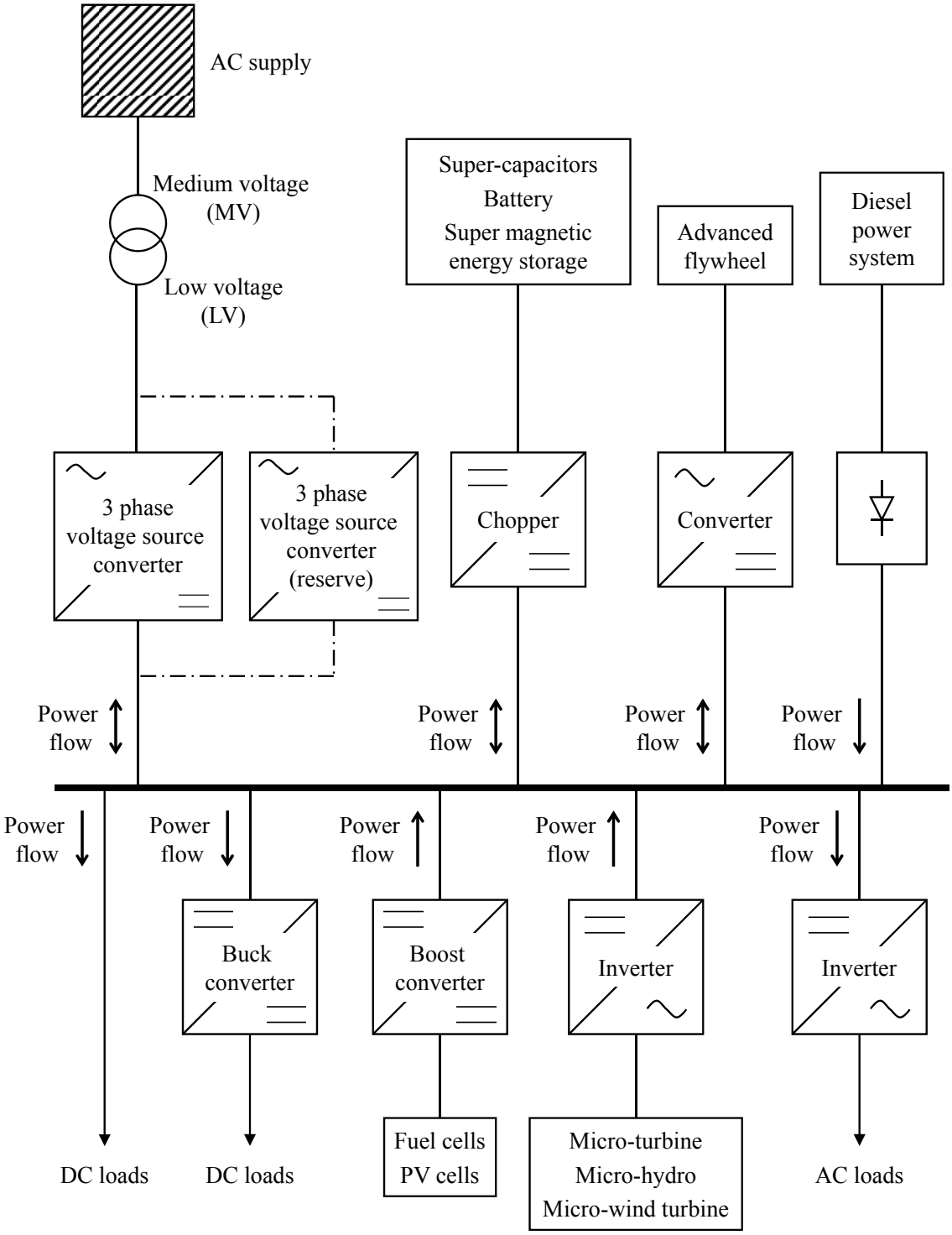

Figure 1.1: *Layout of the low-voltage DC distribution system [10].*

1.2 Advantages of DC distribution system

A substantial number of researchers have investigated the advantages of DC distribution system, which can be summarized as follows [3]:

1. The total system losses of DC distribution system decrease compared to AC system or mixed AC-DC system under the assumption of a substantial reduction in semiconductor losses [11]. This means that for the same energy delivered, less energy must be produced from the available sources, thereby indirectly reducing the environmental impact of energy production. Moreover, the system efficiency will be improved.

2. With DC system, DC renewable energy resources could be much more readily incorporated into a premise DC bus. This would eliminate conversions processes resulting in saving the developed energy.

3. In DC system, battery storage must be provided, leading to continuous supply of electrical power during fault conditions such as unplanned outages. Consequently, the reliability will be greatly improved.

4. The development of DC superconducting cables with the inherent low loss and high current capability could make it feasible to use low-voltage DC superconducting distribution system [12].

In spite of many advantages of DC distribution systems, it is indicated that the efficient application of such systems will be limited by the efficiencies of the power converters used and the percentage of the consumed power of DC loads to the total consumed power of the system as represented in Figure 1.2 [13]. DC distribution system actually has lower losses when more than 60% of the loads are DC and DC/DC converters with efficiencies of 95% or higher are used.

Based on the advantages of DC distribution system, it could be utilized effectively in special applications as will be detailed in the next section.

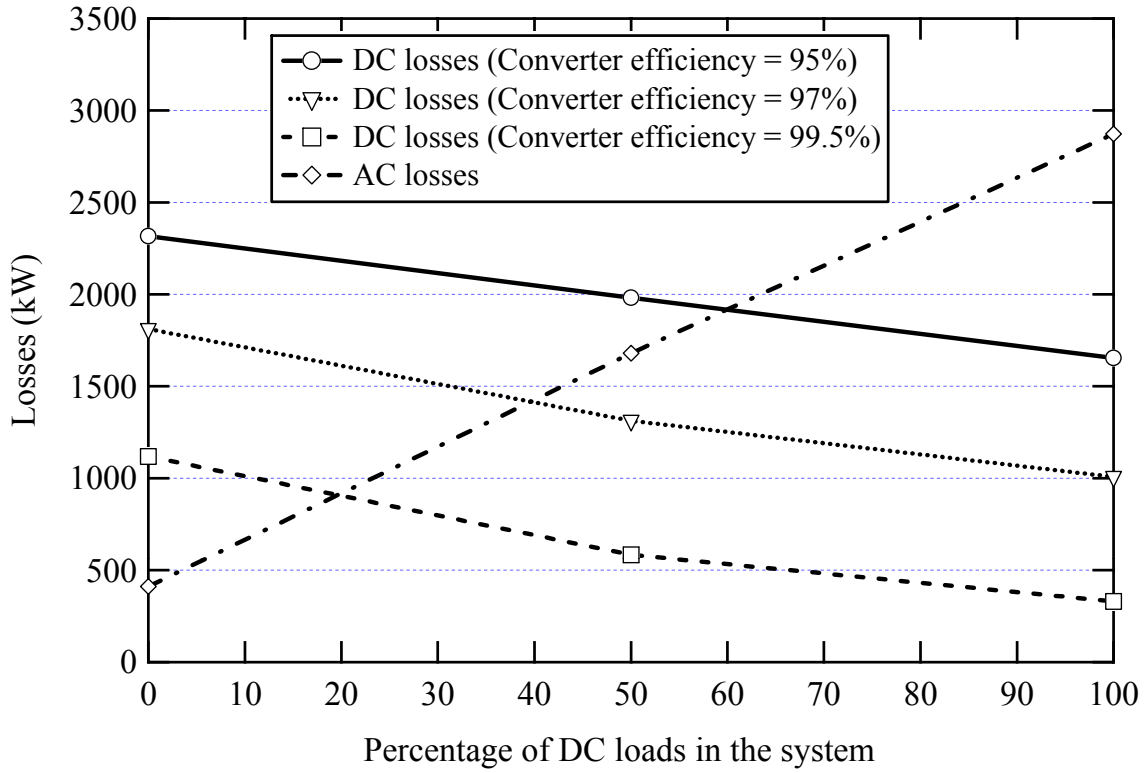

Figure 1.2: *Losses in AC and DC power systems [13].*

1.3 Applications of DC distribution system

1.3.1 Telecommunications and data centers

Telecommunications and data centers are constructed to transfer, store and process large amount of electronic information. Thus, a power system supplying such facilities might be basically required to have high reliability, safety to personnel, high efficiency and low electrical energy cost. As a suitable approach, the use of low voltage DC distribution system is highly recommended for such facilities [14][15]. Figure 1.3 shows the basic elements of a telecommunications DC power system [16]. These elements are rectifier system, battery system, charge bus, discharge bus, primary distribution system, secondary distribution system and voltage conversion. Rectifier system converts the AC voltage to DC one to power the loads when commercial AC power is available while battery system powers the loads during prime power AC outages. Charge bus provides a centralized location for connecting rectifiers to

the battery. The charge bus carries equipment load current and battery charge current during normal operation. Discharge bus provides a centralized location for connecting the battery and rectifiers to the primary DC power distribution system. The primary distribution system has the first protective device for over-current (either fuse or circuit breaker) between the discharge bus and the load. Although the primary distribution system can directly feed loads if desired, a secondary distribution system may be used. The secondary distribution system is an intermediate protected distribution network between the primary distribution network and the load equipment. There can be one or more secondary distribution systems, which serve individual loads or groups of loads downstream from the primary distribution system. Voltage converters are categorized by two basic types: DC/DC converters and inverters. DC/DC converters change the voltage of battery system and rectifier one to other utilization voltages. Inverters are used for AC loads that require an uninterruptible, or protected, AC supply. Each voltage conversion system usually has its own distribution system for connecting and protecting load circuits.

DC distribution system for telecommunications and data centers most often operates at nominal voltages of 24 or 48 volts dc. However, higher voltage DC has been also proposed as energy efficient option for both types of facilities [17].

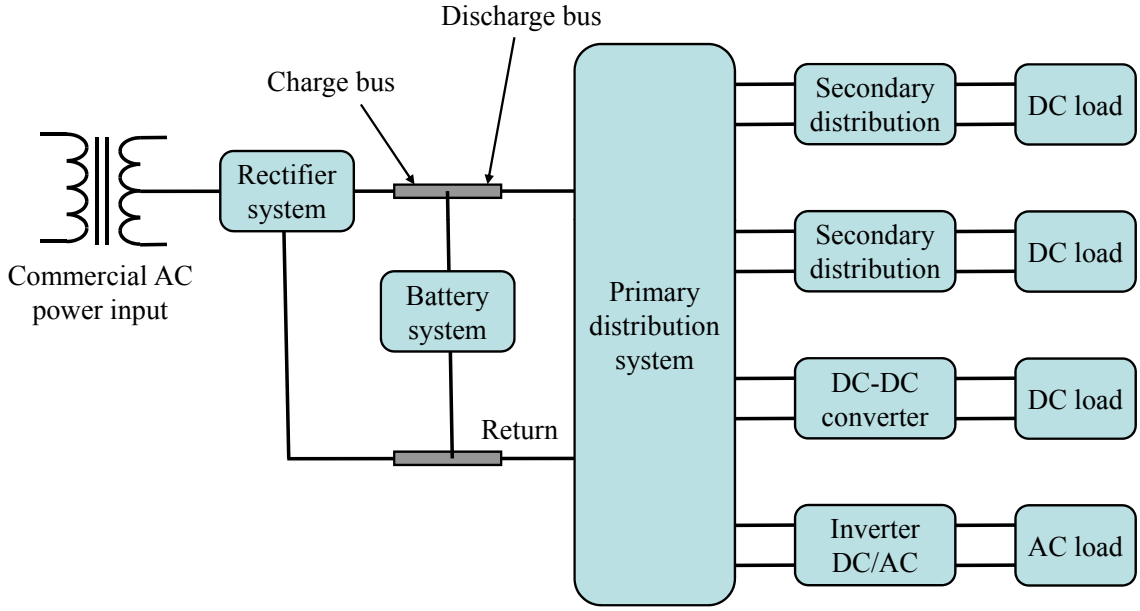

Figure 1.3: *Basic elements of a telecommunications DC power system [16].*

1.3.2 Residential and commercial facilities

Several studies regarding the use of DC in residential and commercial buildings have been presented [18–20]. Residential and commercial buildings often have a large amount of nonlinear electronic loads, such as personal computers, monitors, lighting and motors for air conditioner, refrigerators and washing machines, which are almost controlled by the electric devices. These may give rise to electromagnetic compatibility (EMC) and power quality (PQ) problems. Also, special office buildings have critical computer systems which must not be affected by transients and outages on the utility power grid. A common way to protect these loads is to install uninterruptible power supplies (UPSs) and standby diesel-generator sets. With a DC distribution system, these loads can be powered more effectively [6]. By choosing a proper system voltage level and connecting the battery block directly to the system, some conversion stages can be saved leading to reduced losses. So, in general, with a DC distribution system, a much lower number of converters will be needed and reliable supply to sensitive loads will be ensured [18].

1.3.3 Automotive applications and shipboards

For automotive applications, cost, volume, and weight are three major items to be considered in the development and manufacturing. This is also true for hybrid electric vehicles, which are attracting more and more attention due to increasing fuel costs and air pollution. Since the energy distribution system causes a significant share of the volume and the cost, DC distribution system is used for such applications [21][22] due to the simplicity and conservation of space.

The DC distribution is also considered for shipboard electric power distribution [4, 23]. The ever-increasing high-power load on ships, which need reliable power supply with very high-quality, made conventional AC systems very hard to maintain. The DC distribution system envisioned for the shipboard is illustrated in Figure 1.4 [4]. Two or more generators supply power to the DC distribution bus through power electronic converters, which rectify AC to DC and regulate the DC-bus voltage. The loads in a given zone are served through a DC-DC converter. The AC loads within the zone are served through the inverters which

convert DC to AC. In this system, the DC-DC converters isolate the loads in the zone from the rest of the system, and thus any fault and disturbance within a zone is confined within that zone. The rectifiers, similarly, isolate the AC generators from the system. The rectifiers also eliminate the tight frequency regulation and synchronization required on the AC generators. The DC bus itself might become immune to the ground faults by proper grounding.

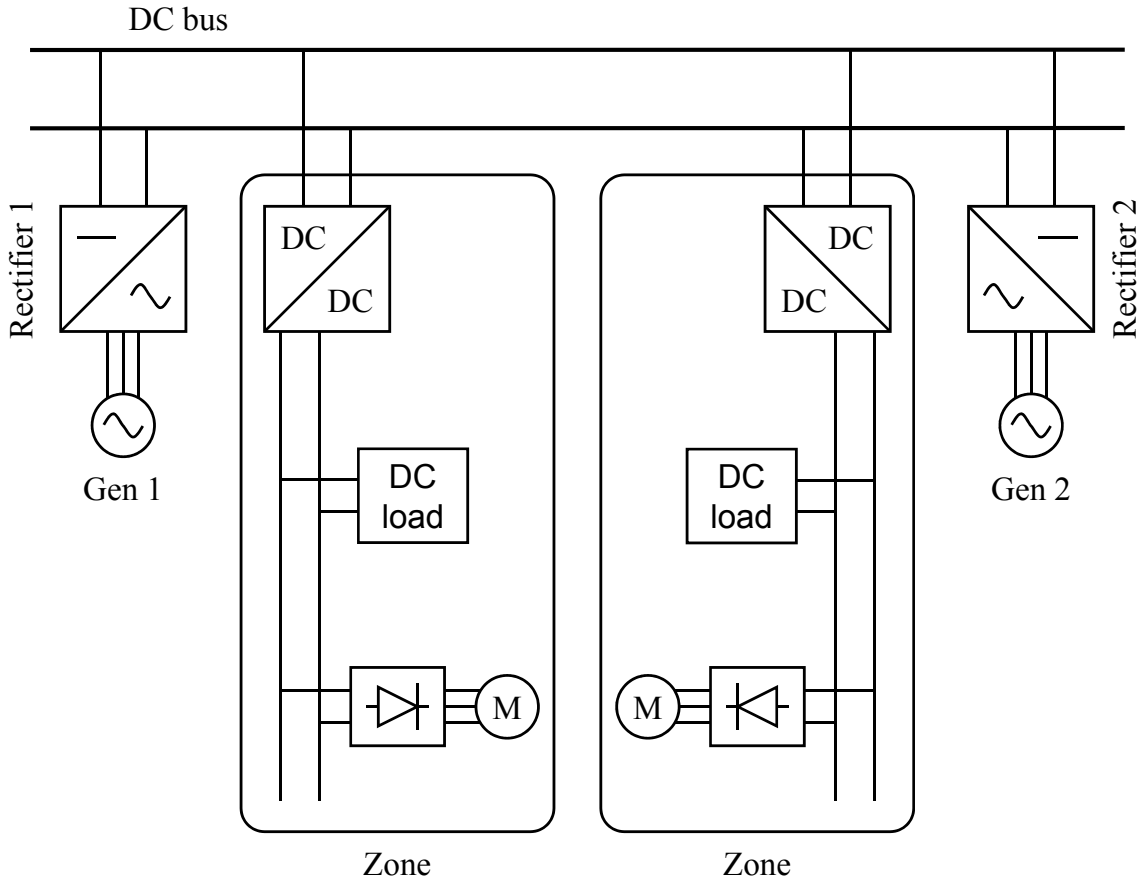

Figure 1.4: *DC shipboard distribution system [4].*

1.4 Voltage instability in DC distribution system

Voltage stability is defined as the ability of a power system to maintain steady voltages at all nodes in the system under operating condition and after being subjected to a disturbance. Voltage instability stems from the attempt of load dynamics to restore power consumption

beyond the capability of the combined transmission and generation system [24]. Instability can be occurred in the form of a fall or rise of voltage at certain nodes as shown in Figure 1.5.

In DC distribution systems, multiple power electronic converters are used to supply needed power at different voltage levels in both DC and AC forms. From the viewpoint of voltage stability studies, the main concern is the way that dynamics at each converter affects other converters and bus voltages throughout the system. Most of the power electronic converters, when they are tightly regulated, behave as constant power loads [25]. In constant power loads, the incremental impedance is always negative ($dV/dI < 0$), which might impact the stability of the multi-converter systems. If the voltage across a constant power load decreases, the current through it increases causing more reduction in the load voltage. In this case, if the system failed to regain to a stable operating point, the load voltage will continue to decrease towards zero resulting in voltage instability. There are many factors that determine the ability of a DC distribution system to regain or not to a stable operating point. These factors include the operating voltage, distribution feeder parameters, such as feeder length and cross-section [26], and load parameters [27]. It was also found that adding capacitance and/or damping resistance can enhance the system stability [28, 29].

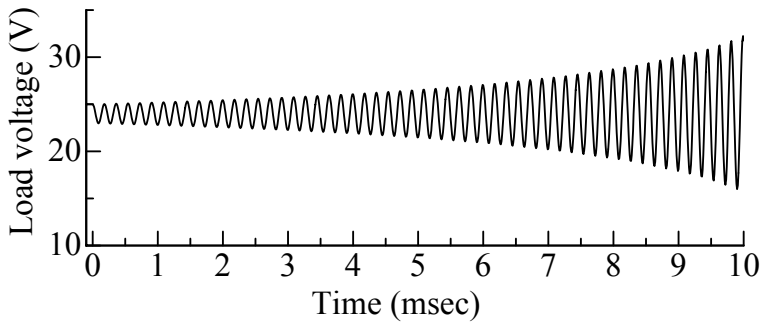

Figure 1.5: *Voltage instability in DC distribution system.*

1.5 Purpose and outline of the thesis

As mentioned in the previous sections, DC distribution system has been proposed as a prospective way to replace the conventional AC distribution system. However, in spite of that

many studies have confirmed the occurrence of voltage instability in DC distribution systems, less attention has been paid for studying the characteristics of deliverable power capability based on such instability phenomenon. From this viewpoint, this thesis aims to investigate the deliverable power characteristics in low-voltage DC distribution system based on voltage stability.

First, in Chapter 2, the electrical loads in DC distribution system are modeled as a preliminary stage for the analysis of voltage stability and deliverable power characteristics. The DC load model constructed from steady state unit, defined by non-linear resistor with voltage sensitivity parameter, and transient unit, defined by R_{in}, L_{in}, and C_{in} circuit. Both steady state and transient units are obtained from experimental measurements of the load power and its waveform.

After modeling the electrical loads in DC distribution system, Chapter 3 discusses the voltage instability phenomenon in DC distribution system and how this can limit the capability of deliverable power in the system. Hurwitz stability criterion is used in determining the stability conditions, and consequently, the upper limitation of deliverable power P_{lim}. The effect of voltage sensitivity parameter is also addressed.

Since the distribution line parameters are important factors in voltage instability and determining P_{lim}, the dependence of P_{lim} on these parameters is clarified in Chapter 4. Distribution line parameters include line cross-section, line length and inductance per meter. The effect of each parameter is evaluated, and then, improving the deliverable power characteristics is investigated by adding capacitor at the receiving end. Also, an experimental setup simulating a DC distribution system is built and experimental results are obtained in order to verify the theoretical calculations of P_{lim}.

In Chapter 5, the effect of load parameters on P_{lim} is examined. First, the effect of considering the transient unit of the DC load model and the magnitudes of R_{in}, L_{in}, and C_{in} is determined. Then, the effect of the number of loads and power sharing among them is also considered.

Finally, Chapter 6 summarizes the main contributions of this thesis. Also, ideas for future work are suggested.

Bibliography

[1] *International Energy Agency, World Energy Outlook 2009*,Chapter 1, Organization for Economic Co-operation and Development, 2009.

[2] R. F. Arritt, R. C. Dugan, D. L. Brooks, T. A. Short and K. Forsten, "Techniques for Analyzing Distribution System Efficiency Alternatives," *IEEE Power and Energy Society General Meeting,*, 2009.

[3] D. J. Hammerstrom, "AC versus DC distribution systems-Did we get it right?," *IEEE Power Engineering Society General Meeting*, June 2007.

[4] M. E. Baran and N. R. Mahajan, "DC distribution for Industrial Systems: Opportunities and Challenges," *IEEE Transactions Industry Applications*, vol. 39, No. 6, pp.1596 -1601, November/December 2003.

[5] K. Engelen, E. Leung Shun, P. Vermeyen, I. Pardon, R. D'hulst, J. Driesen and R. Belmans, "The Feasibility of Small-Scale Residential DC Distribution Systems," *32nd Annual Conference on IEEE Industrial Electronics*, pp. 2618-2623, 2006.

[6] D. Salomonsson and A. Sannino, "Low-voltage DC distribution system for commercial power systems with sensitive electronic loads," *IEEE Transactions Power Delivery*, vol. 22, no. 3, pp. 1620-1627, July 2007.

[7] R. Magureanu, M. Albu, A.-M. Dumitrescu and M. Priboianu, "A Practical Solution for Grid Connected Dispersed Generation from Renewable Sources: DC Connection," *International Symposium on Power Electronics, Electrical Drives, Automation and Motion*, pp. 1228 -1231, 2006.

[8] H. Pang, E. Lo and B. Pong, "DC Electrical Distribution Systems in Buildings," *2nd International Conference on Power Electronics Systems and Applications*, pp. 115-119, 2006.

[9] B. Axelrod, Y. Berkovich and A. Ioinovici, "Switched Coupled-Inductor Cell for DC-DC Converters with Very Large Conversion Ratio," *32nd Annual Conference on IEEE Industrial Electronics*, pp. 2366-2371, 2006.

[10] M. Brenna, G. C. Lazaroiu and E. Tironi, "High Power Quality and DG Integrated Low Voltage dc Distribution System," *IEEE Power Engineering Society General Meeting*, 2006.

[11] D. Nilsson and A. Sannino, "Efficiency Analysis of Low- and Medium- Voltage DC Distribution Systems," *IEEE Power Engineering Society General Meeting*, pp. 2315-2321, 2004.

[12] M. Furuse, S. Fuchino, N. Higuchi and I. Ishii, "Feasibility Study of Low-Voltage DC Superconducting Distribution System," *IEEE Transactions on Applied Superconductivity*, Vol. 15, No. 2, pp. 1759-1762, 2005.

[13] M. R. Starke, L. M. Tolbert and B. Ozpineci, "AC vs. DC Distribution: A Loss Comparison," *IEEE/PES Transmission and Distribution Conference and Exposition*, 2008.

[14] D. Salomonsson, L. Soder and A. Sannino, "An Adaptive Control System for a DC Microgrid for Data Centers," *IEEE Transactions on Industry Applications*, Vol. 44, No. 6, pp. 1910-1917, 2008.

[15] C. Foster and M. Dickinson, "High Voltage DC Power Distribution for Telecommunications Facilities," *30th International Telecommunications Energy Conference*, 2008.

[16] W. D. Reeve, "DC Power System Design for Telecommunications," *the Institute of Electrical and Electronics Engineers*, Inc., 2007.

[17] A. Pratt, P. Kumar and T. V. Aldridge, "Evaluation of 400V DC Distribution in Telco and Data Centers to Improve Energy Efficiency," *29th International Telecommunications Energy Conference*, pp. 32-39, 2007.

[18] A. Sannino, G. Postiglione and M. H. J. Bollen, "Feasibility of a DC Network for Commercial Facilities," *IEEE Transactions on Industry Applications*, Vol. 39, No. 5, pp. 1499-1507, 2003.

[19] Kakigano, Y. Miura, T. Ise, T. Momose and H. Hayakawa, "Fundamental Characteristics of DC Microgrid for Residential Houses with Cogeneration System in Each House," *IEEE Power and Energy Society General Meeting*, 2008.

[20] K. Techakittiroj and V. Wongpaibool, "Co-existance between AC-Distribution and DC-Distribution: In the View of Appliances," *Second International Conference on Computer and Electrical Engineering*, pp. 421-425, 2009.

[21] A. Emadi, M. Ehsani and J. M. Miller, Vehicular Electric Power Systems: Land, Sea, Air, and Space Vehicles, *Marcel Dekker*, Inc., 2004.

[22] H. Plesko, J. Biela, J. Luomi and J. W. Kolar, "Novel Concepts for Integrating the Electric Drive and Auxiliary DCDC Converter for Hybrid Vehicles," *IEEE Transactions on Power Electronics*, Vol. 23, No. 6, pp. 3025-3034, 2008.

[23] J. G. Ciezki and R. W. Ashton, "Selection and Stability Issues Associated with a Navy Shipboard DC Zonal Electric Distribution System," *IEEE Transactions on Power Delivery*, Vol. 15, No. 2, pp. 665-669, 2000.

[24] T. V. Cutsem and C. Vournas, Voltage Stability of Electric Power Systems, *Springer*, 2007.

[25] A. Emadi, A. Khaligh, C. H. Rivetta, and G. A. Williamson, "Constant Power Loads and Negative Impedance Instability in Automotive Systems: Definition, Modeling, Stability, and Control of Power Electronic Converters and Motor Drives," *IEEE Transactions on Vehicular Technology*, vol. 55, no. 4, pp. 1112-1125, 2006.

[26] M. Maruyama, Y. Nozaki, A. Fukui and K. Hirose, "Stability Analysis of High-Voltage DC Power Distribution System Including Long Feeders," *29th International Telecommunications Energy Conference*, pp. 211-215, 2007.

[27] H. Zhang, C. Saudemont, B. Robyns, N. Huttin and R. Meuret, "Stability analysis on the DC Power Distribution System of More Electric Aircraft," *13th International Power Electronics and Motion Control Conference*, pp. 1523-1528, 2008.

[28] T. Tanaka, T. Serada and T. Sakai, "Simulation Analysis of DC Power-supply System Stability," *16th Annual IEEE Applied Power Electronics Conference and Exposition*, pp. 759-764, 2001.

[29] D. L. Logue, and P. T. Krein, "Preventing instability in DC distribution systems by using power buffering," *IEEE Power Electronics Specialists Conference, PESC 2001*, vol. 1, pp. 33-37, June 2001.

Chapter 2
Modeling of Electrical Loads in DC Distribution System

2.1 Introduction

The validity of any theoretical analysis in a power system, like stability or load flow, greatly depends on the accuracy of the models representing its components. One of the major source of concern in modeling of power system components is directed to the load modeling [1]. Therefore, a lot of work has been carried out for the development of more accurate load models [2–5]. Consequently, this chapter aims to model the electrical loads in DC distribution system as a preliminary stage for the analysis of voltage stability and deliverable power characteristics. The proposed model takes into account not only the steady state but also the transient state of the load in order to obtain an accurate load modeling. Several electrical loads are considered such as DC/DC converter and personal computer.

The proposed DC load model consists of two units, steady state unit and transient unit as shown in Figure 2.1. The development of the model is based on the load consumed power in steady and transient states. In order to obtain such load model, the steady state unit must be constructed first.

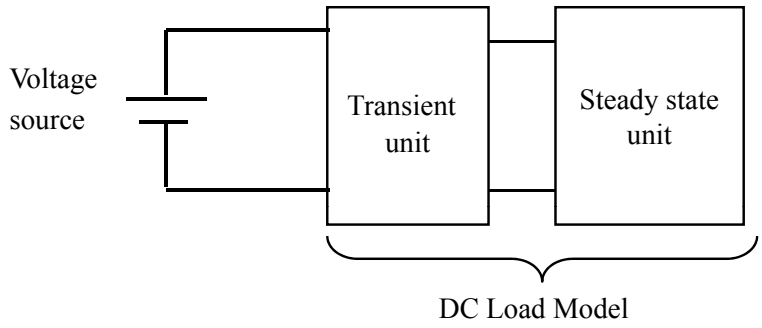

Figure 2.1: *Scheme of DC load model.*

In the steady state unit, the consumed load power at steady state condition is represented by an non-linear resistor defined by the voltage sensitivity parameter. The voltage sensitivity parameter is determined from the steady state experiments which measured the consumed power of the load for various applied voltages at the load terminals. Then, the transient unit is constructed to simulate the transient behavior of the load during the period of voltage variation at the load terminals. The configuration of this unit is determined on the basis of the shape of consumed power waveform in the load obtained from the experimental measurements during the transient condition. The transient unit is represented by an electrical circuit consisting of a resistor, an inductor and a capacitor.

2.2 Construction of steady state unit

2.2.1 Definition of voltage sensitivity parameter

In a power system, there are different types of loads which can be classified into constant current, constant power and constant impedance loads. For proper specification of such loads, the voltage sensitivity parameter is used [1]. The voltage sensitivity parameter, which is denoted as α, defines the dependence degree of load power consumption on the applied voltage variations as given by the following equation:

$$p = \frac{P}{V^{\alpha}} v^{\alpha}. \tag{2.1}$$

where p, v are the instantaneous load power and voltage, respectively, and P, V are the consumed power and load voltage at nominal state, respectively.

It is noticed that, in the case of constant impedance loads, α is equal to 2 where the load power consumption is proportional to the square of the terminal voltage as can be easily deduced from Ohm's law. However, in constant current loads, the load power is linearly proportional to the applied voltage giving α equal to 1. In constant power loads, α is 0, where the load power is considered to be constant at different applied voltages. Figure 2.2 illustrates the load power dependence on the applied voltage and the corresponding voltage sensitivity parameter for different types of loads.

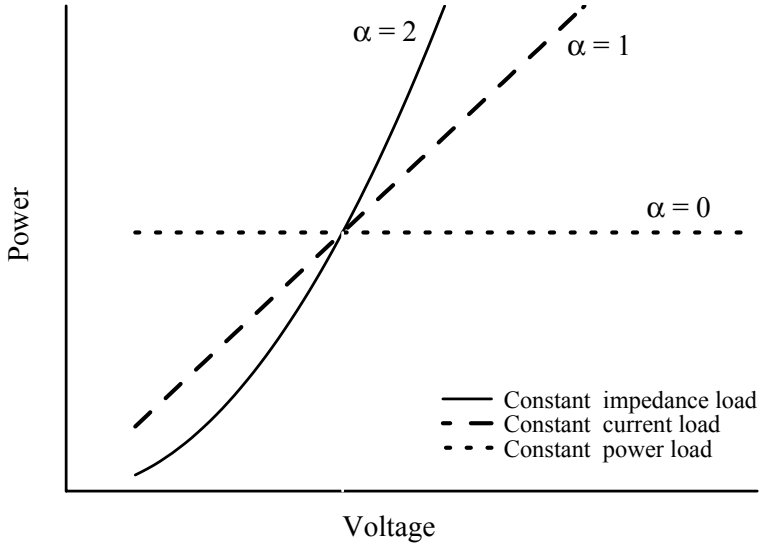

Figure 2.2: *Load power consumption and voltage sensitivity parameters for different types of loads.*

For N loads connected in parallel at the same bus-bar, the total α is given by:

$$\alpha_{\text{total}} = \sum_{j=1}^{N}(\alpha_j P_j)/\sum_{j=1}^{N} P_j. \tag{2.2}$$

where, α_j and P_j are the voltage sensitivity and consumed power of each load [1].

Based on the concept of voltage sensitivity, the steady state unit in our model is represented by a non-linear resistor. The consumed power p of this resistor is related to the applied voltage v in terms of α as in equation (2.1). Therefore, determining the voltage sensitivity parameter of the load is the first step in constructing the steady state unit.

2.2.2 Evaluation procedures of voltage sensitivity parameter

The experimental setup used in measuring the load consumed power under steady and transient states is shown in Figure 2.3. In this setup, the load was powered from a controllable DC voltage source. The voltage at the load terminals V and the current I through the load were measured and recorded by a voltmeter and an ammeter, respectively. In addition, an oscilloscope was used to observe the voltage and current waveforms. This experimental was performed for several loads such as DC fan, DC motor, DC/DC converter and personal computer is presented. The rating of these loads is shown in table 2.1

First, the voltage V applied to the load was varied and the resultant current I was measured. This step was repeated until V reaches 1.2 times the rated voltage of the load (V_0). The consumed power of the load P is determined by multiplying the obtained current I by the applied voltage V. Then, the load power can be plotted as a function of the applied voltage. By fitting the obtained relation between V and P based on equation (2.1), the voltage sensitivity parameter α was determined. Figure 2.4 shows the flow chart to determine α.

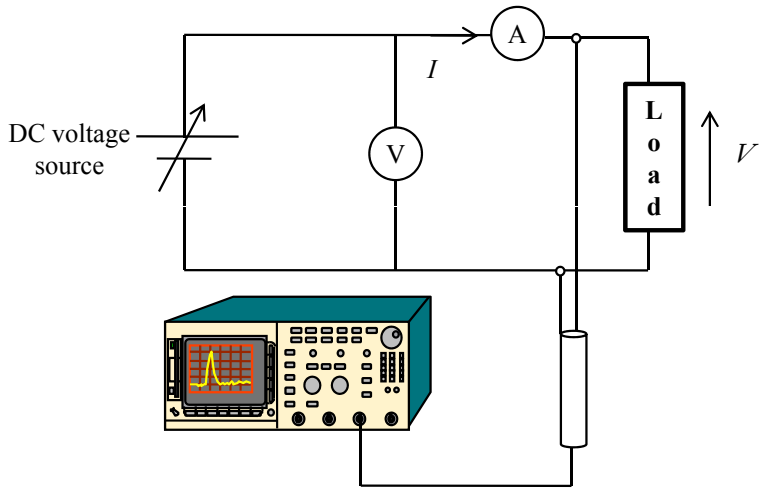

Figure 2.3: *Scheme of the experimental setup for steady-state measurement.*

Load	Rated voltage	Rated power
DC fan	12 V	2.76 W
DC motor	24 V	204 W
DC/DC converter	24 V	120 W
Personal computer	16 V	17 W

Table 2.1: *Rating of DC fan, DC motor, DC/DC converter and personal computer used in determining voltage sensitivity parameter.*

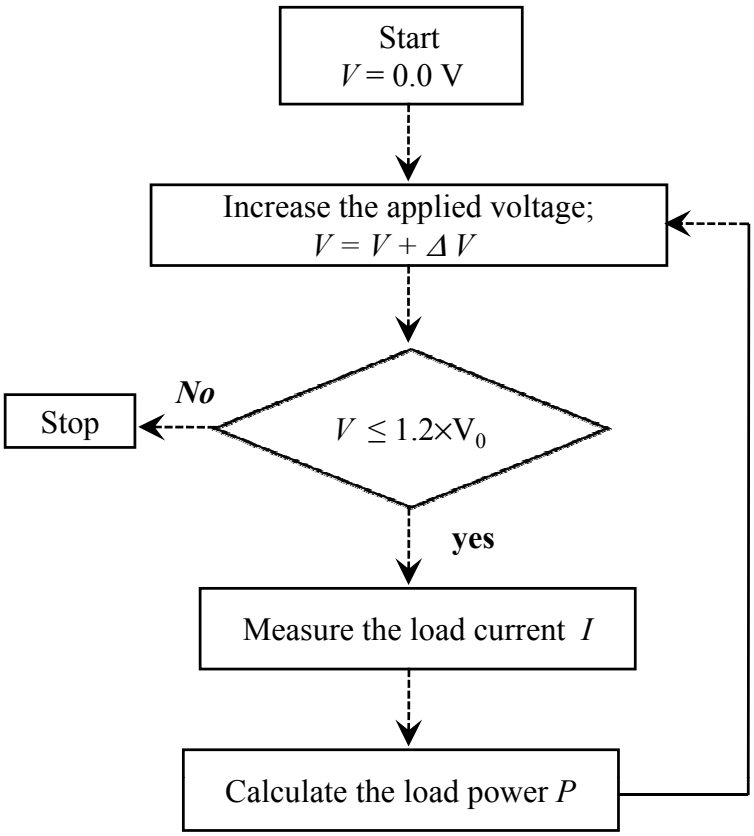

Figure 2.4: *Flow chart of experimental procedures for determining the voltage sensitivity parameter* α.

2.2.3 Voltage sensitivity parameter of DC fan

The voltage sensitivity is determined for a 12 V-DC fan shown in Figure 2.5 which is used in removing the heat in the electronic equipments. The DC fan is connected to a DC voltage source as illustrated in Figure 2.3. Following the previous experimental procedures, α of the DC fan is determined. Figure 2.6 presents the measured waveforms of the current i and the consumed power p of the DC fan for applied voltage v of 3, 5, 9 and 12 V.

This figure shows that the current of the fan increased with the increase in the applied voltage. This increase is almost linear as illustrated from the averaged values of the fan input current presented in Figure 2.7. In order to obtain the voltage sensitivity parameter of the DC fan, the average consumed power was plotted against the applied voltage as shown in Figure 2.8. By fitting the obtained results on the basis of equation (2.1), α was equal to 1.89. This value of α reveals that the consumed power of the DC fan is highly depending on the applied voltage.

Figure 2.5: *12 V-DC fan used in determining voltage sensitivity parameter.*

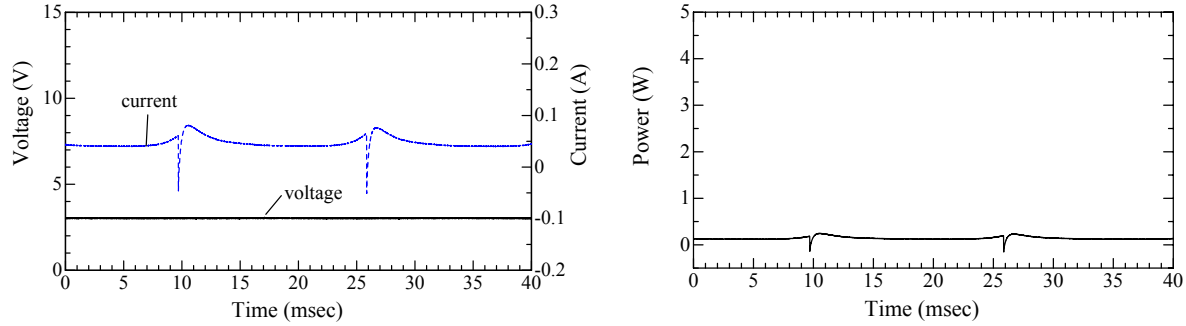

(a) Voltage, current and power of DC Fan at V_{in} = 3 V.

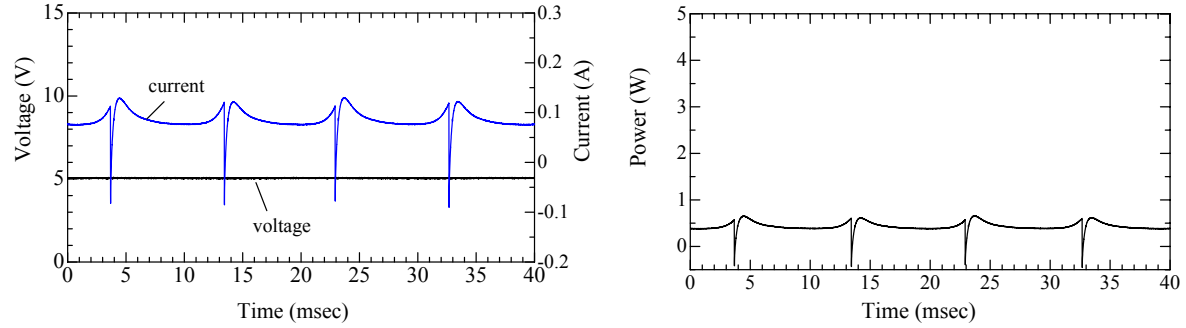

(b) Voltage, current and power of DC Fan at V_{in} = 5 V.

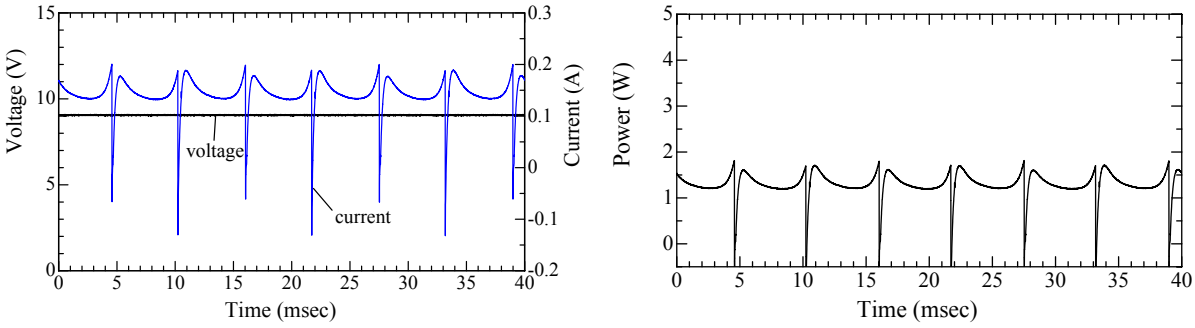

(c) Voltage, current and power of DC Fan at V_{in} = 9 V.

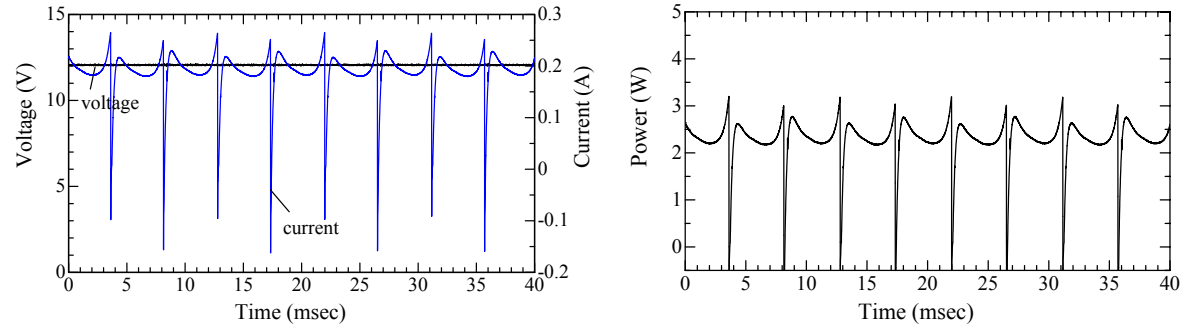

(d) Voltage, current and power of DC Fan at V_{in} = 12 V.

Figure 2.6: *Voltage, current and power of DC Fan at various input voltage.*

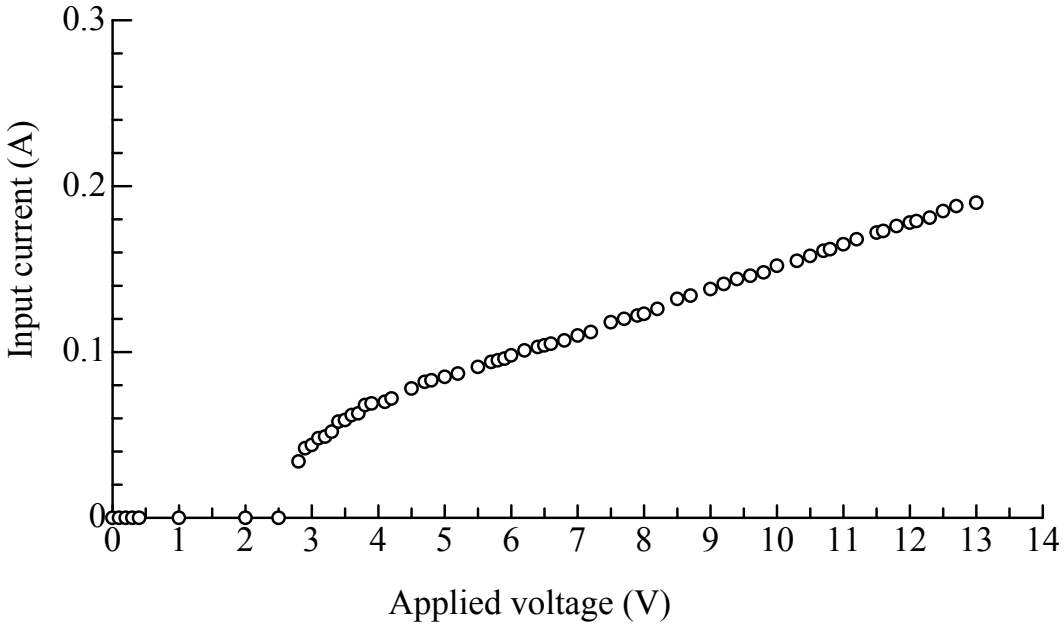

Figure 2.7: *DC Fan voltage-current characteristic.*

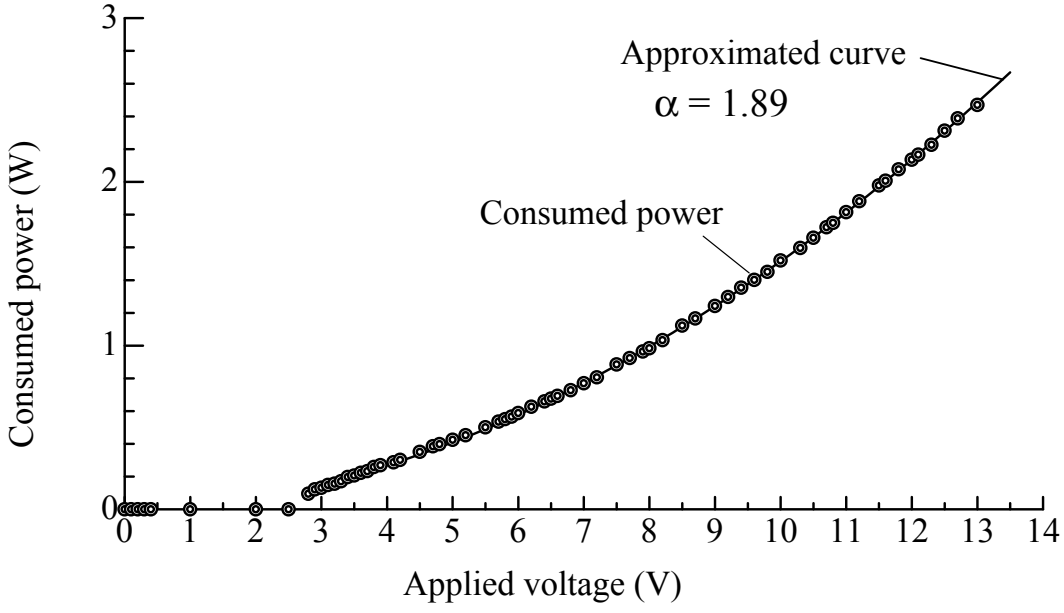

Figure 2.8: *Voltage and power relationship of DC Fan.*

2.2.4 Voltage sensitivity parameter of DC motor

In this section, the voltage sensitivity parameter is determined for a DC motor with rated voltage 24 V, rated current 8.5 A and rated speed 3300 rpm shown in Figure 2.9. The motor was loaded by a constant power mechanical load, in which the torque is inversely proportional to the speed as can be found in cutting tools, mixers and drilling machines.

In order to simulate the constant power mechanical load, a DC generator and constant power electrical load was coupled with the DC motor as shown in Figure 2.10. This combination (DC generator and electrical load) proved to have the characteristics of constant power mechanical load as illustrated in Figure 2.11, where the motor input current was inversely proportional to the applied voltage for various load powers, 20, 30, 40 and 50 W. For example, in the case of 20 W, the current reduces from 3.5 to 2.5 A as the applied voltage increases from 12 to 17 V.

Figure 2.12 shows the consumed power of the DC motor as a function of applied voltage. Fitting this relationship enabled to determine α. For 50 W load, α was determined to be 0.39. Similar magnitude of α was obtained for different load powers. That is to say, α of this motor is found to be 0.4 and independent of the load power.

Figure 2.9: *24 V-DC motor used in determining voltage sensitivity parameter.*

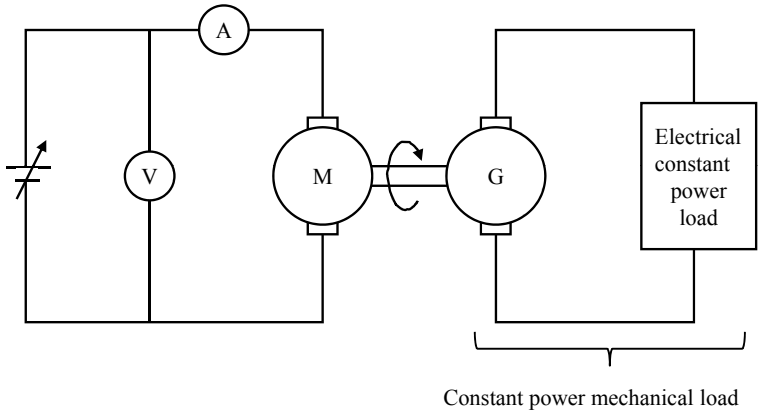

Figure 2.10: *DC motor coupled with constant power mechanical load.*

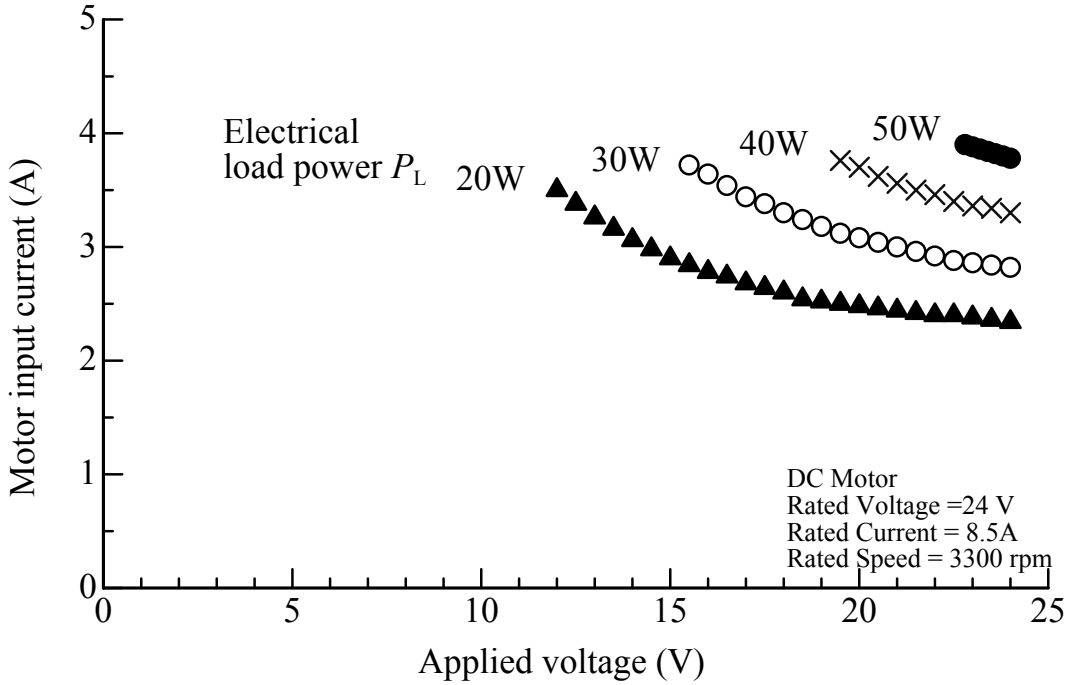

Figure 2.11: *DC motor voltage-current characteristic.*

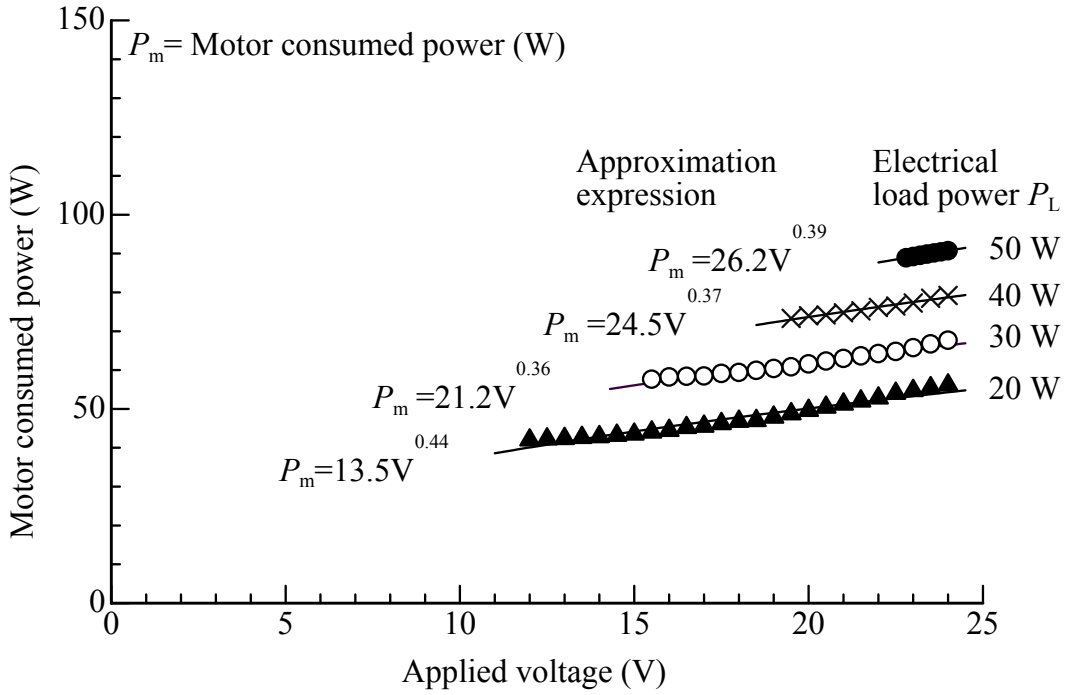

Figure 2.12: *Voltage and power relationship of DC motor.*

2.2.5 Voltage sensitivity of DC/DC converter

The voltage sensitivity parameter is determined for a DC/DC converter shown in Figure 2.13, which loaded by a personal computer. The operating voltage of the DC/DC converter is 24 V. The consumed power by the converter and the personal computer was measured for the different applied voltages from 22.5 to 25.5 V. Figure 2.14 shows the consumed power as a function of the applied voltage. By fitting the experimental results, α was found to be equal to 0. Therefore, the consumed power of DC/DC converter is independent of the applied voltage variations, giving the characteristic of constant power load.

Figure 2.13: *24 V-DC/DC converter used in determining voltage sensitivity parameter.*

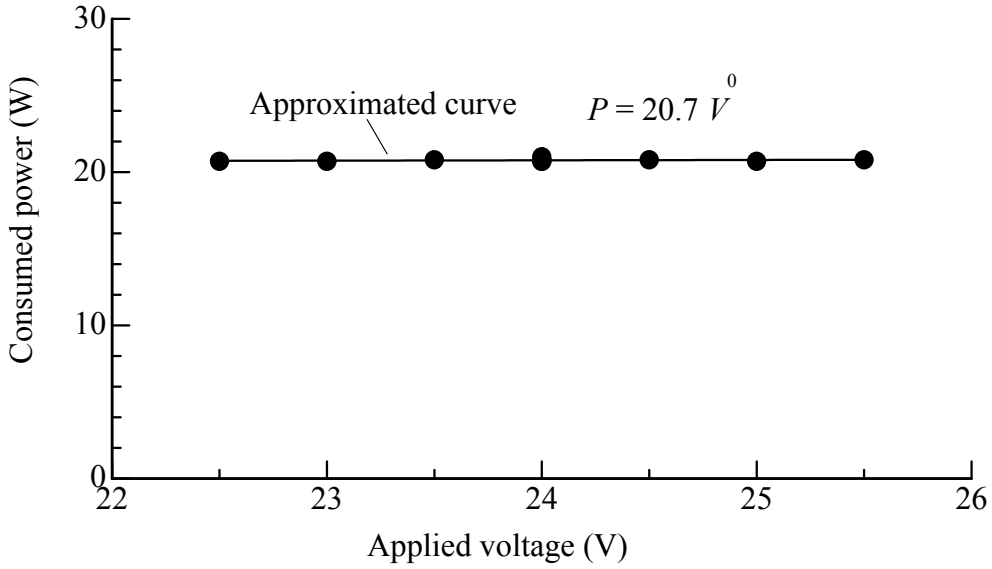

Figure 2.14: *Voltage and power relationship of DC/DC converter.*

2.2.6 Voltage sensitivity of personal computer

The voltage sensitivity parameter is determined for a personal computer shown in Figure 2.15. This computer was directly connected to the DC voltage source without using DC/DC converter. The rated voltage and power of the personal computer are 16 V, 17 W, respectively. The consumed power was determined as the applied voltage was changed from 14.3 to 17.5 V. Figure 2.16 shows the consumed power as a function of the applied voltage. By fitting the experimental results, α was found to be equal to 0.13. Therefore, the variations in the applied voltage slightly affects the load consumed power.

Figure 2.15: *A personal computer used in determining voltage sensitivity parameter.*

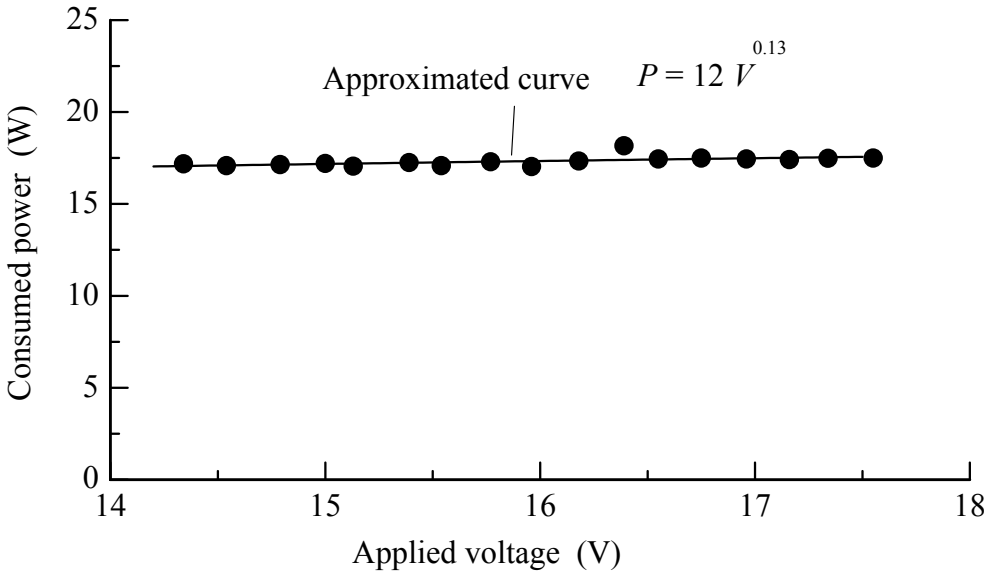

Figure 2.16: *Voltage and power relationship of personal computer.*

2.3 Construction of transient unit

This section presents the construction of the transient unit in the proposed DC load model. This unit simulates the behavior of the load under transient state. Measurements of the consumed power under transient state are carried out and according to the shape of the consumed power, the configuration of the transient unit is determined. The transient unit is obtained for a personal computer and a loaded DC/DC converter.

2.3.1 Configuration of transient unit

The experimental setup shown in Figure 2.3 was used in these measurements. In order to study the transient state, the following procedures were performed:

1. A step change was done in the applied voltage. Each load was subjected to different step-up and step-down values in the applied voltage.
2. Waveforms of the load current and consumed load power were recorded by an oscilloscope.

Figure 2.17 and Figure 2.18 present the obtained waveforms of the load current and the consumed load power of a personal computer and a loaded DC/DC converter, respectively, as a response to a step change in the applied voltage.

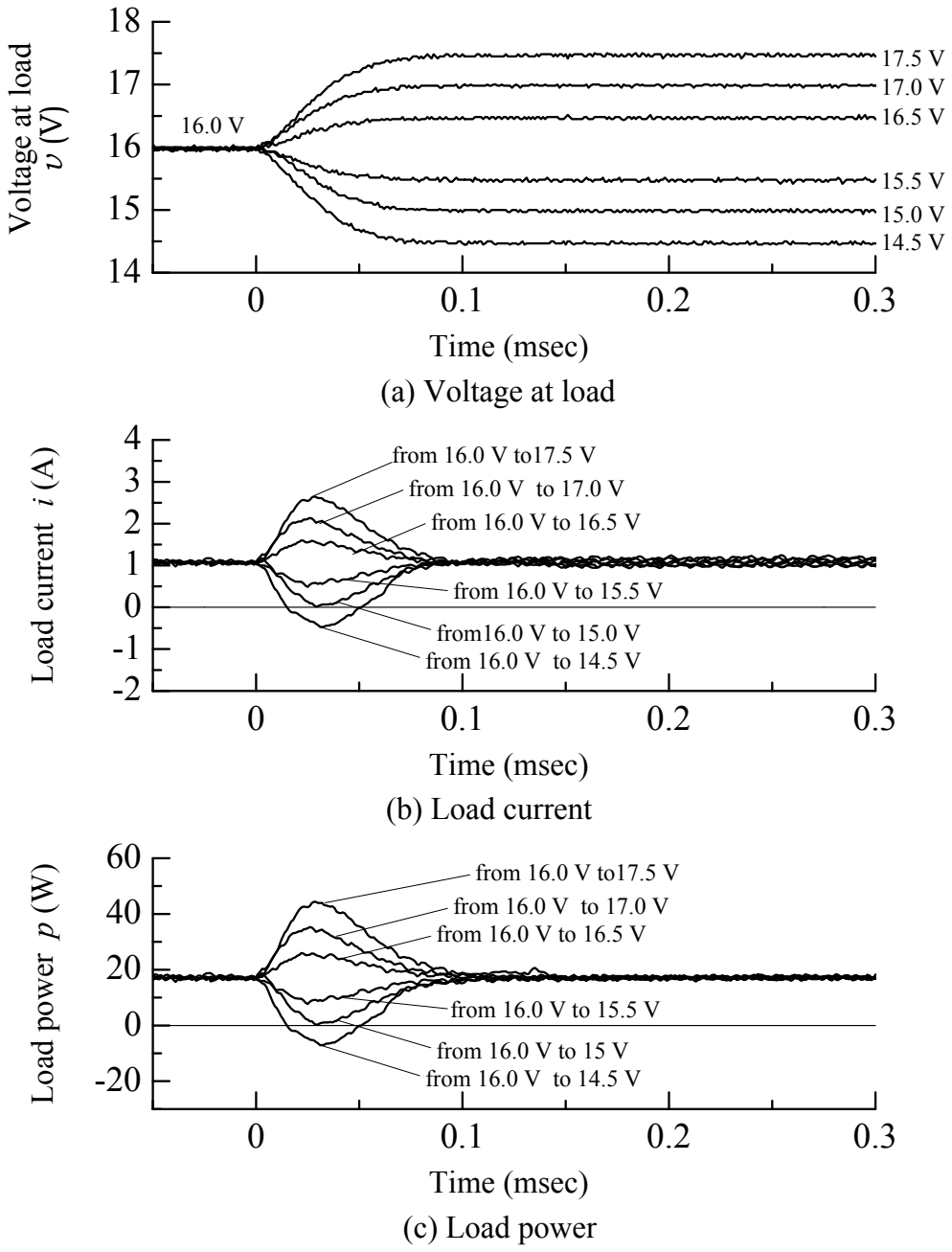

Figure 2.17: *Transient behavior of personal computer.*

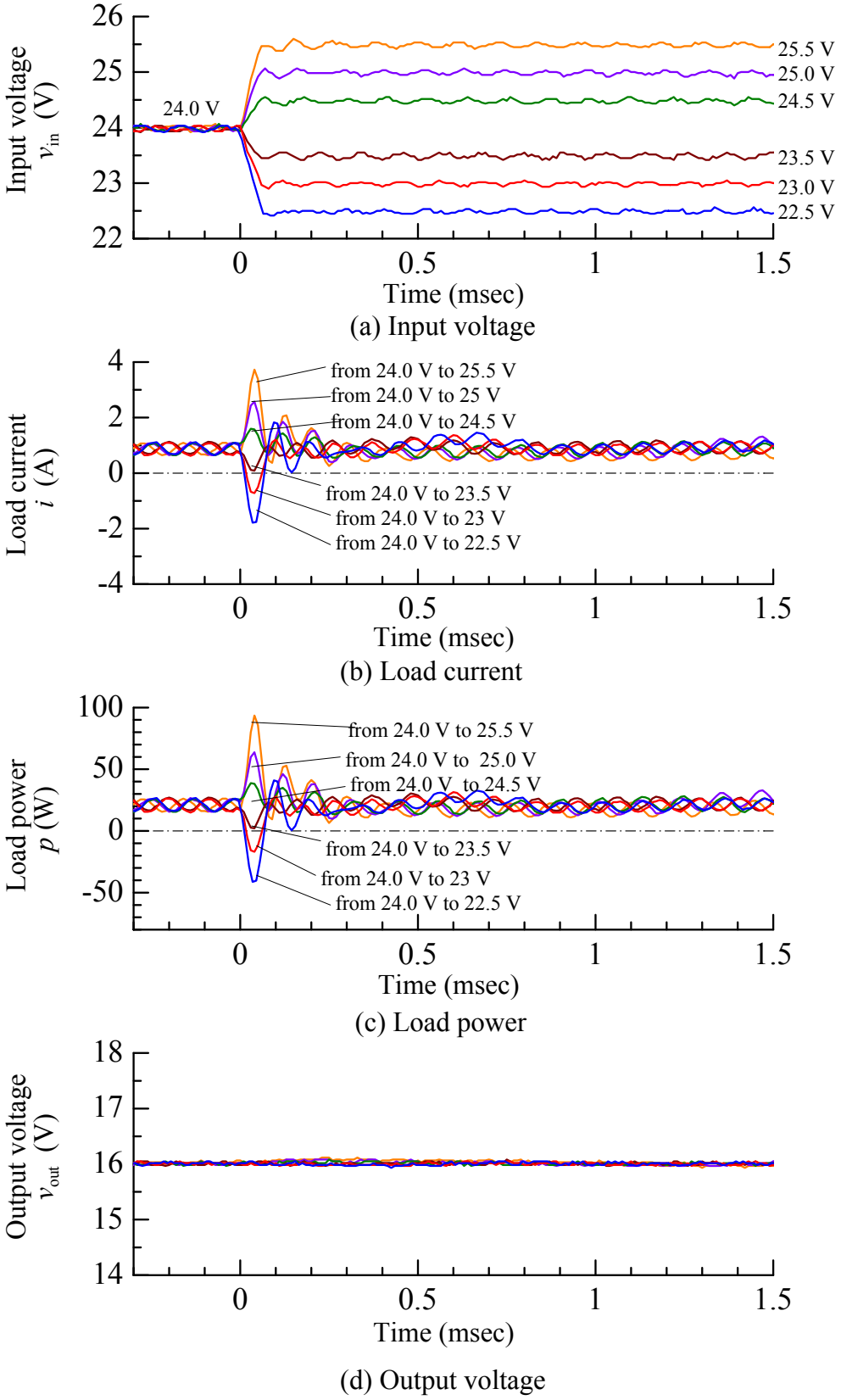

Figure 2.18: *Transient behavior of loaded DC/DC converter.*

For the personal computer in Figure 2.17, when a step change occurred in the applied voltage from 16 V to 17.5 V, the load current increased from 1.07 A to 2.65 A and then decreased to 0.99 A. The consumed load power also increased from 17.1 W to 44.3 W and then decreased to 17.3 W. Similar behavior was observed for the other values of step change in the applied voltage. For the loaded DC/DC converter in Figure 2.18, it is noticed that the load current and the consumed load power behaves in the transient state similarly to the personal computer.

The steady state values of load current and consumed load power in both loads are determined based on the steady state operation as represented by the non-linear resistor. On the other hand, the transient behavior of both loads are similar to the response of a RLC circuit. Therefore, the transient unit is proposed to be constructed with a resistor R_{in}, an inductor L_{in} and a capacitor C_{in} as shown in Figure 2.19. This proposed arrangement is considered in order to take into account the inductance on the conducting wires, as the resistance of the conducting wires is very small.

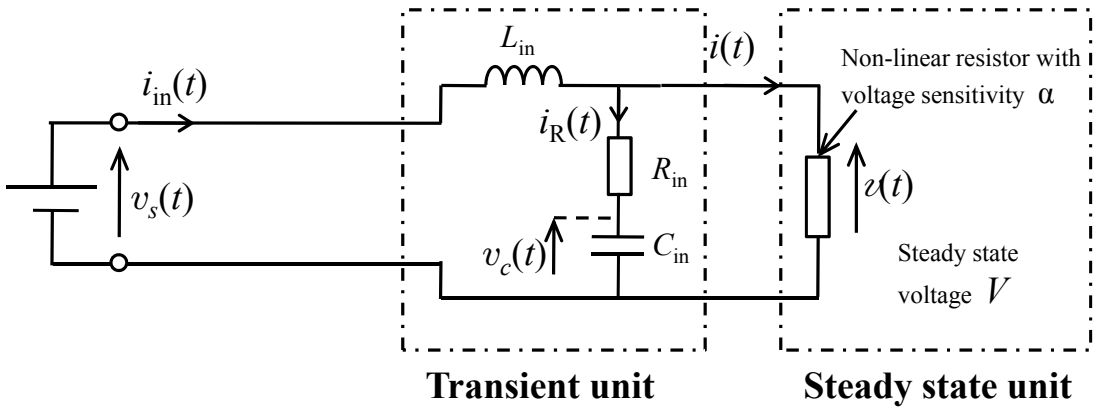

Figure 2.19: *Equivalent circuit of DC load model.*

2.3.2 Calculation of transient unit parameters

After determining the configuration of the transient unit in the proposed DC load model, the next step is to calculate the magnitudes of transient unit components, resistor R_{in}, inductor L_{in} and capacitor C_{in}. The calculation procedure is illustrated in the flow chart of Figure 2.20. As shown in this flow chart, the initial values of the components R_{in}, L_{in} and C_{in} were specified and then the transient responses of the current through the DC load model i_{in} was simulated

to the stepwise change in the applied voltage which was measured in the previous section. The detailed calculation procedure is described below. This calculation is repeated for various magnitudes of the components until the calculated current agree with the measured one.

The circuit equations describing the DC model presented in Figure 2.19 can be derived as follows:

$$v_{\mathrm{s}}(t) = L_{\mathrm{in}}\frac{di_{\mathrm{in}}(t)}{dt} + R_{\mathrm{in}}i_{\mathrm{R}}(t) + v_{\mathrm{c}}(t), \tag{2.3}$$

$$i_{\mathrm{in}}(t) = i_{\mathrm{R}}(t) + i(t), \tag{2.4}$$

$$i_{\mathrm{R}}(t) = C_{\mathrm{in}}\frac{dv_{\mathrm{c}}(t)}{dt}, \tag{2.5}$$

$$i(t) = \frac{P}{V^{\alpha}}v(t)^{\alpha-1} \text{ and} \tag{2.6}$$

$$v(t) = v_{\mathrm{c}}(t) + R_{\mathrm{in}}i_{\mathrm{R}}(t). \tag{2.7}$$

Using Taylor-series, equation (2.6) is expanded as:

$$i(t) = \frac{P}{V} + (\alpha-1)\frac{P}{V^2}(v(t) - V). \tag{2.8}$$

Using these equations and based on the trapezoidal rule, equation (2.3) is expressed as:

$$v_{\mathrm{s}}(t) = L_{\mathrm{in}}[\frac{i_{\mathrm{in}}(t+\Delta t) - i_{\mathrm{in}}(t)}{\Delta t}] + R_{\mathrm{in}}C_{\mathrm{in}}[\frac{v_{\mathrm{c}}(t+\Delta t) - v_{\mathrm{c}}(t)}{\Delta t}] + v_{\mathrm{c}}(t). \tag{2.9}$$

By integrating both sides from t to $t+\Delta t$, the voltage v_{c} across the capacitor C_{in} at $t+\Delta t$ is given by:

$$\begin{aligned} v_{\mathrm{c}}(t+\Delta t) &= \frac{1}{R_{\mathrm{in}}C_{\mathrm{in}} + \frac{\Delta t}{2}}[\frac{\Delta t}{2}(v_{\mathrm{s}}(t+\Delta t) + v_{\mathrm{s}}(t)) - L_{\mathrm{in}}(i_{\mathrm{in}}(t+\Delta t) - i_{\mathrm{in}}(t)) \\ &+ (R_{\mathrm{in}}C_{\mathrm{in}} - \frac{\Delta t}{2})v_{\mathrm{c}}(t)]. \end{aligned} \tag{2.10}$$

By the same way, the total load current $i_{\mathrm{in}}(t)$ in equation (2.4) is expressed as:

$$\begin{aligned} i_{\mathrm{in}}(t) &= C_{\mathrm{in}}\frac{v_{\mathrm{c}}(t+\Delta t) - v_{\mathrm{c}}(t)}{\Delta t} + \frac{P}{V} \\ &+ (\alpha-1)\frac{P}{V^2}\{v_{\mathrm{c}}(t) + R_{\mathrm{in}}C_{\mathrm{in}}(\frac{v_{\mathrm{c}}(t+\Delta t) - v_{\mathrm{c}}(t)}{\Delta t}) - V\}, \end{aligned} \tag{2.11}$$

By integrating both sides from t to $t+\Delta t$,

$$\begin{aligned} \frac{(i_{\mathrm{in}}(t+\Delta t) + i_{\mathrm{in}}(t))\Delta t}{2} &= C_{\mathrm{in}}(v_{\mathrm{c}}(t+\Delta t) - v_{\mathrm{c}}(t)) + \frac{P}{V}\Delta t - (\alpha-1)\frac{P}{V}\Delta t \\ &+ (\alpha-1)\frac{P}{V^2}\frac{\Delta t}{2}(v_{\mathrm{c}}(t+\Delta t) + v_{\mathrm{c}}(t)) \\ &+ (\alpha-1)\frac{P}{V^2}R_{\mathrm{in}}C_{\mathrm{in}}(v_{\mathrm{c}}(t+\Delta t) + v_{\mathrm{c}}(t)), \end{aligned} \tag{2.12}$$

Then,

$$\begin{aligned} i_{\rm in}(t+\Delta t)+i_{\rm in}(t) &= \frac{2P}{V}(2-\alpha)+v_{\rm c}(t)[(\alpha-1)\frac{P}{V^2}-\frac{2C_{\rm in}}{\Delta t}-2R_{\rm in}C_{\rm in}(\alpha-1)\frac{P}{\Delta t V^2}] \\ &+ v_{\rm c}(t+\Delta t)[\frac{2C_{\rm in}}{\Delta t}+(\alpha-1)(\Delta t+2R_{\rm in}C_{\rm in})\frac{P}{\Delta t V^2}]. \end{aligned} \tag{2.13}$$

By substituting for $v_{\rm c}(t+\Delta t)$ from equation (2.10) into equation (2.13), $i_{\rm in}(t+\Delta t)$ is given by:

$$\begin{aligned} i_{\rm in}(t+\Delta t) &= \frac{1}{\gamma V+(\eta+\lambda)L_{\rm in}}[2\gamma P(2-\alpha)-i_{\rm in}(t)\{\gamma V-(\eta+\lambda)L_{\rm in}\} \\ &+ (\eta+\lambda)\frac{\Delta t}{2}v_{\rm s}(t+\Delta t)+v_{\rm s}(t)-\eta\Delta t v_{\rm c}(t)]. \end{aligned} \tag{2.14}$$

where,

$$\begin{aligned} \gamma &= V\Delta t(R_{\rm in}C_{\rm in}+\frac{\Delta t}{2}), \\ \lambda &= P(\alpha-1)(2R_{\rm in}C_{\rm in}+\Delta t) \end{aligned}$$

and

$$\eta = 2V^2C_{\rm in}.$$

On the basis of the expressions of $v_{\rm c}(t+\Delta t)$ in equation (2.10) and $i_{\rm in}(t+\Delta t)$ in equation (2.14) , the numerical solution is carried out using a FORTRAN program in order to determine the magnitude of transient components.

Figure 2.21 shows the load current and consumed load power waveforms of a personal computer corresponding to a step change in the applied voltage from 16 V to 17 V. The current and power are calculated at the magnitudes of $R_{\rm in}$, $L_{\rm in}$ and $C_{\rm in}$ obtained from the FORTRAN program. Then, these calculated values are compared to the actual measured ones. It is cleared that the calculated current agrees with the measured load current as noticed from Figure 2.21 (b). The same agreement occurs between the calculated load power and the actual load power in Figure 2.21 (c). The error between the measured and the calculated load current is regarded to be very small where the maximum obtained error is 0.2 A as presented in Figure 2.21 (d).

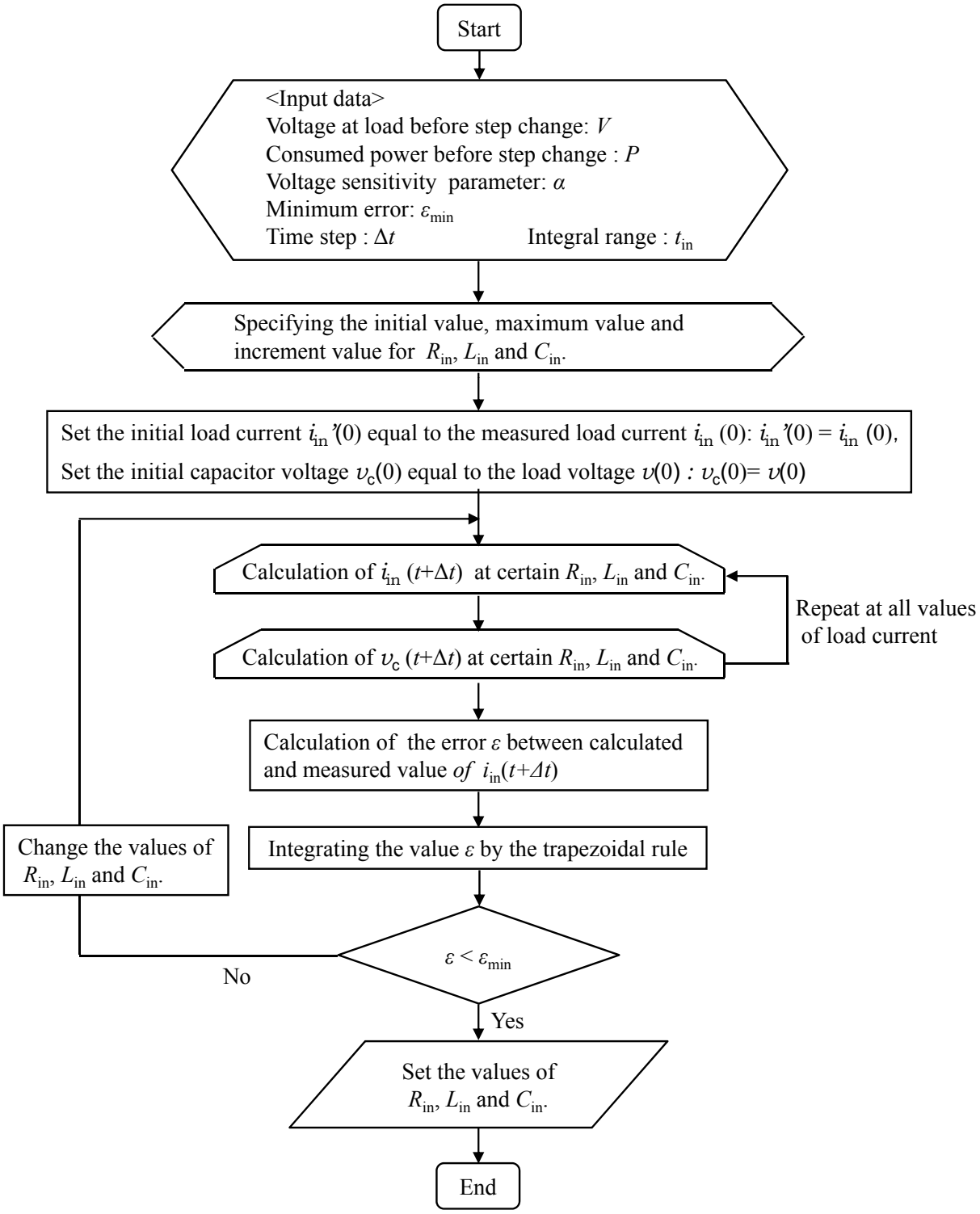

Figure 2.20: *Calculating procedures of the transient unit components.*

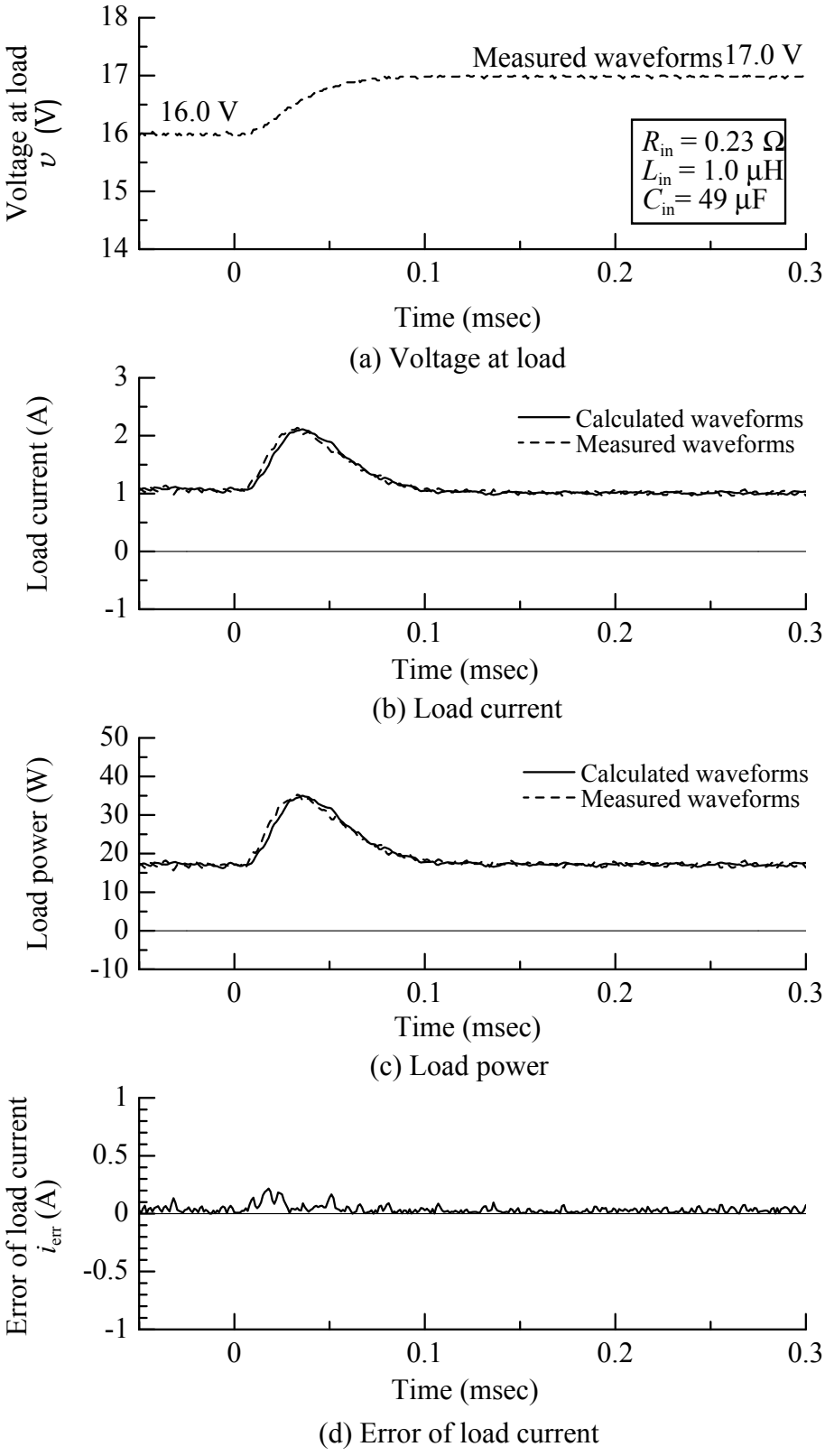

Figure 2.21: *Load current and consumed load power of personal computer using the calculated resistance, inductance and capacitance.*

Based on the calculated magnitudes of R_{in}, L_{in} and C_{in}, the complete model of the personal computer simulating the steady state and the transient state is constructed as shown in Figure 2.22 .

Following the same procedures, the transient components a DC/DC converter loaded with personal computer and a DC/DC converter loaded with resistive load are obtained. The complete models of these loads are presented in Figure 2.23 and Figure 2.24, respectively. Almost the obtained transient unit parameters are the same because of the dependence on the DC/DC converter.

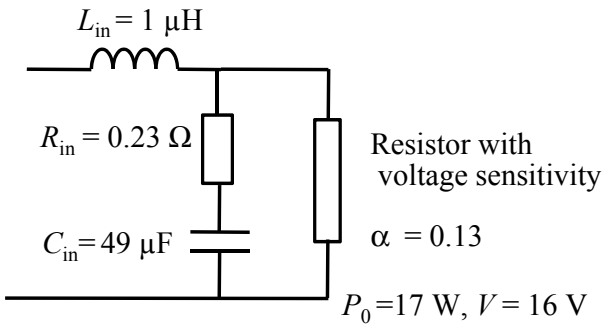

Figure 2.22: *Equivalent DC load model of personal computer.*

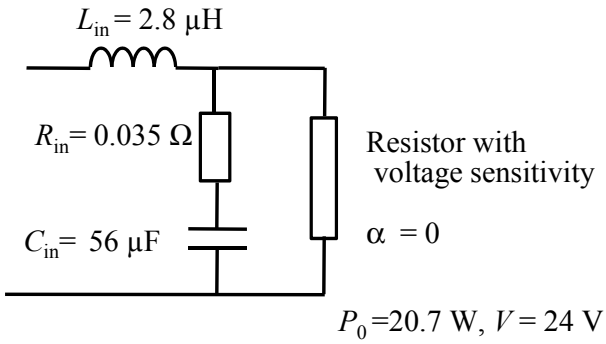

Figure 2.23: *Equivalent DC load model of DC/DC converter loaded by a personal computer.*

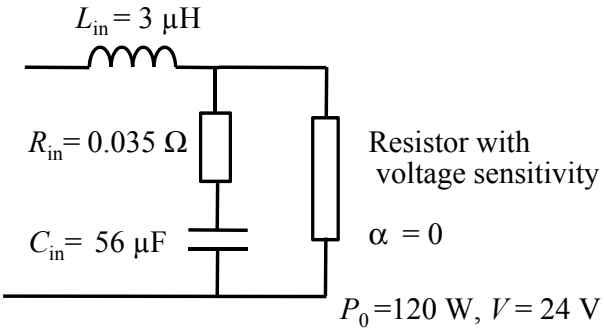

Figure 2.24: *Equivalent DC load model of DC/DC converter loaded by a resistor.*

2.4 Conclusion

In this chapter, a DC load model was proposed as a preliminary stage for the analysis of voltage stability and deliverable power characteristics. This model consisted of steady state unit and transient unit in order to simulate the load performance in both states. The load consumed power in steady state was represented using a non-linear resistor defined by the voltage sensitivity parameter α. The voltage sensitivity parameter was calculated for different loads from steady state measurements of the load powers at various applied voltages. For DC fan, α was equal to 1.89, indicating that the consumed power is highly depending on the applied voltage. For DC motor loaded with a constant power load, α was found to be 0.4. however, for DC/DC converter and personal computer, the consumed power was approximately independent of the applied voltage, giving α equal to 0 and 0.13, respectively.

For constructing the transient unit, the waveforms of consumed load power during step changes in the applied voltage were used. The response was similar to that of RLC circuit. Therefore, the transient unit was represented by a resistor R_{in}, an inductor L_{in} and a capacitor C_{in}. The magnitude of these components were obtained from the numerical solution of the circuit equations until the calculated load current and consumed load power agree with the measured ones. R_{in}, L_{in} and C_{in} were obtained for personal computer and DC/DC converter.

The behavior obtained using the proposed DC load model was in good agreement with the behavior of actual load. Thus, this model can be used effectively in the studies of voltage stability and deliverable power characteristics.

Bibliography

[1] J. Arrillaga and N. R. Watson, *Computer Modelling of Electrical Power Systems*, 2nd ed., John Wiley and Sons, LTD, 2001.

[2] A. Emadi, "Modeling of power electronic loads in AC distribution systems using the generalized state-space averaging method," *IEEE Transactions Industrial Electronics*, vol. 51, no. 5, pp. 992-1000, October 2004.

[3] S. Luo and I. Batarseh, "A review of distributed power systems part I: DC distributed power system," *IEEE Aerospace and Electronic Systems Magazine*, vol. 20, no. 8, part 2, pp. 5-16, August 2005.

[4] J. G. Ciezki and R. W. Ashton, "Selection and stability issues associated with a navy shipboard DC zonal electric distribution system," *IEEE Transactions Power Delivery*, vol. 15, no. 2, pp. 665-669, April 2000.

[5] D. L. Logue, and P. T. Krein, "Preventing instability in DC distribution systems by using power buffering," *IEEE Power Electronics Specialists Conference, PESC 2001*, vol. 1, pp. 33-37, June 2001.

Chapter 3
Estimation Procedure of Limitation of Deliverable Power due to Voltage Instability in DC Distribution System

3.1 Introduction

For the efficient operation of the low-voltage DC distribution system, it is important to understand the deliverable power capability of the system. In the AC system, it is well known that the deliverable power capability is limited by the voltage instability phenomenon as well as the power flow one. Therefore, by analogy to the stability limitation of the AC system, it is expected that DC distribution system also has a limitation based on the voltage instability phenomenon. Voltage instability phenomenon was found to occur especially with constant power loads [1]. This is because, if the voltage across a constant power load increases or decreases, the current through it will decrease or increase, respectively, resulting in a destabilizing effect on the DC distribution system.

In spite of several studies have investigated the use of low-voltage DC distribution systems from the viewpoint of efficiency, control and protection [2–4], less insight has been directed for studying the characteristics of deliverable power capability, except the thermal consideration of a conductor. From this viewpoint, in this chapter, the deliverable power capability is studied on the basis of the voltage instability phenomenon. First, the transfer function between receiving end voltage and source voltage is derived. Then, Hurwitz stability criterion is used to determine the necessary conditions for the stable operation of the system. In these calculations, the developed DC model in Chapter 2 is used in simulating the electrical loads. Based on the stability analysis, the maximum value of deliverable power necessary to satisfy stability conditions is obtained. This power is regarded as upper limitation P_{lim} of

deliverable power. Finally, the effect of load types, as expressed by the voltage sensitivity parameter α, on the voltage instability and the limitation of deliverable power is discussed.

3.2 Analysis of voltage stability phenomenon

In order to analyze the voltage stability in a low-voltage DC distribution system, the DC load model developed in Chapter 2 is used. The DC load model is connected to an ideal DC voltage source through a distribution line with lumped parameters (R, L and C) as shown in Figure 3.1, where the capacitor C represents both the distribution line capacitor and an additional external capacitor.

First, under a steady state condition the voltage source generates a constant DC voltage $V_{\rm s}$ to supply a constant DC voltage V across the receiving end, which is applied across the nonlinear resistor. Let us consider that, under this condition, the non-linear resistor consumes a power P resulting in a current flow I. Second, if a disturbance occurs in the voltage source, the source voltage will slightly change from the constant $V_{\rm s}$ to $V_{\rm s} + \Delta v_{\rm s}$. As a result, the voltage across the receiving end varies from V to $V + \Delta v_{\rm R}$ and the voltage across the non-linear resistor varies from V to $V + \Delta v$. Under this condition of disturbance, the non linear resistor consumes a power $p(t)$ with a current $i(t)$ flow through it, where $i(t)$ equals to $I + \Delta i$. The consumed power $p(t)$ is expressed as:

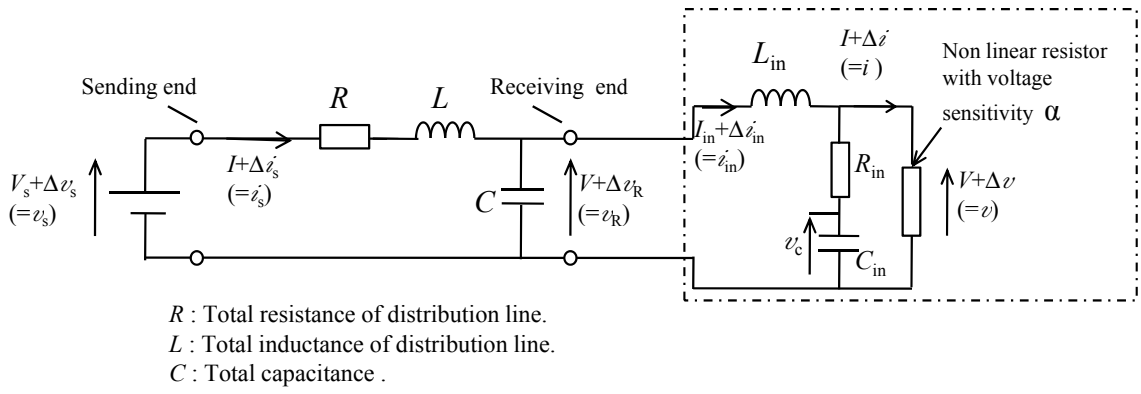

Figure 3.1: *A basic circuit of DC supply with distribution line and DC load.*

$$p(t) = \frac{P}{V^{\alpha}}(V + \Delta v)^{\alpha}. \tag{3.1}$$

Consequently, the current $i(t)$ is given by:

$$i(t) = \frac{P}{V^{\alpha}}(V + \Delta v)^{\alpha-1}. \tag{3.2}$$

For studying the stability, the common approach is to linearize the system around its operating point. Then the stability of the system can be determined using linear system stability analysis methods such as Routh-Hurwitz, root locus, Bode plot or Nyquist criterion. Therefore, Taylor-series expansion is used to linearize the current $i(t)$. In Taylor expansion a function $F(x)$ is expressed as:

$$F(x) = \sum_{j=0}^{n} \frac{1}{j!} \frac{d^j F(x_0)}{dx^j}(x - x_0)^j \tag{3.3}$$

Based on this expansion, $i(t)$ shown in equation (3.2) is linearized around V as a function of Δv as follows:

$$i(t) = \frac{P}{V} + (\alpha - 1)\frac{P}{V^2}\Delta v + (\alpha - 1)(\alpha - 2)\frac{P}{2V^3}\Delta v^2 + ..., \tag{3.4}$$

Starting from 3rd term in this equation, terms are regarded to be very small and can be neglected. Thus, $i(t)$ is approximated as:

$$i(t) = \frac{P}{V} + K\Delta v, \tag{3.5}$$

where

$$K = (\alpha - 1)\frac{P}{V^2}. \tag{3.6}$$

After obtaining the linear expression of $i(t)$, the circuit transient theory can be applied as follows:

$$v_{\mathrm{s}}(t) = i_{\mathrm{s}}(t)R + L\frac{di_{\mathrm{s}}(t)}{dt} + v_{\mathrm{R}}(t), \tag{3.7}$$

$$i_{\mathrm{s}}(t) = C\frac{dv_{\mathrm{R}}(t)}{dt} + i_{\mathrm{in}}(t), \tag{3.8}$$

$$i_{\mathrm{in}}(t) = C_{\mathrm{in}}\frac{dv_{\mathrm{c}}(t)}{dt} + i(t), \tag{3.9}$$

$$v_{\mathrm{R}}(t) = L_{\mathrm{in}}\frac{di_{\mathrm{in}}(t)}{dt} + v(t), \tag{3.10}$$

and

$$v(t) = R_{\mathrm{in}}C_{\mathrm{in}}\frac{dv_{\mathrm{c}}(t)}{dt} + v_{\mathrm{c}}(t). \tag{3.11}$$

Transferring these equation from time-domain to $s-$domain yields:

$$v_{\rm s}(s) = i_{\rm s}(s)(R + Ls) + v_{\rm R}(s), \tag{3.12}$$

$$i_{\rm s}(s) = Csv_{\rm R}(s) + i_{\rm in}(s), \tag{3.13}$$

$$i_{\rm in}(s) = C_{\rm in}sv_{\rm c}(s) + Kv(s), \tag{3.14}$$

$$v_{\rm R}(s) = sL_{\rm in}i_{\rm in}(s) + v(s), \tag{3.15}$$

$$v(s) = v_{\rm c}(s)(1 + sC_{\rm in}R_{\rm in}). \tag{3.16}$$

By solving these equations, the characteristic equation $X(s)$ of the transfer function that relates the receiving voltage $v_{\rm R}$ to the source voltage $v_{\rm s}$ can be obtained with and without considering the terminal capacitance C as follows:

(1) Considering the terminal capacitance C. The function $X(s)$ is represented in the following form:

$$X(s) = a_4s^4 + a_3s^3 + a_2s^2 + a_1s + a_0. \tag{3.17}$$

where

$$a_4 = (KR_{\rm in} + 1)L_{\rm in}LC_{\rm in}C, \tag{3.18}$$

$$a_3 = (KR_{\rm in} + 1)RCL_{\rm in}C_{\rm in} + (KL_{\rm in} + R_{\rm in}C_{\rm in})LC, \tag{3.19}$$

$$a_2 = (KR_{\rm in} + 1)(L + L_{\rm in})C_{\rm in} + LC + (KL_{\rm in} + R_{\rm in}C_{\rm in})RC, \tag{3.20}$$

$$a_1 = (KR_{\rm in} + 1)RC_{\rm in} + (L + L_{\rm in})K + R_{\rm in}C_{\rm in} + RC \tag{3.21}$$

and

$$a_0 = KR + 1. \tag{3.22}$$

(2) Considering the case of $C = 0$, the function of $X(s)$ is expressed as

$$X(s) = b_2s^2 + b_1s + b_0, \tag{3.23}$$

where

$$b_2 = (KR_{\rm in} + 1)(L + L_{\rm in})C_{\rm in}, \tag{3.24}$$

$$b_1 = (KR_{\rm in} + 1)RC_{\rm in} + (L + L_{\rm in})K + R_{\rm in}C_{\rm in} \tag{3.25}$$

and

$$b_0 = KR + 1. \tag{3.26}$$

In order to determine the system stability, which refers to the ability of the system to restore its stable operating condition, the Hurwitz criterion is used. This criterion is one of the methods used for determining the stability of a linear system without solving for the roots of the characteristics equation of the system [5]. According to this criterion, the necessary and sufficient conditions for stability are as follows:

1. All the coefficients of the characteristic equation $X(s)$ are positive.
2. All the Hurwitz determinants: $H_1; H_2, ...H_n$ are positive.

The Hurwitz determinants can be built by using the following scheme of the characteristic equation coefficients a_n:

H_1	a_{n-1}	a_n	0	0	0
H_2	a_{n-3}	a_{n-2}	a_{n-1}	a_n	0
H_3	a_{n-5}	a_{n-4}	a_{n-3}	a_{n-2}	a_{n-1}
H_4	a_{n-7}	a_{n-6}	a_{n-5}	a_{n-4}	a_{n-3}
...	...	...	...	...	...

In the case of considering capacitance C at the load terminals, there are 4-determinants H_1, H_2, H_3 and H_4. That are,

$$H_1 = \quad a_3 \tag{3.27}$$

$$H_2 = \begin{vmatrix} a_3 & a_4 \\ a_1 & a_2 \end{vmatrix} \tag{3.28}$$

$$H_3 = \begin{vmatrix} a_3 & a_4 & 0 \\ a_1 & a_2 & a_3 \\ 0 & a_0 & a_1 \end{vmatrix} \tag{3.29}$$

$$H_4 = \begin{vmatrix} a_3 & a_4 & 0 & 0 \\ a_1 & a_2 & a_3 & a_4 \\ 0 & a_0 & a_1 & a_2 \\ 0 & 0 & 0 & a_0 \end{vmatrix} \tag{3.30}$$

Therefore, the stability conditions for the voltage Δv_{R} in this case are:

$$a_4 > 0,\ a_3 > 0,\ a_2 > 0,\ a_1 > 0,\ a_0 > 0, \tag{3.31}$$

$$H_1 = a_3 > 0, \tag{3.32}$$

$$H_2 = a_3 a_2 - a_4 a_1 > 0, \tag{3.33}$$

$$H_3 = a_1 a_2 a_3 - a_3^2 a_0 - a_4 a_1^2 > 0 \tag{3.34}$$

and

$$H_4 = a_0 H_3 > 0. \tag{3.35}$$

In the case of considering capacitance C =0 the system is 2nd order. Consequently, in Hurwitz criterion the system is stable if and only if all coefficients are positive. Thus, the stability conditions for the voltage Δv_{R} in the case of C =0 are written as

$$b_2 > 0, b_1 > 0 \text{ and } b_0 > 0. \tag{3.36}$$

From these stability conditions it is noticed that, all variables $a_{\mathrm{j}}(j = 4, 3, ..., 0)$, $H_{\mathrm{j}}(j = 4, 3, 2, 1)$ and $b_{\mathrm{j}}(j = 2, 1, 0)$ include the parameter K expressed in equation (3.6). The value of K depends on the consumed power P and the voltage sensitivity parameter α of the load, considering constant operating voltage V in the DC system. Therefore at certain α, the consumed power P has a maximum value for satisfying all of the stability conditions. This maximum value corresponds to the upper limitation P_{lim} of a deliverable power.

Based on the concept of the upper limitation of a deliverable power, if a disturbance occurs when the DC system delivers the power of P_{lim} or below, the voltage v_{R} across the receiving end and the voltage v across the non-linear resistor restore to a constant DC voltage after the disturbance completion. In contrast, let us consider the other situation that the DC system attempts delivering power above P_{lim}. In this case, once a disturbance occurs, the voltages v_{R} and v never restore to a constant DC voltage even after the disturbance completion.

3.3 The upper limitation of the deliverable power

In order to determine the magnitude of P_{lim}, the procedures illustrated in Figure 3.2 are built in a FORTRAN program. These procedures can be explained as follows:

1. The amplitude of P is set to be zero, as the initial magnitude.
2. A small amount ΔP is added to P.
3. From the modified $P + \Delta P$, the amplitudes of all variables b_0, b_1 and b_2 are calculated.
4. The above procedures (2) and (3) are iterated until at least one of the variables shows a magnitude of zero or below. Then, the obtained power P will be P_{lim}.

In the stability conditions, it is found that the upper limitation P_{lim} of the deliverable power depends on a variety of factors. These factors are listed below.

1. Distribution line parameters: line resistance R, inductance L and the terminal capacitance C. These parameters depend on the line cross-section S, line length ζ and inductance per meter l.
2. Load parameters: the magnitude of load components R_{in}, L_{in} and C_{in} as well as voltage sensitivity parameter α. These parameters depend on the load type and the number of connected loads.
3. The magnitude of the operating voltage V of the distribution system. In this study, the operating voltage of 24 V is considered.

The dependence of P_{lim} on distribution line parameters and load parameters will be investigated extensively in the subsequent chapters.

3.4 Discussion

As shown in the stability conditions, the parameter K depends on the consumed power P and the voltage sensitivity parameter α of the load.

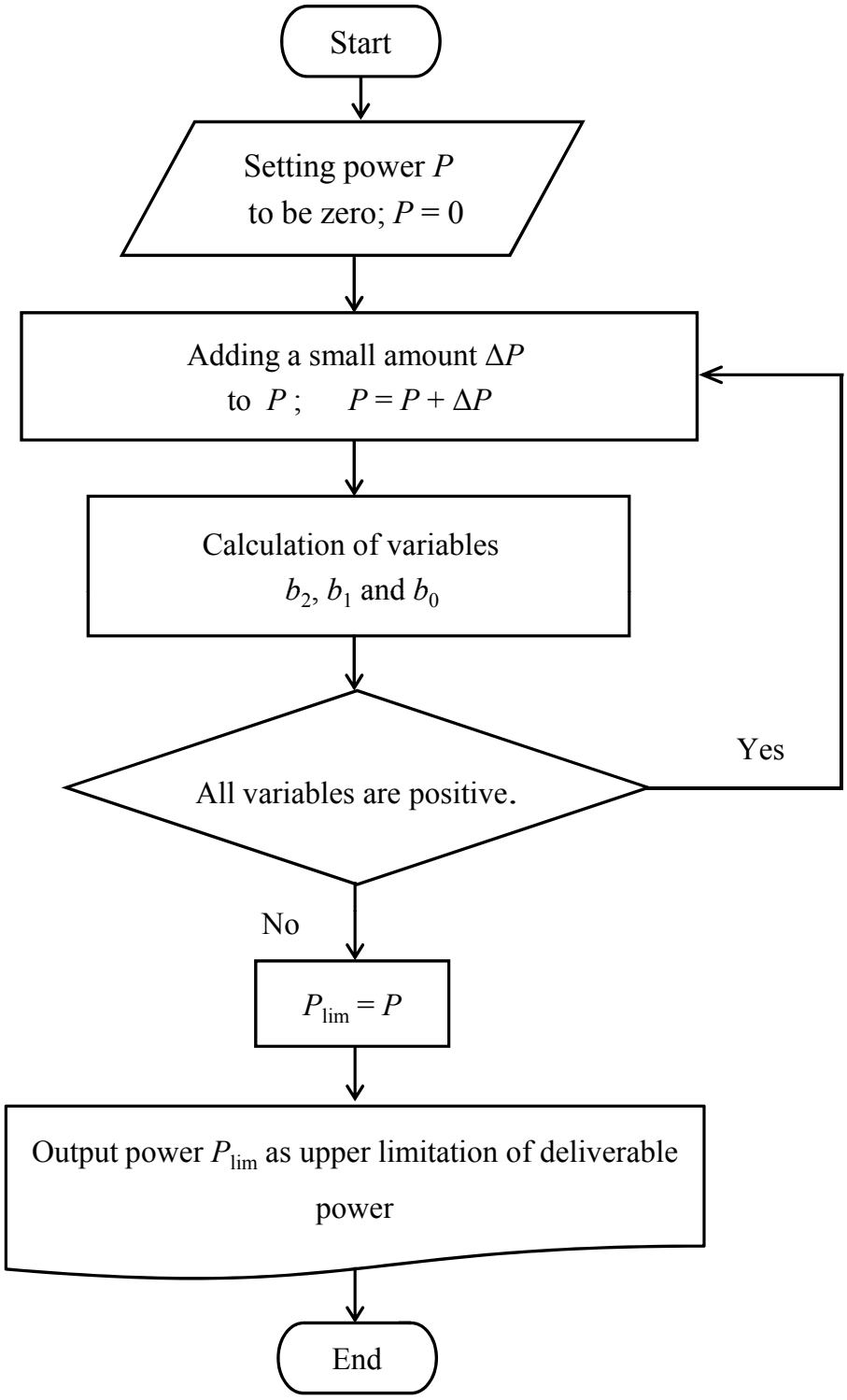

Figure 3.2: *The procedures of calculating the limitation of the delivered power.*

The polarity of parameter K (positive or negative) depends on the load type defined by α. For loads of $\alpha > 1$ such as constant impedance and constant current loads, K is a positive magnitude that increases linearly with the increase in P. Therefore, all the stability conditions b_0, b_1 and b_2 are positive for all values of load consumed power P. Thus, in the situation of using these loads, the system is stable for all values of the consumed power and only the thermal characteristics of the conductors are considered for the limitation of deliverable power.

On the other side, for loads of $\alpha < 1$, such as constant power loads, K is a negative magnitude declining with the increase in P. This reduction in K would cause that one or multiple of the stability conditions b_0, b_1 and b_2 becomes zero or negative resulting in voltage instability. Therefore, the limitation of deliverable power caused by the voltage instability phenomenon is considered as another limitation in addition to the thermal characteristics of the conductors.

As an example, Figure 3.3 shows the value of the coefficient b_1 as a function of the deliverable power P at distribution line resistance $R = 10$ mΩ, inductance $L = 12$ μH and capacitance $C = 0$ μF. In this Figure, increasing in P beyond 98 W causes this coefficient to be negative value. So, the power 98 W corresponds to the upper limitation of the deliverable power P_{lim}.

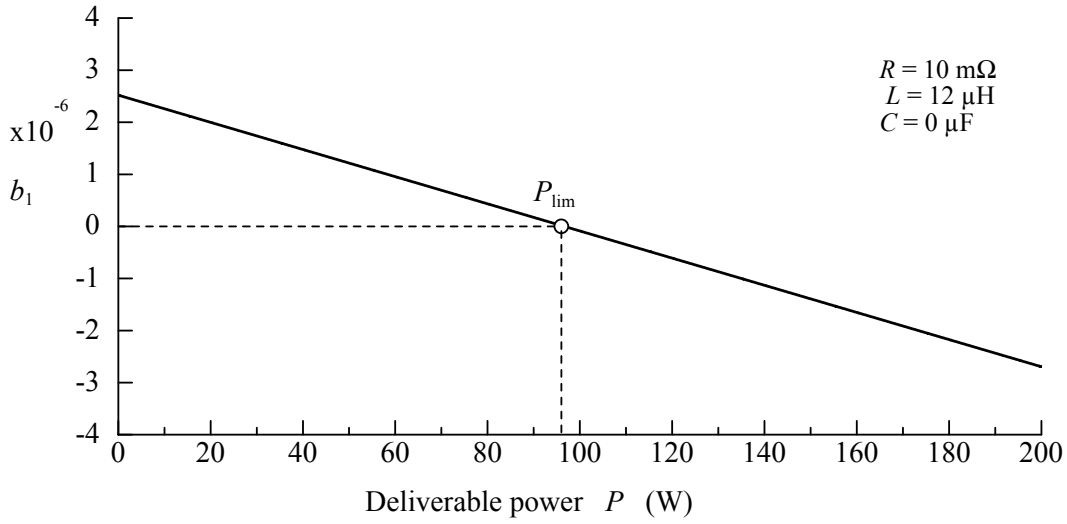

Figure 3.3: *Change of coefficient b_1 with deliverable power.*

It is important here to point out that, when any load is connected to the DC distribution system through power converter, the combination will behave as constant power loads and will have $\alpha < 1$. Accordingly, it is essential to study the limitation of deliverable power in DC distribution system containing such loads.

The essential factor causing the voltage instability is an inductance component. Let us depicts a simplified DC distribution system as shown in Figure 3.4. The circuit shown in this figure is indented to be simplified to offer essential explanation of the voltage-instability phenomenon. The distribution line consists of only inductor and load consists of only non-linear resistor of α <1.

Let us consider α to be zero, as a representative of of the load of α <1. For the load of α =0, the dependence of a current i on a voltage v_{R} across the receiving ends is expressed in the following form: $i = P/v_{\mathrm{R}}$, where P is a power consumed by the load. Fat curve in Figure 3.5 shows $i$as a function of v_{R}. As confirmed in this figure, reduction in voltage v_{R} raises the current i.

1. Steady state: Firstly, let us consider a steady state; the voltage source generates a completely constant DC voltage V to supply the DC voltage V across the receiving ends. Since a current of I (= P/V) flows through the distribution line, the system operate at a point 'A' shown in Figure 3.4.

2. Occurrence of disturbance: Secondly, let us suppose that, the source voltage slightly increases from V to $V + \Delta V_{\mathrm{s}}$ at a time t of 0 and then maintains at $V + \Delta V_{\mathrm{s}}$ during $t > 0$, where ΔV_{s} >0. Owing to this disturbance, the following phenomenon occurs:

   (a) t =0; the law of the constant flux linkage enables us to find out that the current i remains to be I. The receiving-ends voltage v_{R} thus remains to be V. Since the source voltage v_{s} (= $V + \Delta V_{\mathrm{s}}$) is higher than v_{R} (= V), a voltage v_{L} (= $v_{\mathrm{s}} - v_{\mathrm{R}}$) across the inductor is positive.

   (b) t >0; since v_{L} >0, the current i increases. This increase in i reduces v_{R}, because the load has the characteristic expressed by $v_{\mathrm{R}} = P/i$. This reduction in v_{R} leads to further augment in v_{L} (= $V + \Delta V_{\mathrm{s}} - v_{\mathrm{R}}$).

(c) Above process b) continues with a passage of time. The voltage v_{R} therefore maintains to decrease with a passage of time.

(d) In summary, v_{R} never converges to a steady DC voltage, once the disturbance occurs.

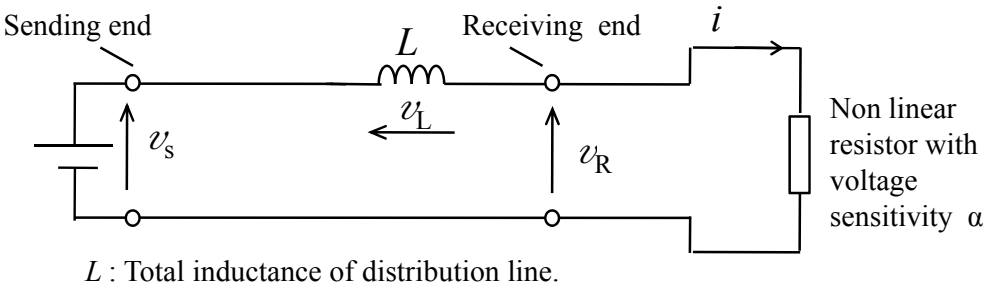

Figure 3.4: *Simplified DC distribution system.*

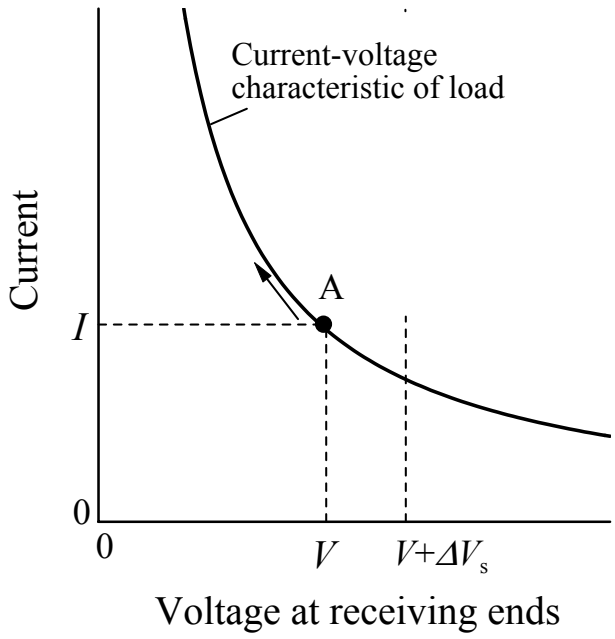

Figure 3.5: *Current-voltage characteristic for constant power load.*

3.5 Conclusion

In this chapter, the deliverable power in low-voltage DC distribution system proved to have an upper limitation P_{lim}, owing to the voltage instability phenomenon. This limitation is defined only for the electrical loads with the voltage sensitivity parameter less than 1. It was found that, the essential factor causing the voltage instability is an inductance component. Hurwitz criterion was used in determining the stability conditions. The loads were simulated by the DC model presented in chapter 2. The theoretical calculation showed that the upper limitation of deliverable power depends on distribution line parameters, load parameters and the operating voltage.

Bibliography

[1] A. Emadi, A. Khaligh, C. H. Rivetta, and G. A. Williamson, "Constant Power Loads and Negative Impedance Instability in Automotive Systems: Definition, Modeling, Stability, and Control of Power Electronic Converters and Motor Drives", *IEEE Transactions on Vehicular Technology*, vol. 55, no. 4, pp. 1112-1125, 2006.

[2] D. Nilsson and A. Sannino, "Efficiency Analysis of Low- and Medium- Voltage DC Distribution Systems", *IEEE Power Engineering Society General Meeting*, pp. 2315-2321, 2004.

[3] H. Kakigano, Y. Miura, T. Ise and R. Uchida, "DC Voltage Control of the DC Micro-grid for Super High Quality Distribution, *Power Conversion Conference*, pp. 518-525, 2007.

[4] D. Salomonsson, L. Soder and A. Sannino, "Protection of Low-Voltage DC Microgrids, *IEEE Transactions on Power Delivery*, Vol. 24, No. 3, pp. 1045-1053, 2009.

[5] W. S. Levine, *The Control Handbook*, Vol. 1, CRC Press, 1996.

Chapter 4
Influence of Distribution Line Parameters on Deliverable Power in DC Distribution System

4.1 Introduction

Distribution line parameters are considered as important factors affecting the voltage instability phenomenon of DC distribution system. Consequently, these parameters should be discussed in determining the upper limitation P_{lim} of the deliverable power. The distribution line parameters include distribution line cross-section, line length and inductance per meter. The distribution line capacitance C is set to 0 μF, because the capacitance of the low-voltage cable is regarded to be very small [1].

From this viewpoint, the first objective of this chapter is to clarify the dependence of P_{lim} on the aforementioned parameters. The theoretical calculations were performed using FORTRAN program. The second objective is to improve deliverable power characteristics by adding capacitor at the receiving end. The minimum capacitance required to deliver the load power is obtained. Finally, experimental measurements are carried out in order to confirm the validity of the theoretically calculated limitation of the deliverable power. A loaded DC/DC converter is used as a representative of the electrical loads with $\alpha < 1$, which causes voltage instability phenomenon as discussed in chapter 3.

4.2 Influence of distribution line cross-section on P_{lim}

Figure 4.1 shows the basic circuit of a DC distribution system connected to the model of the loaded DC/DC converter.

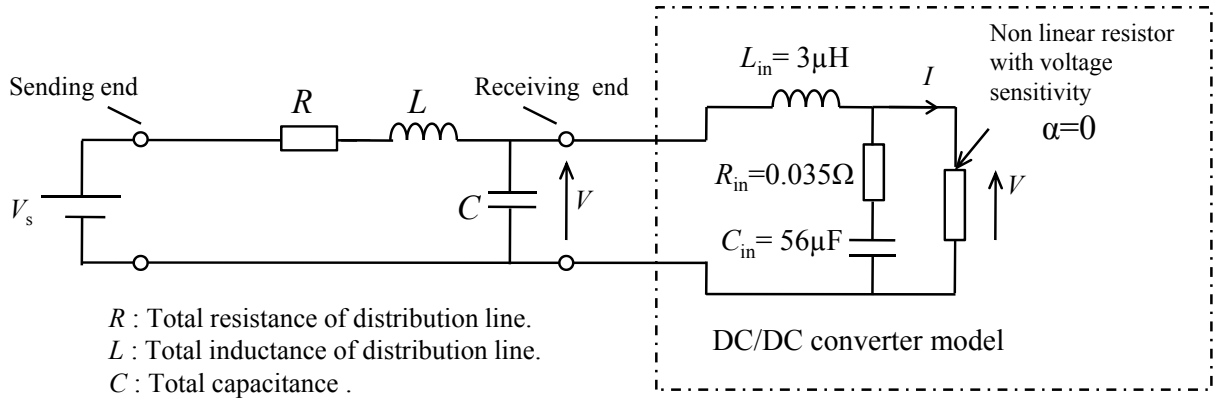

Figure 4.1: *A basic circuit of DC distribution system with loaded DC/DC converter model.*

For a fixed distribution line length ζ, the line resistance R is the main parameter, that is related to the cross-section S by the following equation:

$$R = \frac{\rho\zeta}{S}. \tag{4.1}$$

where ρ is the resistivity of the copper conductor, which equal to 24 nΩm. Therefore, in this section the power P_{lim} is evaluated as a function of distribution line resistance R. The distribution line was considered to have the total length ζ of 40 m. The inductance per meter l was selected 0.3 μH/m as a typical value in low-voltage cables. This corresponds to a total inductance L of 12 μH for the distribution line. The total resistance R was set to be in the range from 5 to 30 mΩ, which corresponds to a cross-section S from 192 mm^2 to 32 mm^2. The parameters α, R_{in}, L_{in} and C_{in} of the loaded DC/DC converter presented in chapter 2 were used, namely α = 0, R_{in} = 0.035 Ω, L_{in} = 3.0 μH and C_{in} = 56 μF. This converter operates around 24 V. In accordance with this operating voltage, the calculation described in this section adopts 24 V as the voltage V at the receiving end.

Figure 4.2 depicts the magnitude of the maximum deliverable power P_{lim} by a bold curve as a function of distribution line resistance. All points on and below this curve satisfy the stability conditions clarified in chapter 3. Therefore, if the load power located on or under this curve, the DC voltage across the load would be restored to the steady state after occurrence of a disturbance. However, if the power required by the load locates beyond this curve, the load voltage never restores after a disturbance to a constant DC voltage.

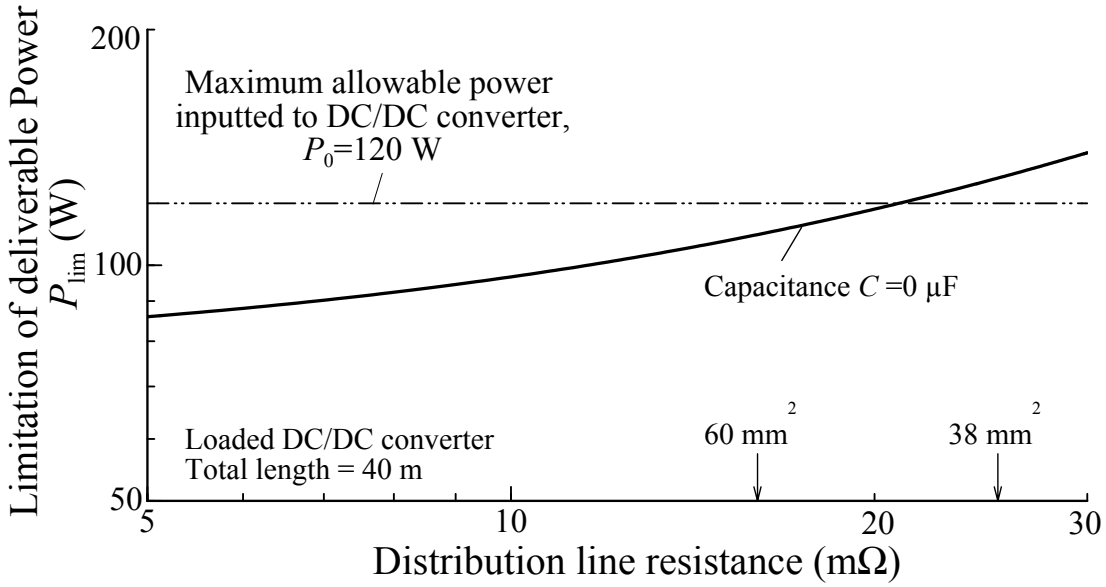

Figure 4.2: *Upper limitation of deliverable power as a function of distribution line resistance for a loaded DC/DC converter.*

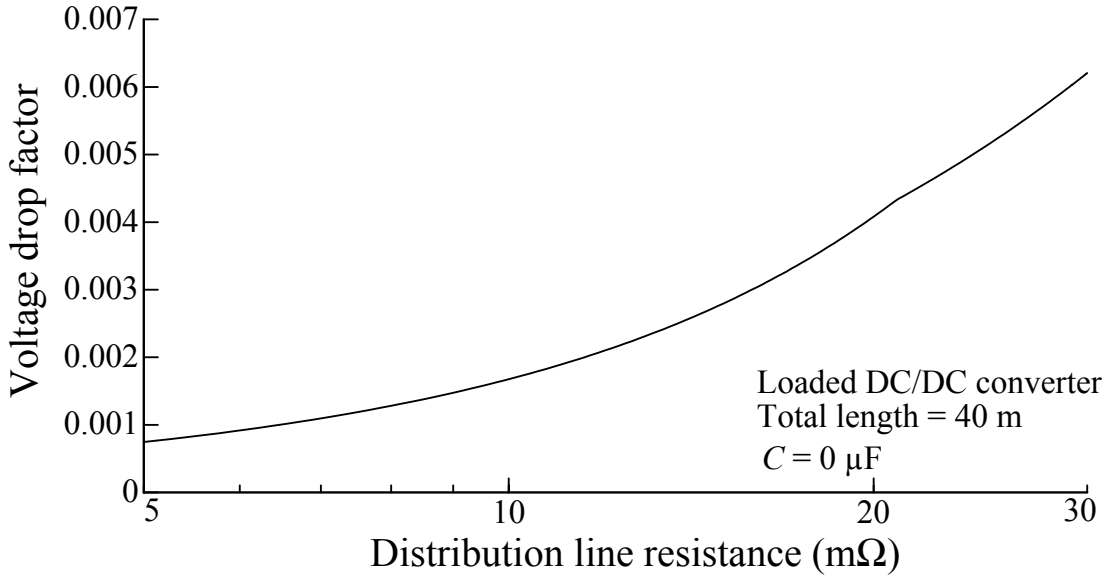

Figure 4.3: *The voltage drop factor as a function of distribution line resistance for a loaded DC/DC converter.*

As shown from Figure 4.2, the upper limitation of the deliverable power $P_{\lim}$ declines with reduction in R and increase in S. Higher deliverable power can be obtained with distribution lines of larger resistance. So, from the viewpoint of deliverable power characteristics, larger distribution line resistance will be preferred. However, with larger line resistance R, the voltage drop factor ϵ between the sending and receiving voltages will be higher as presented in Figure 4.3. The voltage drop factor ϵ is calculated from the following equation:

$$\epsilon = \frac{V_s - V}{V_s}. \tag{4.2}$$

According to the operating manual of the DC/DC converter adopted in this calculation, this converter has a capacity for receiving power P_0 up to 120 W at the inputted terminals as shown by a chain double-dashed line in Figure 4.2. It is noted that, $P_{\lim}$ is less than P_0 for $R < 20$ mΩ. This obtained fact indicates that the voltage instability phenomenon would limit delivering P_0 to the load terminals for certain values of line resistance R. In addition, in the situation of power delivery to several loads or larger load capacity, the DC system adopts distribution lines of wider S i. e. lower R. As a result, this situation seems to give the DC system more pronounced difficulty in delivering the required power. This situation will be discussed in details in chapter 5

The higher deliverable power characteristic with larger distribution line resistance can be explained by the damping property provided by the resistance. When a disturbance occurs, the larger resistance will damp the oscillations following the disturbance, and the system time response will be reduced. However, a compromise between higher deliverable power and larger voltage drop factor have to be arranged when using distribution lines with larger resistance.

4.3 Influence of distribution line inductance per meter on $P_{\lim}$

In this section, $P_{\lim}$ is evaluated as a function of distribution line inductance per meter l. This is because l somewhat varies, depending on the structure of the distribution line. Similar to the

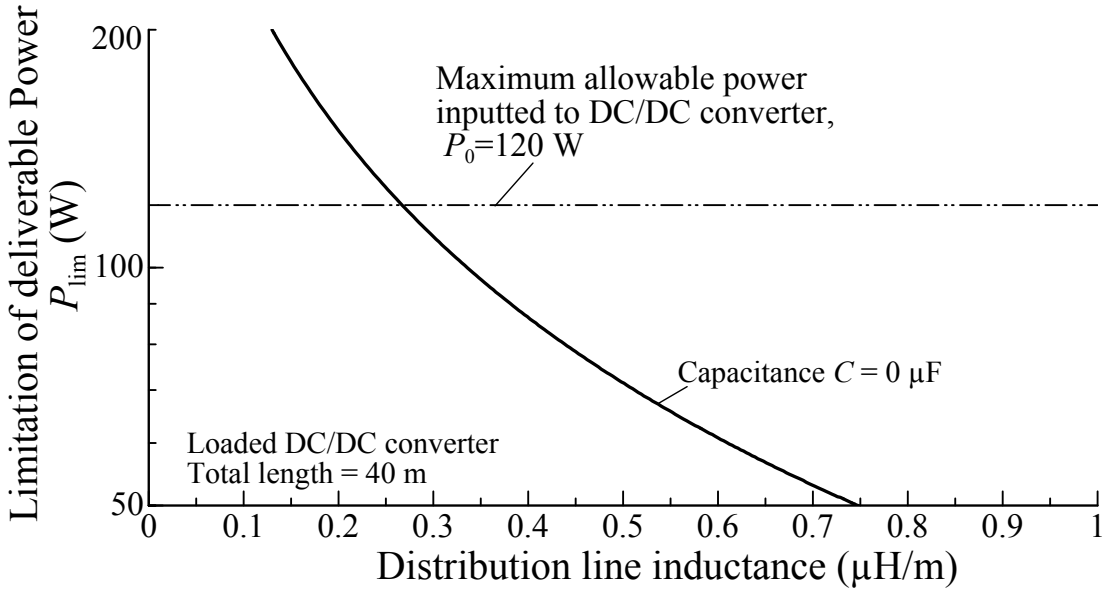

Figure 4.4: *Upper limitation of deliverable as a function of distribution line inductance per meter for a loaded DC/DC converter.*

previous section, the distribution line length ζ was fixed at 40 m. The total resistance R is set to 16 mΩ, which corresponds to a distribution line cross-section of 60 mm^2. The distribution line inductance per meter varies in the range from 0 to 1 μH/m. In this calculation, the parameters of the loaded DC/DC converter were used.

Figure 4.4 presents the obtained $P_{\rm lim}$ as a function of distribution line inductance per meter. It is evident that the increase of the line inductance per meter results in the reduction of $P_{\rm lim}$, exhibiting different tendency from the distribution line resistance. For instance, as l increased from 0.3 to 0.6 μH/m, $P_{\rm lim}$ decreased drastically from 109 to 60 W. This results agree with the explanation of voltage instability due to inductance presented in chapter 3. Based on this explanation, higher inductance L causes the voltage instability at lower $P_{\rm lim}$.

4.4 Influence of distribution line length on $P_{\rm lim}$

The present section is aimed at describing dependence of $P_{\rm lim}$ on the total length ζ of the distribution line. In this calculation, the resistance r of the distribution line per unit length were fixed to be 0.4 mΩ/m, being equal to that of a low-voltage cable with a conductor

cross-section of 60 mm^2. The inductance per meter l of the distribution line was set to be 0.3 μH/m, as a typical value for low-voltage cables. On the basis of these r and l, the total resistance R and the total inductance L represented in Figure 4.1 were set to be proportion to the whole length ζ of the distribution line; $R = r\zeta$ and $L = l\zeta$. Determination of P_{lim} was performed over a wide range of line length, from 1 m to 100 m.

The dependence of P_{lim} on the distribution line length is represented by a bold curve in Figure 4.5. Increasing distribution line length causes a reduction in the upper limitation of the deliverable power. For example, P_{lim} declines from 154 to 110 W, as the distribution line length increases from 20 to 40 m. In addition, P_{lim} is found to be less than the maximum allowable power inputted to DC/DC converter, $P_0 = 120$ W, at lengths above 33 m. That is to say, the DC system suffers from delivering the power beyond the length of 33 m. The reduction of P_{lim} with increasing line length can be explained by the combined effects of total resistance R and total inductance L.

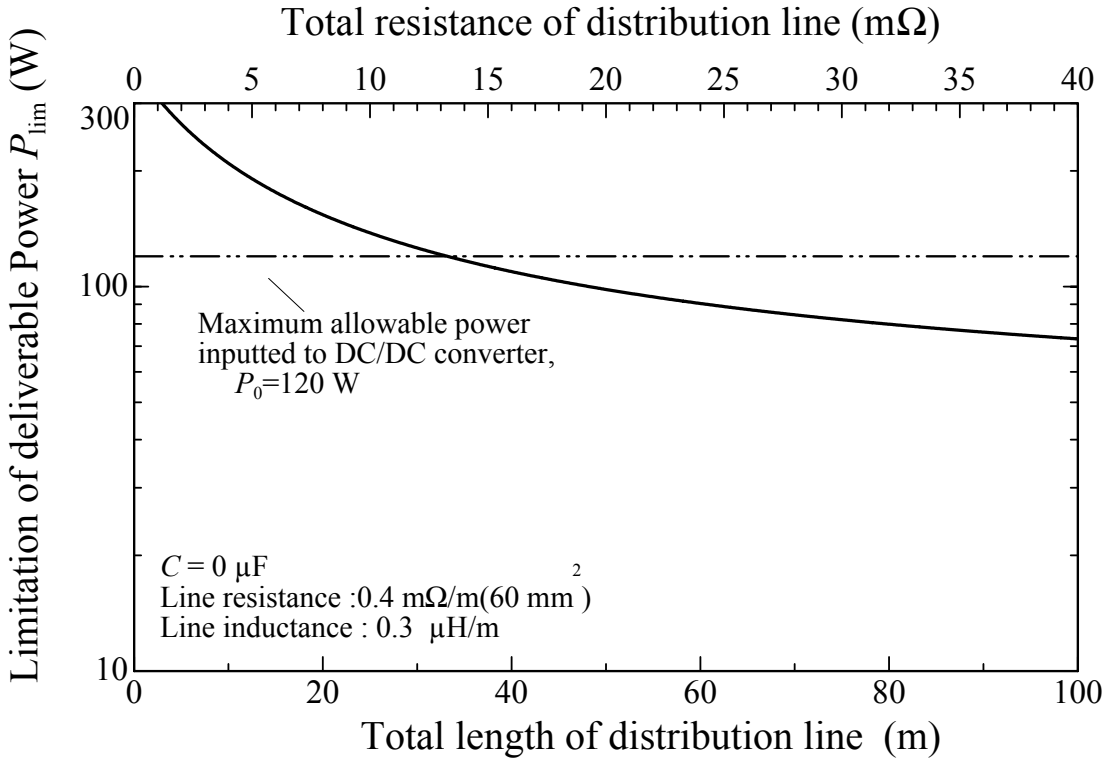

Figure 4.5: *Upper limitation of deliverable power as a function of distribution line-length for a loaded DC/DC converter.*

Increasing the line length must lead to an increase in both R and L with the same rate. But, based on the results obtained in Figure 4.2 and Figure 4.4, the destabilizing effect produced by increasing the inductance appears more dominant than the stabilizing effect produced by increasing the resistance. For example, when ζ increases from 20 to 40 m, line resistance R increases from 8 to 16 mΩ. At these resistances, P_{lim} increases from 92 to 110 W as shown in Figure 4.2. On the other hand, for the same range of ζ, line inductance L increases from 6 to 12 μH. As a result, P_{lim} declines from 182 to 110 W as shown in Figure 4.4. By combining both effects, a reduction in P_{lim} occurs with increasing line length as presented in Figure 4.5.

4.5 Improving deliverable power characteristics using capacitor

Based on the dominant effect of the line inductance in reducing the upper limitation of the deliverable power, it is expected that adding capacitor at the receiving end would help in delivering higher power in low voltage DC distribution system. Therefore, in this section a capacitor is added at the receiving end and the magnitude of P_{lim} is evaluated as a function of ζ for different values of capacitance C as shown in Figure 4.6.

Similar to the previous section, the line cross-section and inductance per meter were set at 60 mm^2 and 0.3 μH/m, respectively. The considered capacitances values are 0, 50 and 100 μF. It is found that connecting a capacitor with C of 50 μF raises P_{lim} in the length range from 35 to 100 m. Connecting a capacitor with C of 100 μF causes further increase in P_{lim} in the length range from 20 to 100 m.

These results reveal that connecting the capacitor of the higher capacitance gives more rising effect to P_{lim}, especially for the longer length. This is because the capacitance compensates the effect of line inductance. With respect to the maximum input power P_0 of the DC/DC converter, estimated results indicate that connection of an appropriate C achieves for P_{lim} to be increased above P_0 of the converter even for the cases that P_{lim} is lower than P_0 without additional capacitor.

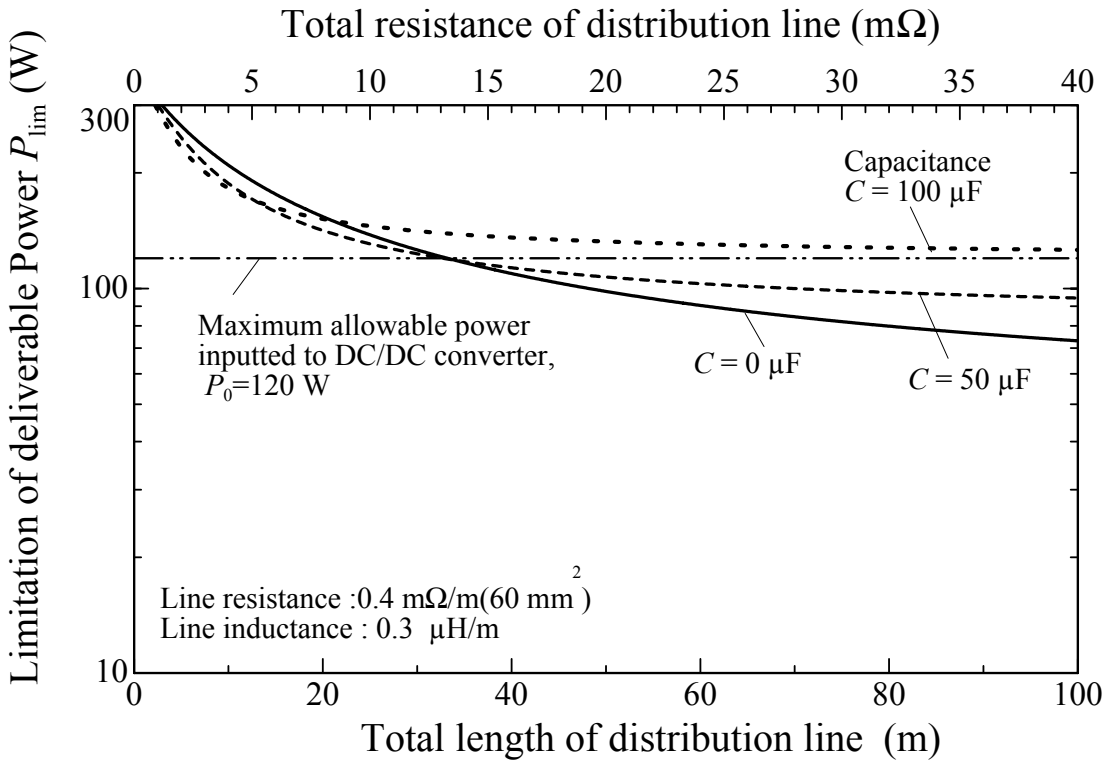

Figure 4.6: *Upper limitation of deliverable power for loaded DC/DC converter with capacitance.*

Thus, it is important to calculate the minimum capacitance required to increase $P_{\lim}$ to P_0. In order to obtain such minimum capacitance under different conditions, the following numerical calculation method is used:

1. The power P in the eq. (3.6) is fixed to be P_0 of the load.
2. For C =0, variables $b_j(j = 2, 1, 0)$ expressed in equations (3.26)−(3.28) are calculated. If all variables b_j show positive amounts, no terminal capacitance is required. If not, the procedures (3)−(5) are performed.
3. A small amount ΔC is added to C.
4. From the modified $C + \Delta C$, the magnitudes of all variables of $a_j(j = 4, 3, 2, 1, 0)$ and $H_j(j = 4, 3, 2, 1)$ are evaluated in accordance with equations (3.15)−(3.19) and equations (3.20)-(3.24).

5. The procedures (3) and (4) are iterated until all variables give positive values.

6. The capacitance $C + \Delta C$ obtained in (5) is the minimum capacitance required to increase P_{lim} to P_0.

Figure 4.7 shows the calculated minimum capacitance as a function of the distribution line length ζ for different values of inductance per meter l. The considered values of l are 0.3, 0.6 and 0.9 μH/m. It is found that, for l of 0.3 μH/m, the minimum capacitance is 52 μF at the length of 33 m. For the same l, this capacitance somewhat increases to 91 μF with the length of 100 m. The minimum capacitance for l of 0.6 and 0.9 μH/m also shows small increase with increasing the length ζ. In Figure 4.7, it is also found that the minimum capacitance extremely increases with increasing the inductance per meter l. For example, the use of distribution line with 0.6 and 0.9 μH/m requires the capacitance of 240 and 400 μF at 33 m. These capacitances are about 5 and 8 times, respectively, as high as that for line with 0.3 μH/m.

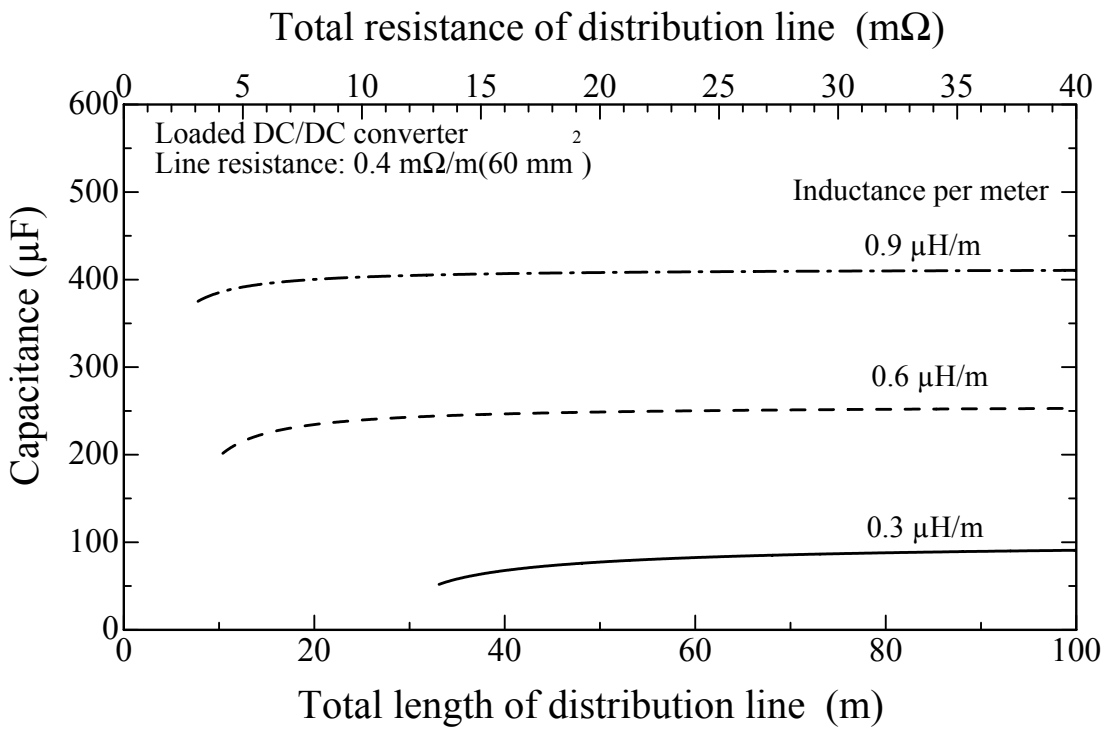

Figure 4.7: *Minimum capacitance for delivering the maximum power consumption of load.*

4.6 Experimental verification

In order to verify the theoretical calculation of the upper limitation of deliverable power, an experimental setup simulating a DC distribution system was built. The experimental measurements were carried out for different distribution line lengths with and without a capacitor at the load terminals. In addition, the measurement of P_{lim} for different line inductances per meter was considered.

4.6.1 Experimental setup

Experimental circuit is illustrated in Figure 4.8 where the different components of a DC distribution system are represented and the corresponding laboratory setup is shown in Figure 4.9. The system consists of a coil and two conductors, which are used to simulate the distribution line inductance and resistance. The system is powered by a stabilized DC voltage source with voltage rating 35 V and current rating 5 A. The voltage applied by the DC voltage source has a ripple of only 0.5 mV. At the load terminals, a step down DC/DC converter is connected. The DC/DC converter is designed for input voltage up to 24 V, output voltage up to 15 V. The switching frequency of the converter is 90 kHz. At the output of the converter, a variable resistive load is used. The voltage waveform across the load terminals (input terminals of the DC/DC converter) is measured by a digital oscilloscope. A capacitor is also connected at the load terminals in order to investigate the improvement of deliverable power characteristics.

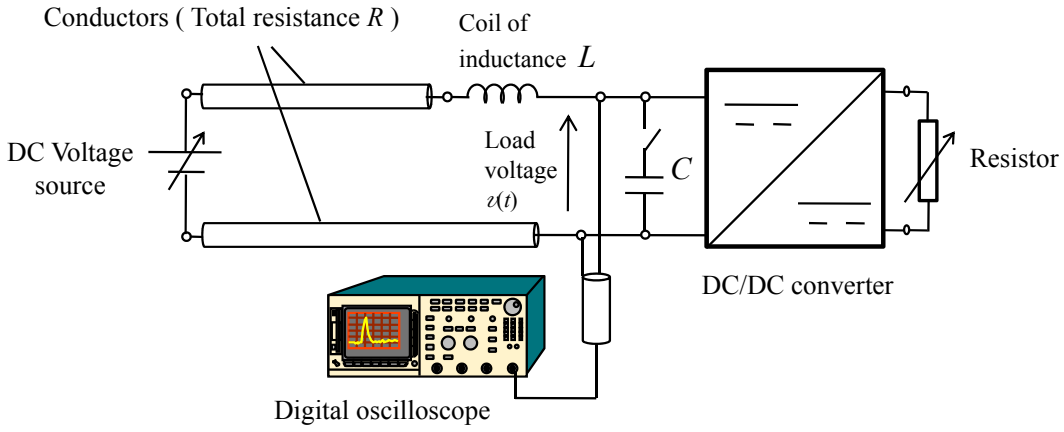

Figure 4.8: *Miniature DC circuit used in measurements.*

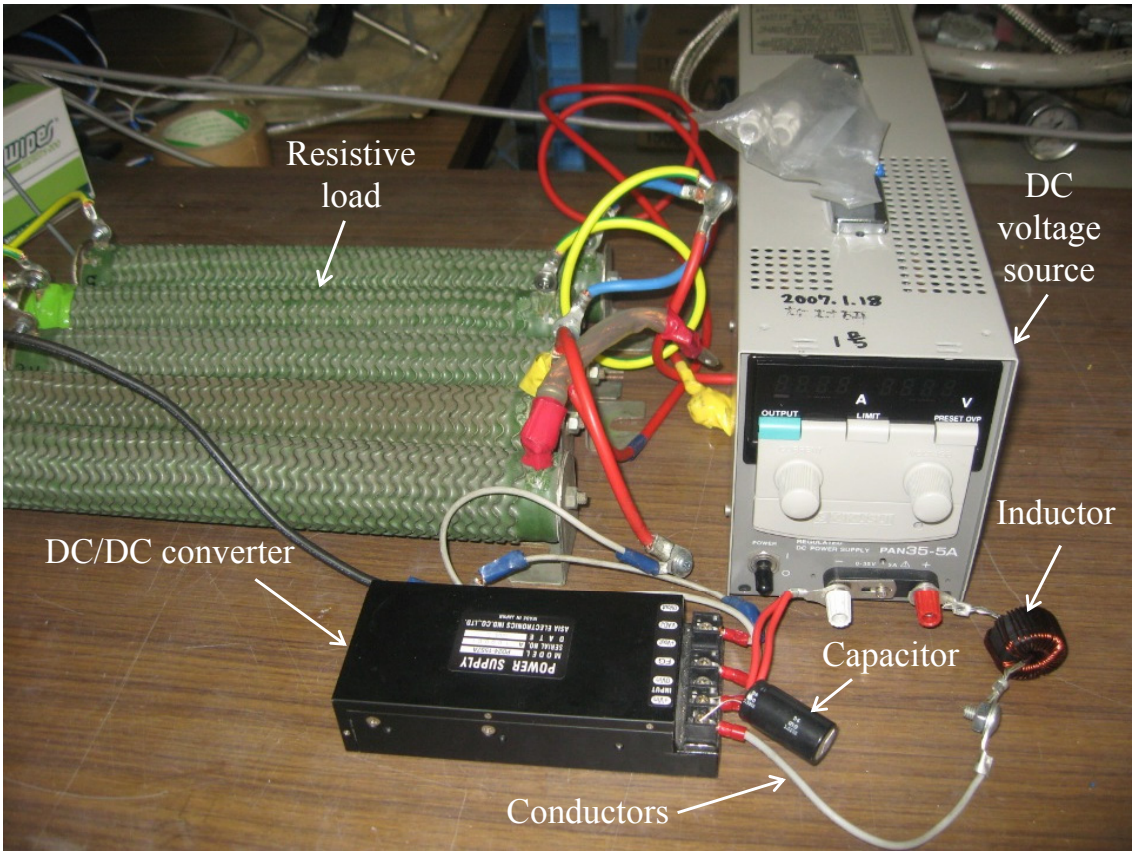

Figure 4.9: *Laboratory setup used in measurements.*

4.6.2 Measurement method

The two conductors and the coil had a total resistance R and a total inductance L. The experimental system has been tested for different combinations of conductors and coils corresponding to different R and L. With respect to the load, the variable resistor was set to 9.6, 4.8, 3.2 and 2.4 Ω giving power consumption of 23, 47, 70 and 94 W at the output terminals of the DC/DC converter. Therefore, the power consumption at the input terminals of the DC/DC converter were 26, 52, 78 and 108 W, taking into consideration the converter efficiency. The ripple of the DC voltage source was considered as the disturbance applied to the system. Then, the voltage waveform across the load terminals $v(t)$ was observed and used as an indicator for the stable operation of the system. If this voltage waveform was free of oscillation, the system would be stable and would deliver the load power. If there was any oscillation in the voltage waveform, the system would be unstable.

4.6.3 Experimental results

In the experimental measurements, the previous theoretical calculations of deliverable power dependence on length, capacitance and line inductance per meter are verified.

1. (The measurements concerning the dependence of the deliverable power on distribution line length are carried out). In this case, distribution line length of 30 m and 57 m are considered. In both lengths, the distribution line has an inductance l of 0.9 μH/m and a resistance r of 0.4 mΩ/m. These measurements were carried out under the condition of terminal capacitance C= 0 μF.

   Figure 4.10 shows the waveforms of the load voltage $v(t)$ for load power 26, 52, 78 and 108 W at distribution line length of 30 m. The total resistance R of the circuit include the coil resistance R_{coil} and the conductor resistance R_{c}. In this experiment, R_{coil} is 5 mΩ. For this distribution line length, R and inductance L were set to 12 mΩ and 27 μH, respectively. In Figure 4.10 (a) and (b) the voltage waveform for the load power of 26 and 52 W are observed to remain at the constant of 24 V, namely at the original DC voltage. These results reveal that the DC circuit delivers the powers of 26 and 52 W in the original DC form, performing stable operation. With increasing the power

consumption to 78 W in Figure 4.10 (c), the load voltage deviates from the constant DC voltage (24 V), giving pronounced oscillation in the waveform. This case corresponds to the unstable operation of the DC system.

From Figure 4.10, it is also noted that, lager power consumption increases the amplitude of voltage oscillation, as shown in Figure 4.10 (d) for the power consumption of 108 W. The amplitude of voltage oscillation in the case of 78 W was 0.5 V. However, this amplitude increased to 1.5 V in the case of 108 W.

Figure 4.11 presents the waveforms of the load voltage $v(t)$ in the case of distribution line length of 57 m. For this distribution line length, R and L were set to 23 mΩ and 51 μH, respectively. For this length, only in the case of power consumption 26 W, the DC state of the load voltage was kept as shown in Figure 4.11 (a). For other load powers, 52, 78 and 108 W, the voltage oscillation occurred indicating unstable operation as shown in Figure 4.11 (b), Figure 4.11 (c) and Figure 4.11 (d). Similar to Figure 4.10 the amplitude of voltage oscillation increases with larger power consumption, as noticed from the obtained waveforms. This amplitude of voltage oscillation reached 2.5 V in the case of 108 W. These results indicate that the increase of distribution line length is accompanied by lowering of power consumption that could be delivered stably.

Figure 4.12 summarizes the obtained experimental results. In this figure, circles denote to no oscillation case, while crosses denote to the occurrence of oscillation. Also, in this figure, the theoretical result of P_{lim} is shown, as calculated for the line resistance r of 0.4 mΩ/m and the line inductance l of 0.9 μH/m.

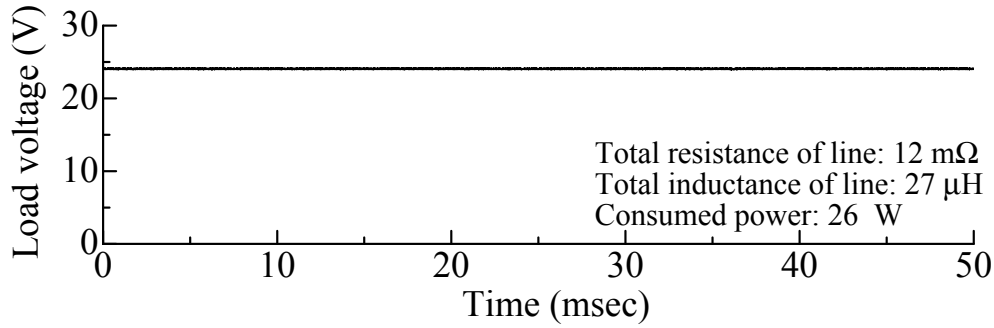

(a) Load voltage for consumed power of 26 W.

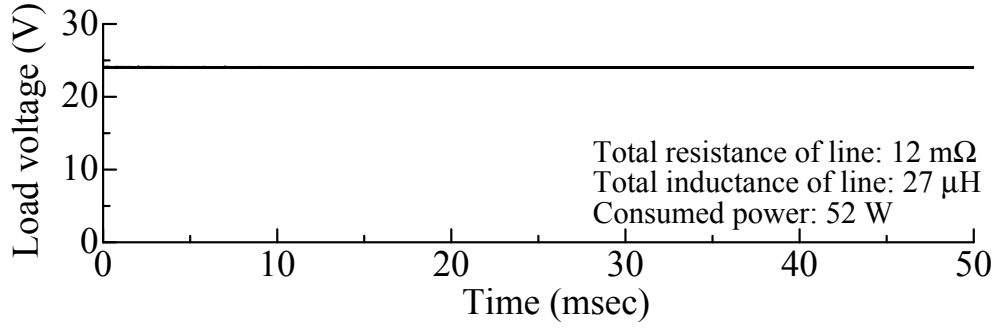

(b) Load voltage for consumed power of 52 W.

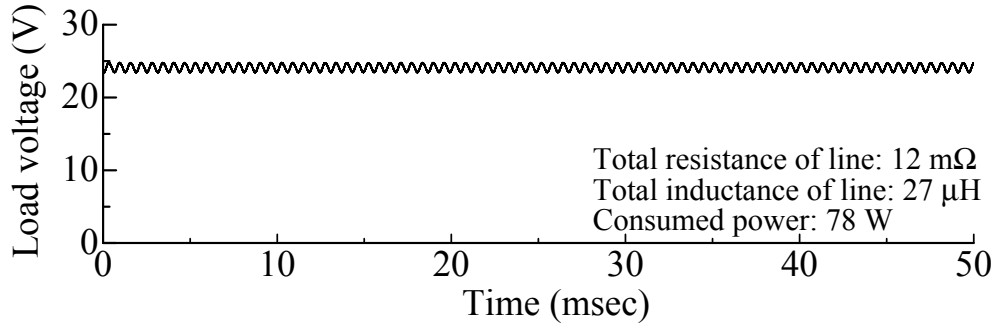

(c) Load voltage for consumed power of 78 W.

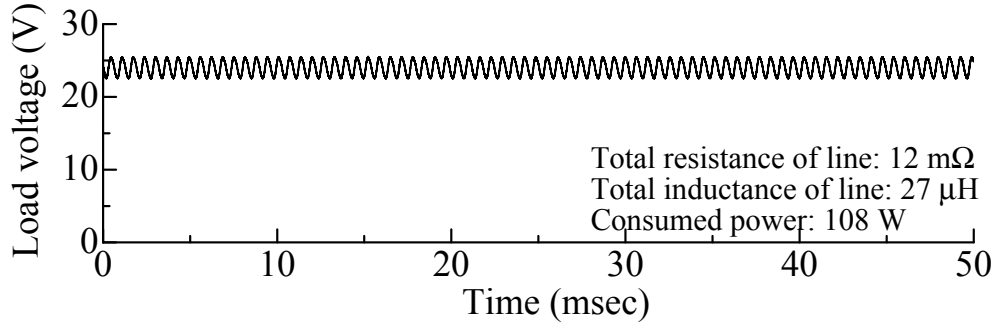

(d) Load voltage for consumed power of 108 W.

Figure 4.10: *The load voltage waveforms of different consumed-power at distribution line length of 30 m.*

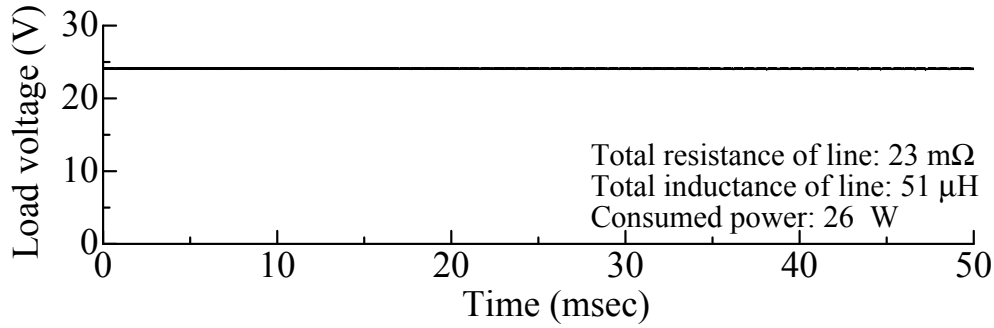

(a) Load voltage for consumed power of 26 W.

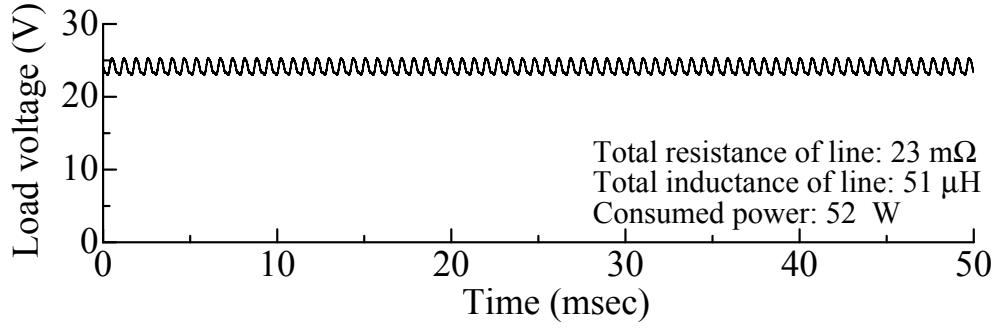

(b) Load voltage for consumed power of 52 W.

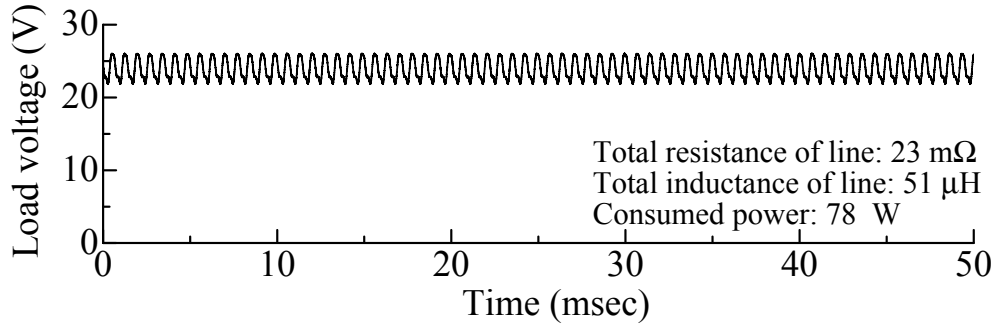

(c) Load voltage for consumed power of 78 W.

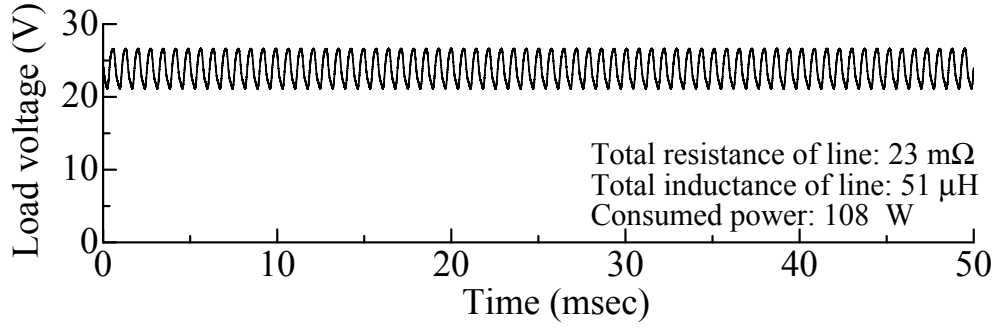

(d) Load voltage for consumed power of 108 W.

Figure 4.11: *The load voltage waveforms of different consumed-power at distribution line length of 57 m.*

The operating points located below the limitation line should be circles, representing a stable operation of the system. However, the operating points located beyond the limitation line should be crosses, indicating an unstable operation of the system. It is evident that the obtained experimental results highly agree with the calculated P_{lim}. This agreement supports the validity of the proposed concept regarding the limitation of the deliverable power to electrical loads due to voltage instability phenomenon. Moreover, this agreement confirms that the deliverable power decreases with longer distribution line length as obtained from the theoretical calculation. Finally, these experimental results support the validity of the load model of the DC/DC converter explained in chapter 2, where the experiments were performed on the actual DC/DC converter.

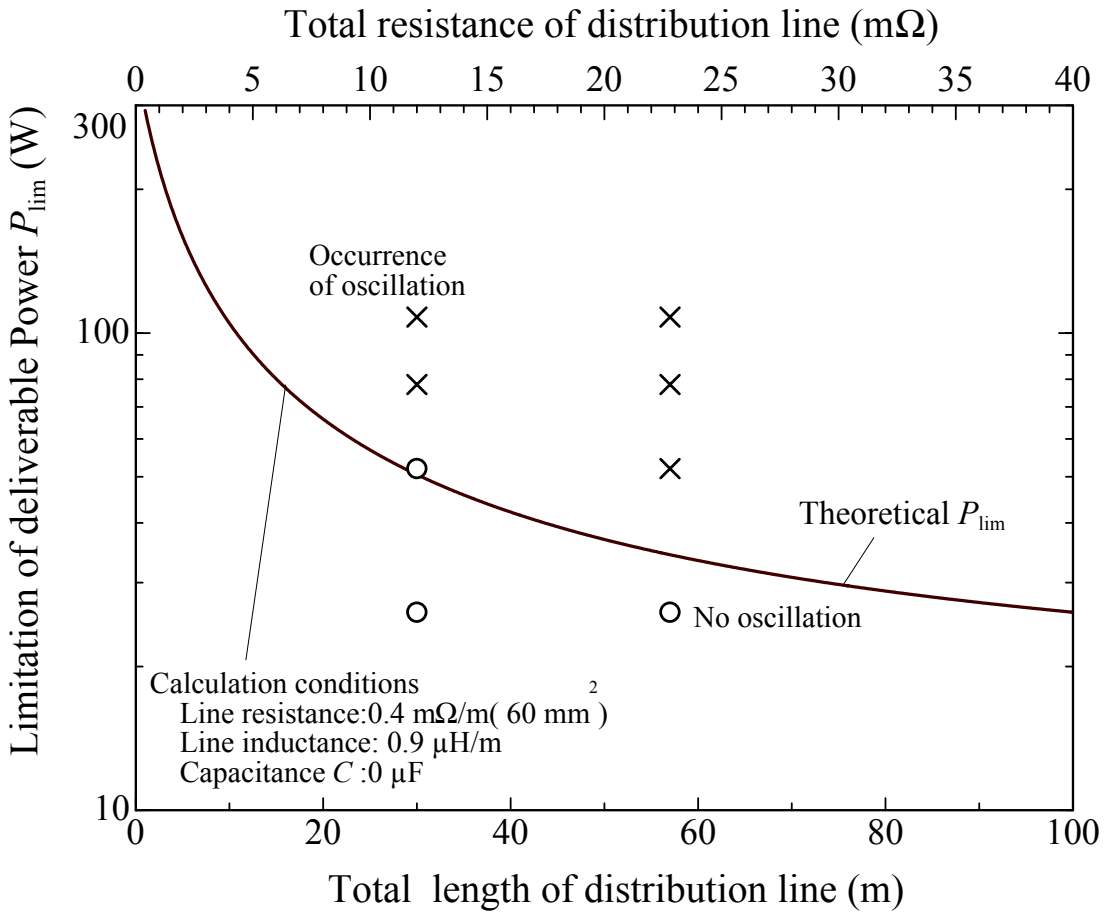

Figure 4.12: *Verification points of P_{lim} for C=0 μF.*

2. (The experimental measurements concerning the dependence of $P_{\lim}$ on the distribution line inductance per meter). In these measurements, two values of line inductance per meter l were considered, 1.3 μH/m and 1.5 μH/m. In both cases, the distribution line has a resistance r of 0.4 mΩ/m. The experiments were carried out for the case of terminal capacitance C= 0 μF. Load powers of 26, 52, 78 and 108 W were used. The experimental measurements were compared with the calculated $P_{\lim}$ for the same conditions. Figure 4.13 shows the obtained experimental results, described by circles and crosses for stable and unstable operating points, respectively. In Figure 4.13 (a), the experimental measurements are obtained considering line inductance per meter l=1.3 μH/m. In this case, the circuit inductance L was set to 26 μH, corresponding to a distribution line length of 20 m. For 20 m line length and r of 0.4 mΩ/m, a resistance R of 8 mΩ was used. The experimental measurements for the line inductance per meter l=1.5 μH/m are shown in Figure 4.13 (b). In this case, L and R were set to 26 μH and 7 mΩ, respectively, corresponding to a distribution line length of 17.5 m. It in noticed that the DC system could deliver the load powers of 26 W and 52 W for the case of l=1.3 μH/m. However, increasing l to 1.5 μH/m made the DC system unable to deliver the load power of 52 W. The obtained results are in good agreement with the theoretical calculations and validate the dependence of deliverable power on distribution line inductance per meter.

3. (The experimental measurements concerning the improvement of deliverable power characteristics). In these measurements a capacitor $C = 270$ μF connected at the input terminals of the DC/DC converter and distribution line lengths ζ of 30 m and 57 m were used. The inductance per meter l and resistance per meter r were set to 0.9 μH/m and 0.4 mΩ/m, respectively. The obtained measurements were compared with the theoretical calculation of $P_{\lim}$ for the same conditions. The summary of the experimental results are presented in Figure 4.14. Comparing these results to that obtained in Figure 4.12, it is noticed that adding a capacitor of 270 μF enables the load power 78 W to be delivered in the case of ζ = 30 m and the load power of 52 W to be delivered in the case of ζ = 57 m. Therefore, these results show good agreement with the theoretical one and confirm the improvement of deliverable power capability of the DC system by using a capacitor at the load terminals.

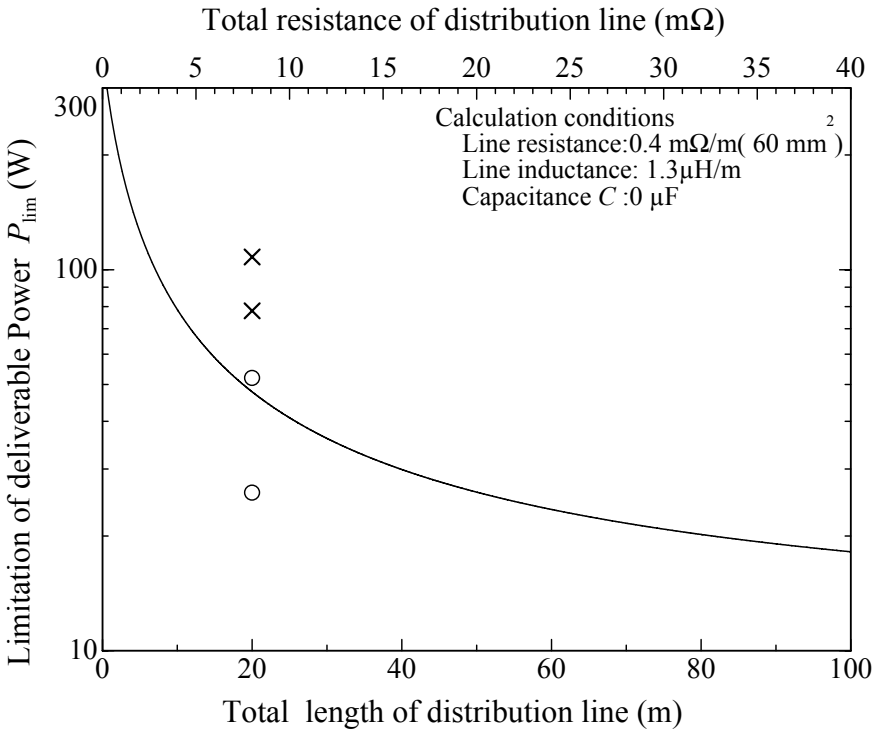

(a) Verification points of $P_{\lim}$ for l=1.3 μH/m.

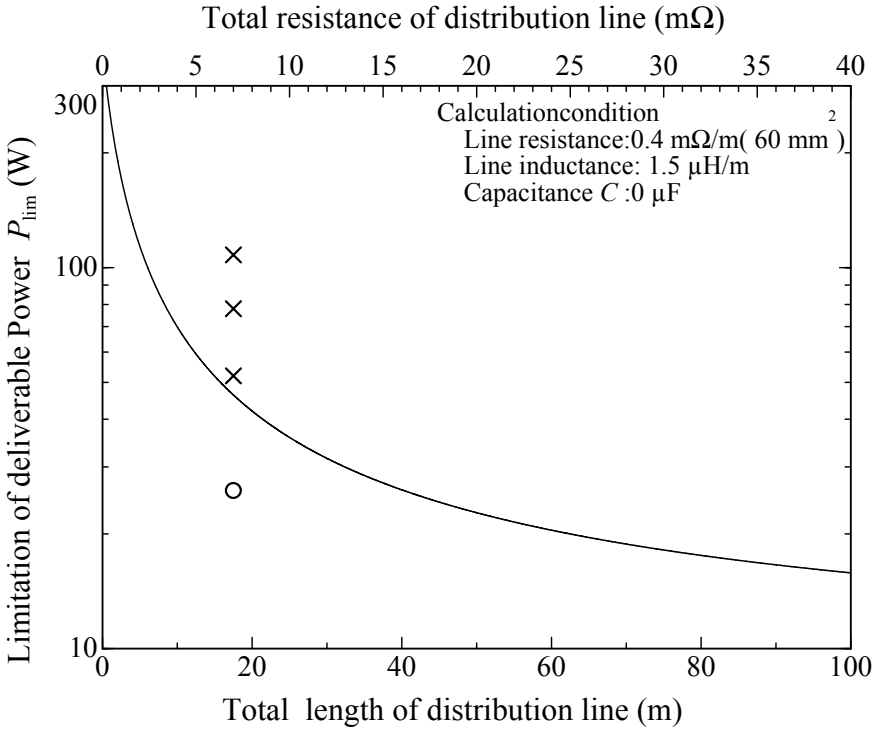

(b) Verification points of $P_{\lim}$ for l=1.5 μH/m.

Figure 4.13: *Verification points of $P_{\lim}$ at various inductance per meter.*

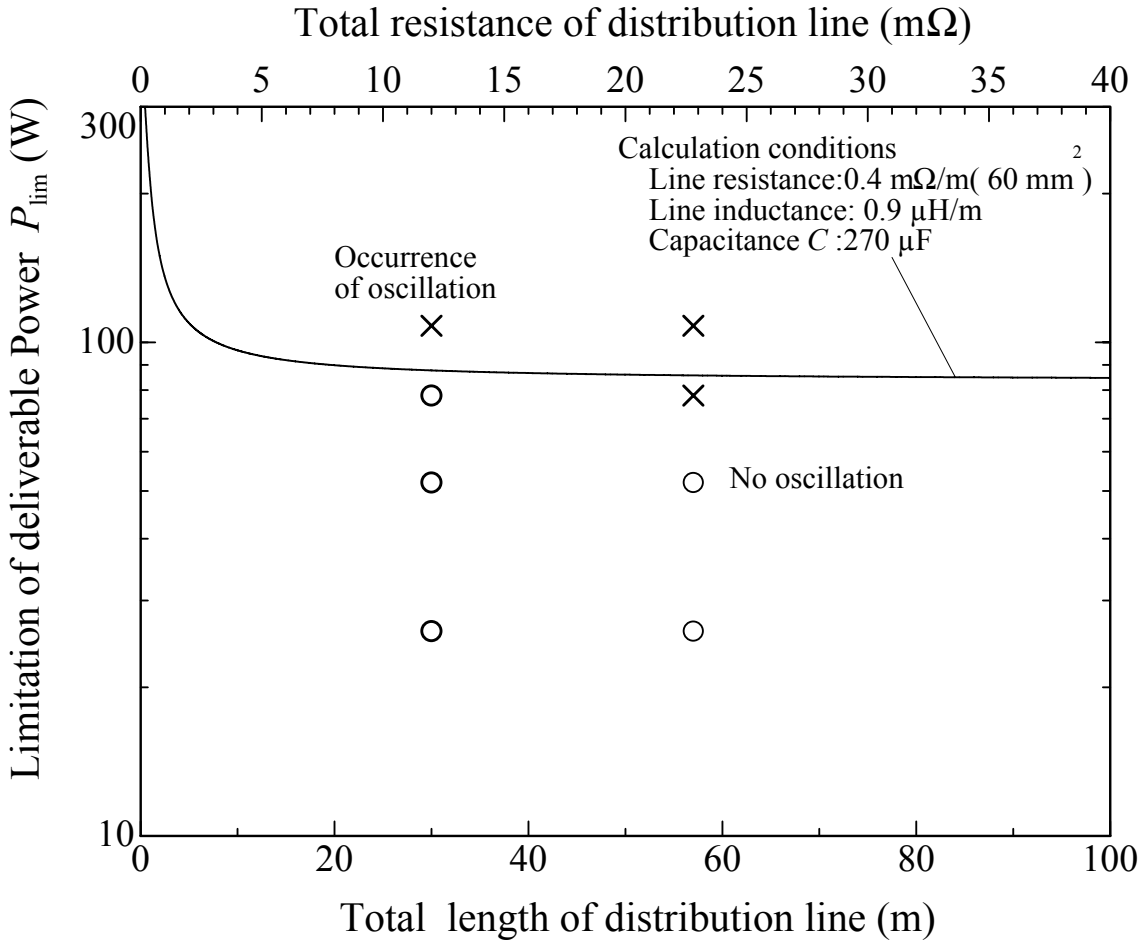

Figure 4.14: *Verification points of P_{lim} for C=270 μF.*

4.7 Conclusion

In this chapter, the influence of distribution line parameters on deliverable power in DC distribution system was studied. These parameters are line cross-section, inductance per meter and line length. Theoretical calculations were performed for the upper limitation P_{lim} of deliverable power under different conditions. Also, the improving of deliverable power characteristics was investigated by adding a capacitor at the load terminals. Finally, an experimental setup was built in order to confirm the obtained theoretical calculations. The obtained findings can be summarized as follows:

1. With decreasing the line cross-section, the line resistance became larger. Larger line resistance could damp the oscillations following a disturbance, and hence, higher deliverable power could be obtained. However, with larger line resistance, the voltage drop would increase. So, a compromise between both effects should be considered.

2. With increasing the line inductance per meter, P_{lim} decreased drastically. This is due to the role played by the inductance in causing voltage instability phenomenon.

3. Increasing the line length resulted in a decrease in P_{lim}, where the destabilizing effect produced by increasing the inductance was more dominant than that produced by increasing the resistance.

4. Adding a capacitor at the load terminals could increase P_{lim}. The minimum capacitance required to deliver the maximum load power was found to depend extremely on the line inductance per meter.

5. The experimental measurements were in good agreement with the theoretical calculations and validate the aforementioned theoretical results. Also, the voltage waveforms under stable and unstable operation could be obtained.

The obtained results in this chapter would be helpful for the efficient operation of a DC distribution system.

Bibliography

[1] L. Sluis, *Transients in Power Systems.*, John Wiley and Sons, LTD, 2001.

Chapter 5
Influence of Load Parameters on Deliverable Power in DC Distribution System

5.1 Introduction

In Chapter 3, it was indicated that the load parameters are important factors in determining the upper limitation P_{lim} of deliverable power in DC distribution system.

From this viewpoint, in this chapter, the effect of load parameters on P_{lim} is investigated. First, the effect of considering the transient unit of the DC load model in determining P_{lim} is discussed. Then, the influence of the magnitude of model parameters, R_{in}, L_{in} and C_{in}, on P_{lim} is evaluated in order to specify the dominant parameter that affecting the deliverable power. In addition, an equivalent representation of several loads connected to the DC distribution system is obtained. Based on this equivalent representation of loads, the limitation of deliverable power for several loads is determined, showing the effect of number of loads on P_{lim}. Finally, the dependence of P_{lim} on the power share between several loads is examined.

5.2 Influence of the transient unit of DC load model on P_{lim}

Several studies discussed the voltage instability phenomenon in DC distribution system [1–4]. In these studies loads were represented by only a non-linear resistor that consumes the load power. On the other hand, in this thesis, the transient performance of the load was discussed and then the transient unit was added to the DC load model of the non-linear resistor as explained in Chapter 2.

In order to discuss the effect of considering the transient unit in determining $P_{\lim}$, in this section, the loaded DC/DC converter is assumed to be represented only by a non-linear resistor with a voltage sensitivity parameter $\alpha = 0$. Then, the upper limitation based on this representation, $P'_{\lim}$, is calculated and compared to the results obtained with considering the transient unit.

Figure 5.1 shows the DC/DC converter model presented by only the non-linear resistor, which is powered with the DC voltage source through a distribution line with lumped parameters R and L. In this calculation, a capacitor C is considered to exist at the load terminals.

First, under a steady state condition the voltage source generates a constant DC voltage $V_{\rm s}$, supplying a constant DC voltage V across the non-linear resistor. Under this condition, the non-linear resistor consumes a power P resulting in a current flow I. Second, if a disturbance occurs in $V_{\rm s}$, the voltage across the non-linear resistor varies from V to $V + \Delta v$. Under this condition of disturbance, the non-linear resistor consumes a power $p(t)$ and a current $i(t)$ flows through it, where $i(t)$ equals to $I + \Delta i$. For this system, the consumed power $p(t)$ and the current $i(t)$ can be expressed in a similar manner to that in Chapter 3 as follows:

$$p(t) = \frac{P}{V^{\alpha}}(V + \Delta v)^{\alpha}. \tag{5.1}$$

$$i(t) = \frac{P}{V} + (\alpha - 1)\frac{P}{V^2}(v(t) - V). \tag{5.2}$$

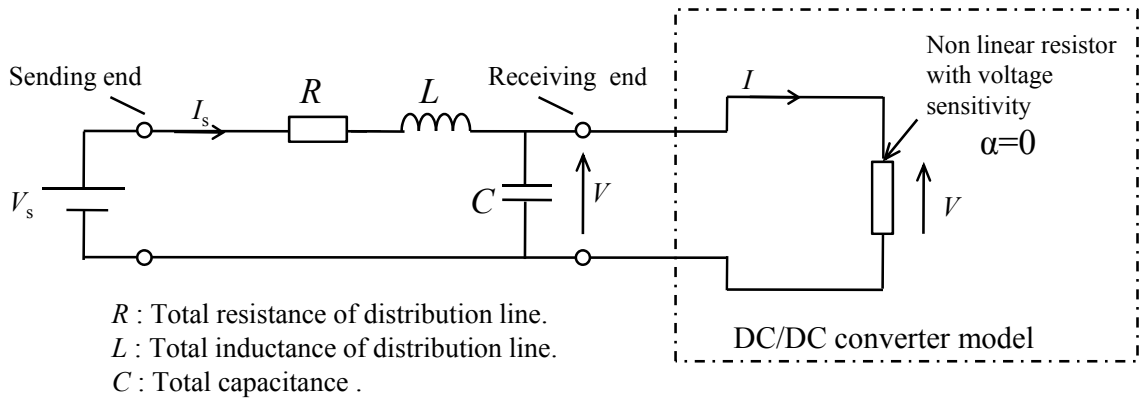

Figure 5.1: *DC distribution system with non-linear resistor of the DC/DC converter model.*

Then, from the circuit equations,

$$i_{\mathrm{s}}(t) = i(t) + C\frac{dv(t)}{dt}, \tag{5.3}$$

$$v_{\mathrm{s}}(t) = i_{\mathrm{s}}(t)R + L\frac{di_{\mathrm{s}}(t)}{dt} + v(t). \tag{5.4}$$

Substituting Eq. (5.2) into these equations and transferring to $s-$domain yield to:

$$i_{\mathrm{s}}(s) = (\alpha - 1)\frac{P}{V^2}v(s) + Csv(s) \tag{5.5}$$

$$v_{\mathrm{s}}(s) = v(s)(sL + R)[Cs + (\alpha - 1)\frac{P}{V^2} + 1]. \tag{5.6}$$

From these relations the transfer function $G(s)$ between v and v_{s} is given by:

$$G(s) = \frac{\frac{1}{LC}}{X(s)}. \tag{5.7}$$

where $X(s)$ is expressed as:

$$X(s) = s^2 + a_1 s + a_0. \tag{5.8}$$

According to Hurwitz criterion, the 2nd order system is stable if and only if all coefficients (a_1 and a_0) of $X(s)$ are positive. Therefore, for this system the stability conditions are:

$$a_1 = \frac{(\alpha - 1)P}{V^2C} + \frac{R}{L} > 0 \tag{5.9}$$

and

$$a_0 = 1 + \frac{(\alpha - 1)PR}{V^2} > 0. \tag{5.10}$$

It is found that, $(\alpha - 1)P\ R/V^2$ is very small negative value for the considered load values. Therefore, the coefficient a_0 is considered to be positive. Thus, the upper limitation P'_{lim} of deliverable power without considering of the transient unit is determined from the condition a_1 as follows:

$$P'_{\mathrm{lim}} = V^2C\frac{R}{L(1-\alpha)}. \tag{5.11}$$

From this expression, P'_{lim} was plotted against the distribution line resistance R for distribution line length of 40 m and terminal capacitance C of 0 and 100 μF as shown in Figure 5.2. The obtained P'_{lim} was compared with the previous calculated P_{lim} that consider the transient unit of the load.

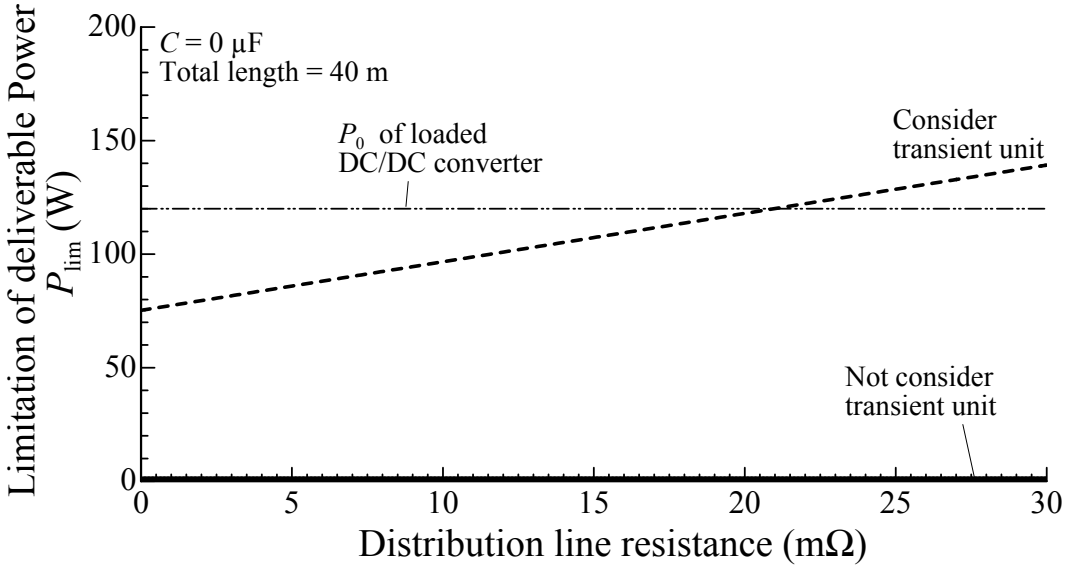

(a) Deliverable power for $C = 0\mu$F.

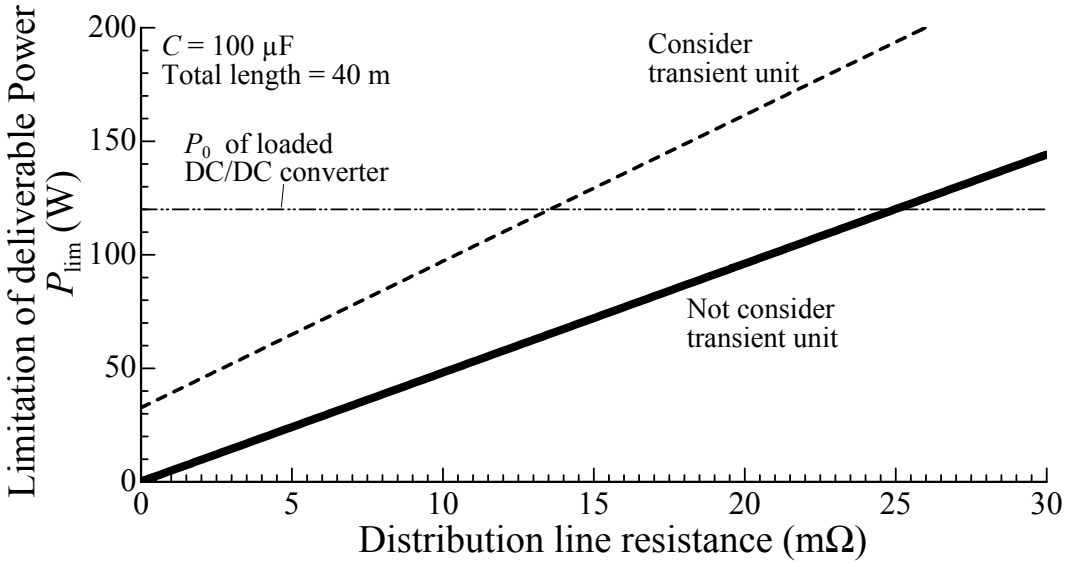

(b) Deliverable power for $C = 100\mu$F.

Figure 5.2: *Limitation of deliverable power for loaded DC/DC converter with and without considering the transient unit of DC load model.*

For the case of C = 0 μF, it is noticed that P'_{lim} is equal to 0 and shows a considerable difference from P_{lim} for the same C as seen in Figure 5.2 (a). However, increasing capacitance to 100 μF reduces the difference between P'_{lim} and P_{lim}. In this case, P'_{lim} is about half of P_{lim}. On the other hand, in Chapter 4, the validity of P_{lim} calculated for our DC load model with transient unit was confirmed by the experimental measurements. These results indicate clearly the importance of considering the transient unit in determining the upper limitation of deliverable power.

5.3 Influence of the DC load model parameters on P_{lim}

As shown in Chapter 2, the transient unit of the DC load model consists of R_{in}, L_{in} and C_{in} and the magnitudes of these parameters varies according to the type of load. Therefore, in this section, the influence of the magnitude of R_{in}, L_{in} and C_{in} on P_{lim} is discussed showing the dominant parameter that affects the deliverable power. The parameter of the DC/DC converter loaded by a resistor in Figure 2.24 is used.

5.3.1 Resistance R_{in}

To evaluate the influence of R_{in} on P_{lim}, R_{in} was varied from the original value 0.035 Ω to a halved and a duplicated magnitudes, 0.0175 and 0.07 Ω, while L_{in} and C_{in} remained at their original magnitude. The calculations were made to determine P_{lim} for C = 0 μF and for the distribution line length of 40 m, in the same manner as that mentioned in Chapter 3.

Figure 5.3 presents P_{lim} for the different magnitudes of R_{in}. It is observed that, as R_{in} increases from 0.035 to 0.07 Ω, P_{lim} increases to about two times of its original value. For example, P_{lim} increases from 97 W to 172 W at a line resistance R of 10 mΩ. On the other hand, reducing R_{in} to 0.0175 Ω leads to decreasing P_{lim} to nearly half of its original value. At R of 10 mΩ only 59 W can be delivered. These results show that the value of R_{in} has a considerable impact on the limitation of deliverable power. Moreover, the effect of R_{in} on P_{lim} is similar to that of the distribution line resistance R.

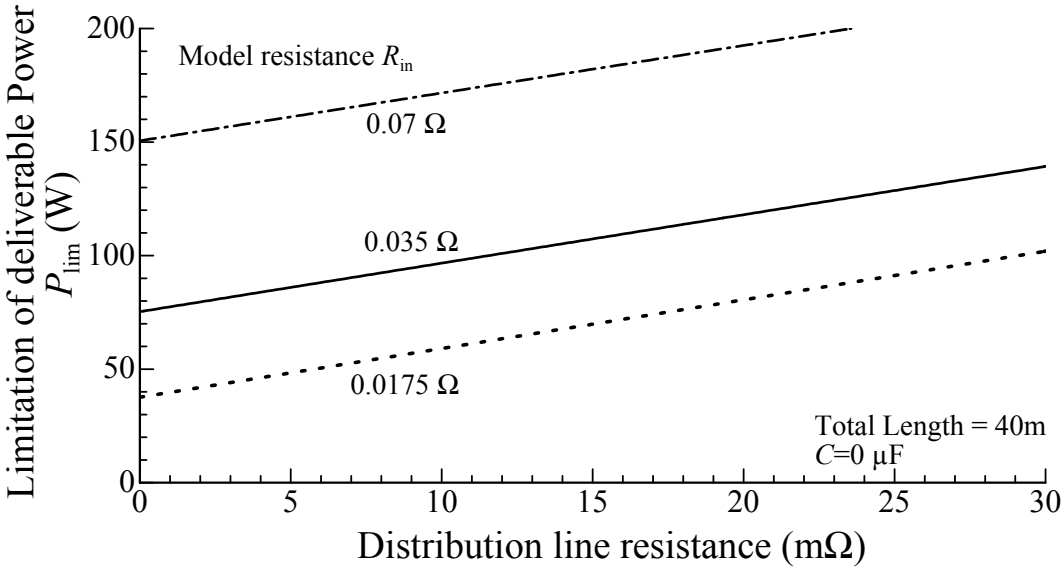

Figure 5.3: *Deliverable power for different values of model resistance.*

5.3.2 Inductance L_{in}

In this case R_{in} and C_{in} were set to their original magnitude. However, L_{in} was varied from 3 μH to 1.5 and 6 μH in order to calculate P_{lim}. Figure 5.4 presents P_{lim} for various L_{in}. As seen in Figure 5.4, increasing L_{in} to the doubled magnitude results in a slight reduction in P_{lim}. For example, P_{lim} reduces from 97 W by 17 W at a line resistance of 10 mΩ. When L_{in} halved to 1.5 μH a small increment occurred in P_{lim}. For example, P_{lim} increments only by 11 W at a line resistance of 10 mΩ. These results reveal that the effect of L_{in} on P_{lim} is considered to be less dominant comparing to the effect of R_{in} shown in Figure 5.3. In addition, the effect of the model inductance L_{in} is similar to that of distribution line inductance L.

5.3.3 Capacitance C_{in}

In this case, R_{in} and L_{in} were kept at their original magnitude. The power P_{lim} was recalculated when C_{in} was varied from 56 μF to 112 and 28 μF. Figure 5.5 shows the obtained results. Increasing C_{in} to 112 μF duplicates P_{lim} and reducing C_{in} to 28 μF decreases P_{lim} by 50 % of its original value. These results indicate that C_{in} extremely affects the deliverable power. Higher deliverable power would be available for loads with large capacitance C_{in}.

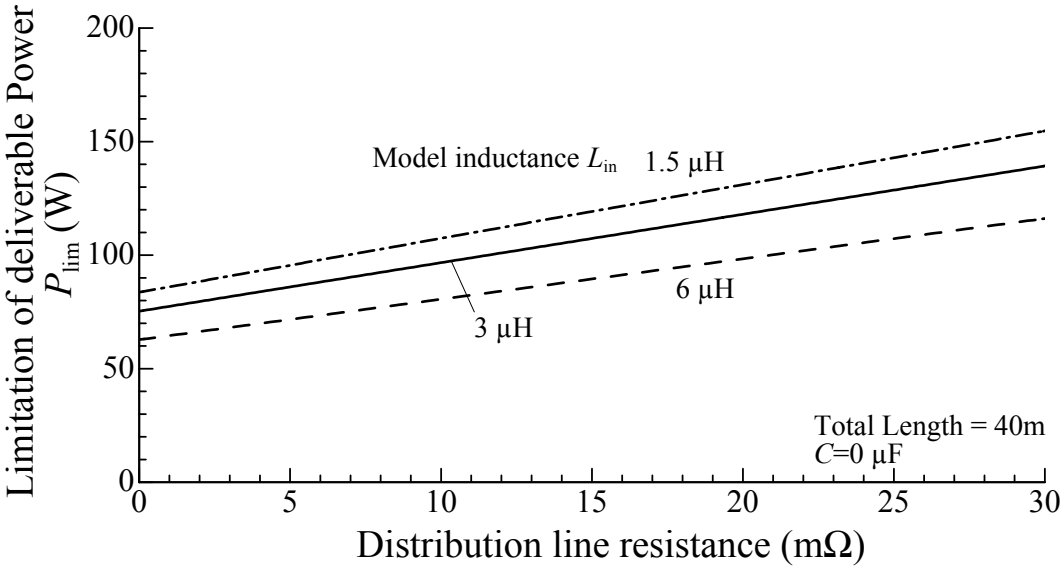

Figure 5.4: *Deliverable power for different values of model inductance.*

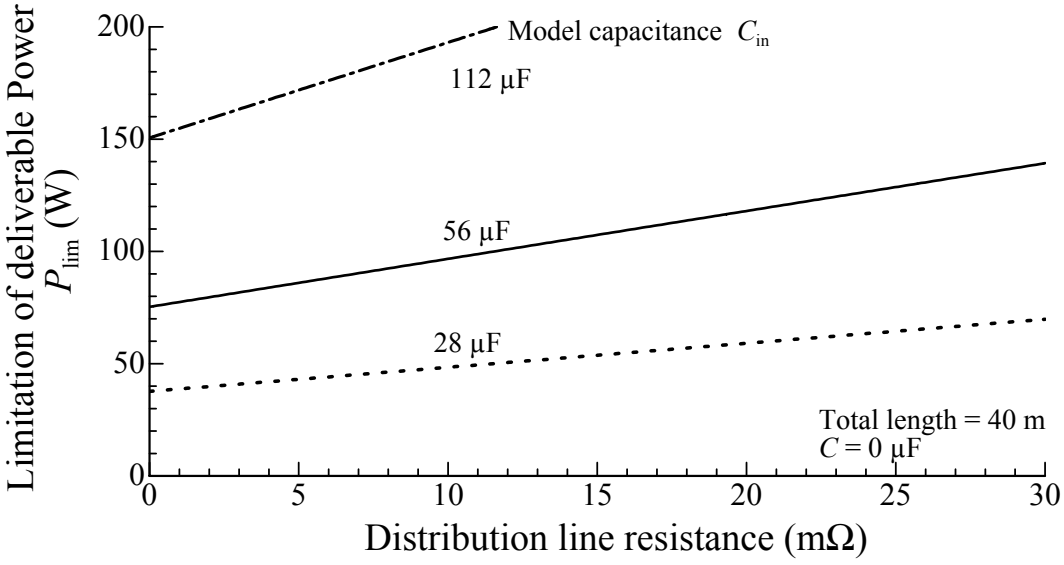

Figure 5.5: *Deliverable power for different values of model capacitance.*

Figure 5.6 summarizes the effect of magnitude of load parameters on the limitation of deliverable power. This Figure reveals that the capacitance of the transient unit of the model has the most dominant effect on P_{lim}. However, the inductance of the DC load model has the smallest effect on the deliverable power.

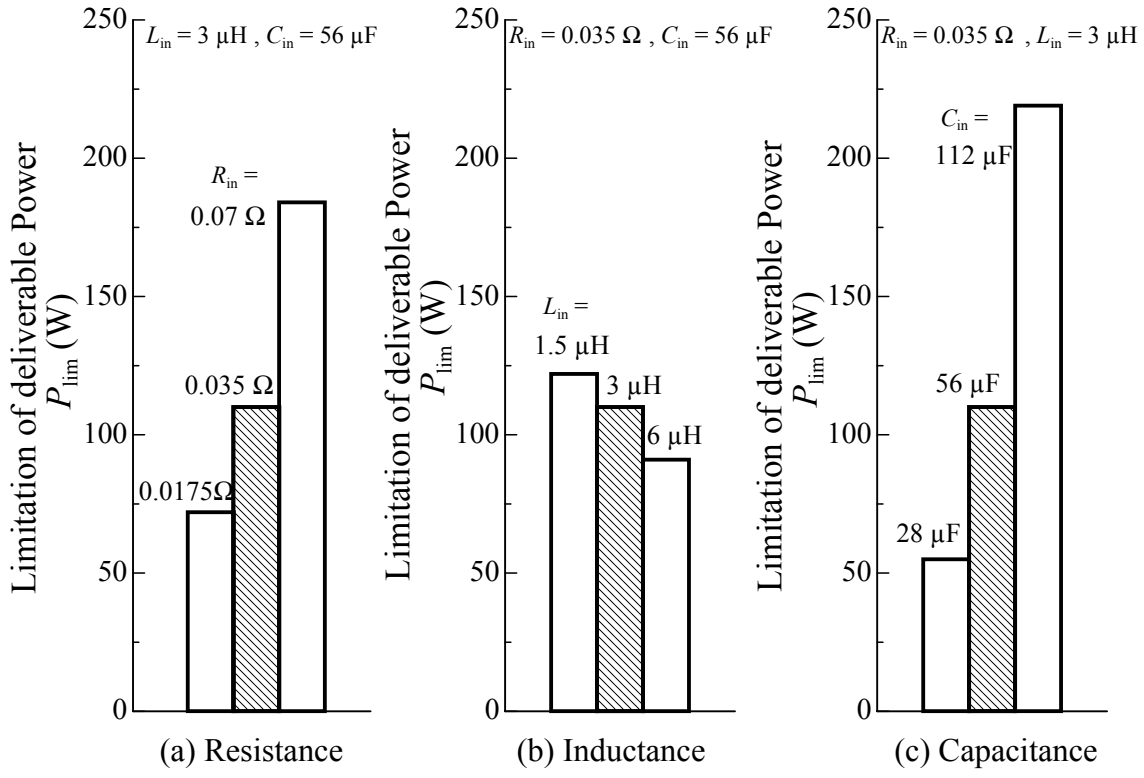

Figure 5.6: *Effect of load parameters on the deliverable power.*

5.4 Upper limitation of deliverable power for several loads

Usually, electrical loads are connected in parallel at the receiving end of the DC distribution system. Therefore, the situation of connecting several loads to the DC distribution system has to be discussed in studying the properties of deliverable power. In the stability analysis presented in Chapter 3, it is found that the limitation of deliverable power is dependent on the magnitude of load parameters, which are expected to be affected by the number of connected loads. Therefore, in the present section the limitation of deliverable power is calculated when several loads are connected at the receiving end. Based on the obtained results, the influence of the number of loads on $P_{\rm lim}$ is discussed.

5.4.1 Equivalent representation of several loads

The number of loads is expressed by a variable 'N'. Figure 5.7 shows the situation that 'N' DC loads are connected at the receiving end. Each load is represented by the DC load model explained in Chapter 2.

In order to calculate the limitation of the deliverable power for $N-$loads, $P_{\rm lim}^{(N)}$, the transfer function $G(s)$ relating the voltage at the receiving end $\Delta v_{\rm R}$ to the source voltage $\Delta v_{\rm s}$ have to be obtained. However, for $N-$loads it is difficult to directly get $G(s)$ by using the current representation of $N-$loads shown in Figure 5.7. Therefore, an equivalent circuit of these loads is needed. As shown in Figure 5.7, each load 'j' has a non-linear resistor with voltage sensitivity α_j and has a transient unit composed of an inductor $L_{{\rm in},j}$, a resistor $R_{{\rm in},j}$ and a capacitor $C_{{\rm in},j}$.

Each load 'j' is assumed to consume a power P_j for an operating voltage V. Let us consider the situation that the voltage across the receiving ends varies from V to $V + \Delta v_{\rm R}$, owing to a disturbance. As a result, the voltage across the non-linear resistor varies from V to $V + \Delta v_j$ $(j = 1, 2, ..., N)$ and the current flowing through the resistor varies from I_j to $I_j + \Delta i_j$. Under this situation, circuit equations for the single load 'j' is written in the form:

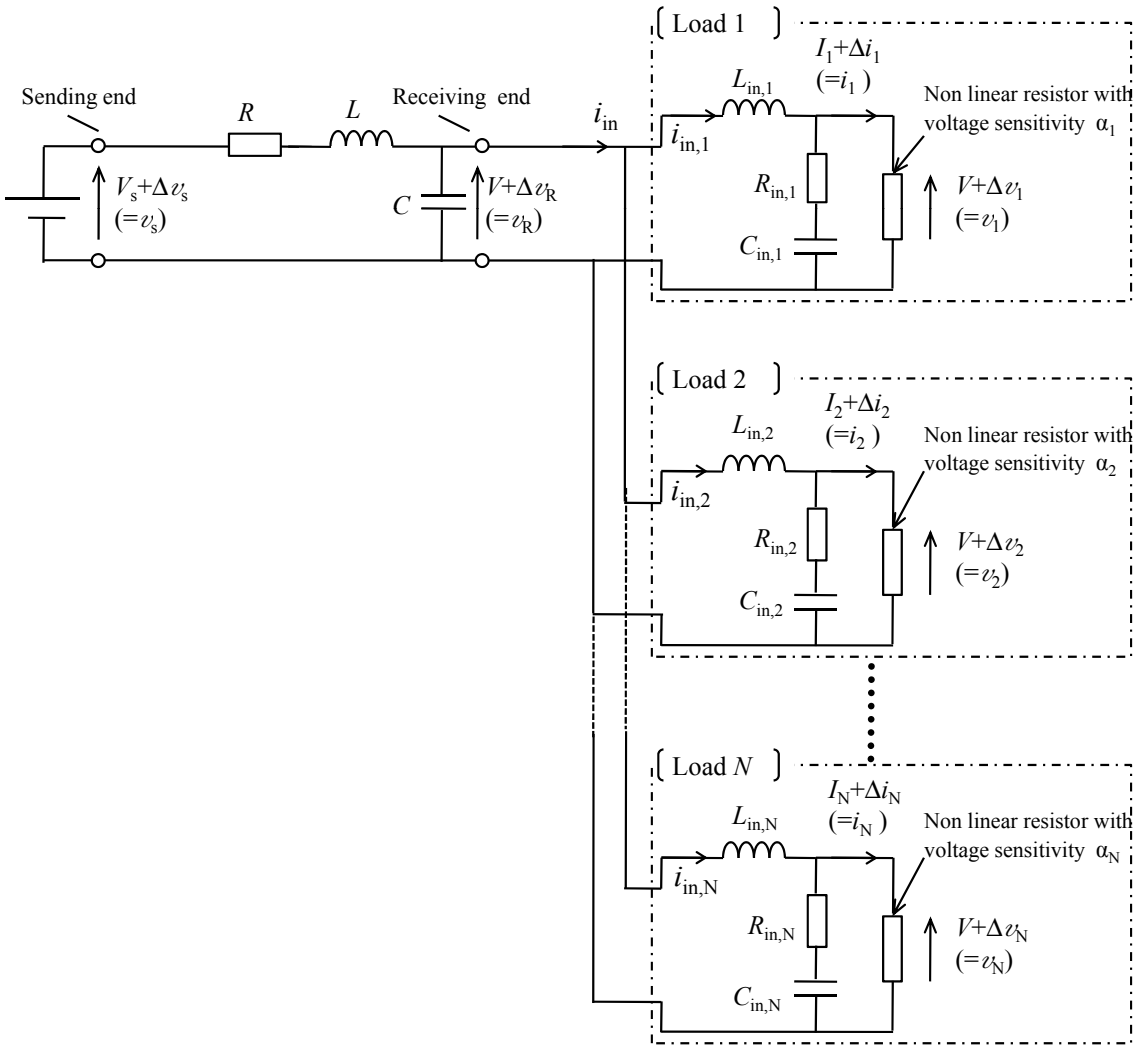

Figure 5.7: *A basic circuit of DC distribution system with several loads.*

$$\begin{aligned}\Delta v_{\mathrm{R}}(t) &= L_{\mathrm{in},j}\frac{d\Delta i_{\mathrm{in},j}(t)}{dt} + R_{\mathrm{in},j}(\Delta i_{\mathrm{in},j}(t) - \Delta i_j(t)) \\ &+ \frac{1}{C_{\mathrm{in},j}}\int(\Delta i_{\mathrm{in},j}(t) - \Delta i_j(t))dt, \qquad (5.12)\end{aligned}$$

and

$$i_j(t) = \frac{P_j}{V} + K_j\Delta v_j(t). \qquad (5.13)$$

where,

$$K_j = (\alpha_j - 1)\frac{P_j}{V^2}. \qquad (5.14)$$

Summing equation (5.12) related to $j = 1, 2, ..., N$ yields:

$$\begin{aligned}N\Delta v_{\mathrm{R}}(t) &= \sum_{j=1}^{N} L_{\mathrm{in},j}\frac{d\Delta i_{\mathrm{in},j}(t)}{dt} + \sum_{j=1}^{N} R_{\mathrm{in},j}(\Delta i_{\mathrm{in},j}(t) - \Delta i_j(t)) \\ &+ \sum_{j=1}^{N}\frac{1}{C_{\mathrm{in},j}}\int(\Delta i_{\mathrm{in},j}(t) - \Delta i_j(t)). \qquad (5.15)\end{aligned}$$

For the sake of simplicity, we assume that

1. All loads are similar in type. This means that all loads have the same α, R_{in}, L_{in} and C_{in}. Accordantly, $\alpha_j \equiv \alpha$, $R_{\mathrm{in},j} \equiv R_{\mathrm{in}}$, $L_{\mathrm{in},j} \equiv L_{\mathrm{in}}$ and $C_{\mathrm{in},j} \equiv C_{\mathrm{in}}$.

2. All loads consume the same power, namely P_j=P.

Based on assumption (1), equation (5.15) becomes

$$\begin{aligned}\Delta v_{\mathrm{R}}(t) &= \frac{L_{\mathrm{in}}}{N}\sum_{j=1}^{N}\frac{d\Delta i_{\mathrm{in},j}(t)}{dt} + \frac{R_{\mathrm{in}}}{N}\sum_{j=1}^{N}(\Delta i_{\mathrm{in},j}(t) - \Delta i_j(t)) \\ &+ \frac{1}{NC_{\mathrm{in}}}\int\sum_{j=1}^{N}(\Delta i_{\mathrm{in},j}(t) - \Delta i_j(t))dt. \qquad (5.16)\end{aligned}$$

Furthermore, application of the assumption (2) to equation (5.16) leads to

$$\begin{aligned}\Delta v_{\mathrm{R}}(t) &= \frac{L_{\mathrm{in}}}{N}\frac{d\Delta i_{\mathrm{in}}(t)}{dt} + \frac{R_{\mathrm{in}}}{N}(\Delta i_{\mathrm{in}}(t) - \Delta i(t)) \\ &+ \frac{1}{NC_{\mathrm{in}}}\int(\Delta i_{\mathrm{in}}(t) - \Delta i(t))dt. \qquad (5.17)\end{aligned}$$

where

$$\begin{aligned} \Delta i(t) &= NK\Delta v \\ &= [(\alpha - 1)\frac{NP}{V^2}]\Delta v. \end{aligned} \tag{5.18}$$

From equation (5.17), the equivalent circuit for $N-$loads is found to have the same construction as that for the single load. Figure (5.8) shows the derived equivalent circuit. The parameters of $N-$loads $\alpha^{(N)}$, $R_{\text{in}}^{(N)}$, $L_{\text{in}}^{(N)}$ and $C_{\text{in}}^{(N)}$ are related to the basic parameters of the individual load α, R_{in}, L_{in} and C_{in} as follows:

$$\alpha^{(N)} = \alpha, \tag{5.19}$$

$$R_{\text{in}}^{(N)} = R_{\text{in}}/N, \tag{5.20}$$

$$L_{\text{in}}^{(N)} = L_{\text{in}}/N \tag{5.21}$$

and

$$C_{\text{in}}^{(N)} = NC_{\text{in}}. \tag{5.22}$$

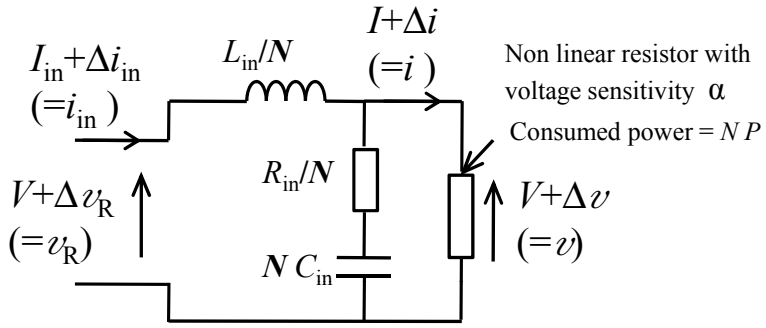

Figure 5.8: *Equivalent circuit of 'N' loads.*

5.4.2 Evaluation procedures of $P_{\text{lim}}^{(N)}$

Use of the equivalent circuit shown in Figure 5.8 allowed calculation of the upper limitation of deliverable power $P_{\text{lim}}^{(N)}$ to 'N' loaded DC/DC converters. This calculation employed the obtained equivalent parameters $\alpha^{(N)}$, $R_{\text{in}}^{(N)}$, $L_{\text{in}}^{(N)}$ and $C_{\text{in}}^{(N)}$ shown in equations (5.19)-(5.22).

Therefore, the coefficients c_j of the characteristic equation for the case of C= 0 as in equations (3.24)-(3.26) are given by:

$$c_2 = (K\frac{R_{\text{in}}}{N}+1)(L+\frac{L_{\text{in}}}{N})NC_{\text{in}}, \tag{5.23}$$

$$c_1 = (K\frac{R_{\text{in}}}{N}+1)RNC_{\text{in}}+(L+\frac{L_{\text{in}}}{N})K+R_{\text{in}}C_{\text{in}} \tag{5.24}$$

and

$$c_0 = KR+1. \tag{5.25}$$

Moreover, the coefficients d_j in the case of $C > 0$ as in equations (3.18)-(3.22) are changed to:

$$d_4 = (K\frac{R_{\text{in}}}{N}+1)L_{\text{in}}LC_{\text{in}}C, \tag{5.26}$$

$$d_3 = (K\frac{R_{\text{in}}}{N}+1)RCL_{\text{in}}C_{\text{in}}+(K\frac{L_{\text{in}}}{N}+R_{\text{in}}C_{\text{in}})LC, \tag{5.27}$$

$$d_2 = (K\frac{R_{\text{in}}}{N}+1)(L+\frac{L_{\text{in}}}{N})NC_{\text{in}}+LC+(K\frac{L_{\text{in}}}{N}+R_{\text{in}}C_{\text{in}})RC, \tag{5.28}$$

$$d_1 = (K\frac{R_{\text{in}}}{N}+1)RNC_{\text{in}}+(L+\frac{L_{\text{in}}}{N})K+R_{\text{in}}C_{\text{in}}+RC \tag{5.29}$$

and

$$d_0 = KR+1. \tag{5.30}$$

On the basis of these new coefficients, the stability conditions by Hurwitz criterion are obtained. Then, $P_{\text{lim}}^{(N)}$ is calculated for $N = 1, 2, 5, 10$ and 20 loads. For constant distribution line length, $P_{\text{lim}}^{(N)}$ is evaluated as a function of distribution line resistance R. The distribution line has an inductance l per meter of 0.3 μH/m and length of 40 m. The case of terminal capacitance C = 0 μF is adopted.

Figure 5.9 shows $P_{\text{lim}}^{(N)}$ for 1, 2, 5, 10 and 20 loads as a function of R. It is evident that larger number of loads increments P_{lim}. These derived results are explained as follows. As the number of loads increases, the parameters of the transient unit are changed as expressed in equations (5.19)-(5.22). In these equations it is noticed that the resistance R_{in} and inductance L_{in} are reduced, but the capacitance C_{in} is increased with larger number of loads. In section 5.3, the effect of changing R_{in}, L_{in} and C_{in} is presented. Based on the obtained results, it

would be concluded that higher capacitance NC_{in} and less inductance L_{in}/N of $N-$loads cause an increase in P_{lim}. Although the reduction in the resistance R_{in}/N decreases P_{lim}, $P_{\text{lim}}^{(\text{N})}$ increases with larger number of loads because the influence of the capacitance C_{in} on $P_{\text{lim}}^{(\text{N})}$ is higher than that of the resistance.

Also, Figure 5.9 depicts that $P_{\text{lim}}^{(N)}$ decreases with the reduction in distribution line resistance regardless the number of loads. For example, in the case of 2-loads, as R reduced from 15 mΩ to 10 mΩ, $P_{\text{lim}}^{(2)}$ diminished from 156 to 132 W. Also, $P_{\text{lim}}^{(10)}$ reduced from 487 to 357 W for the same range of R.

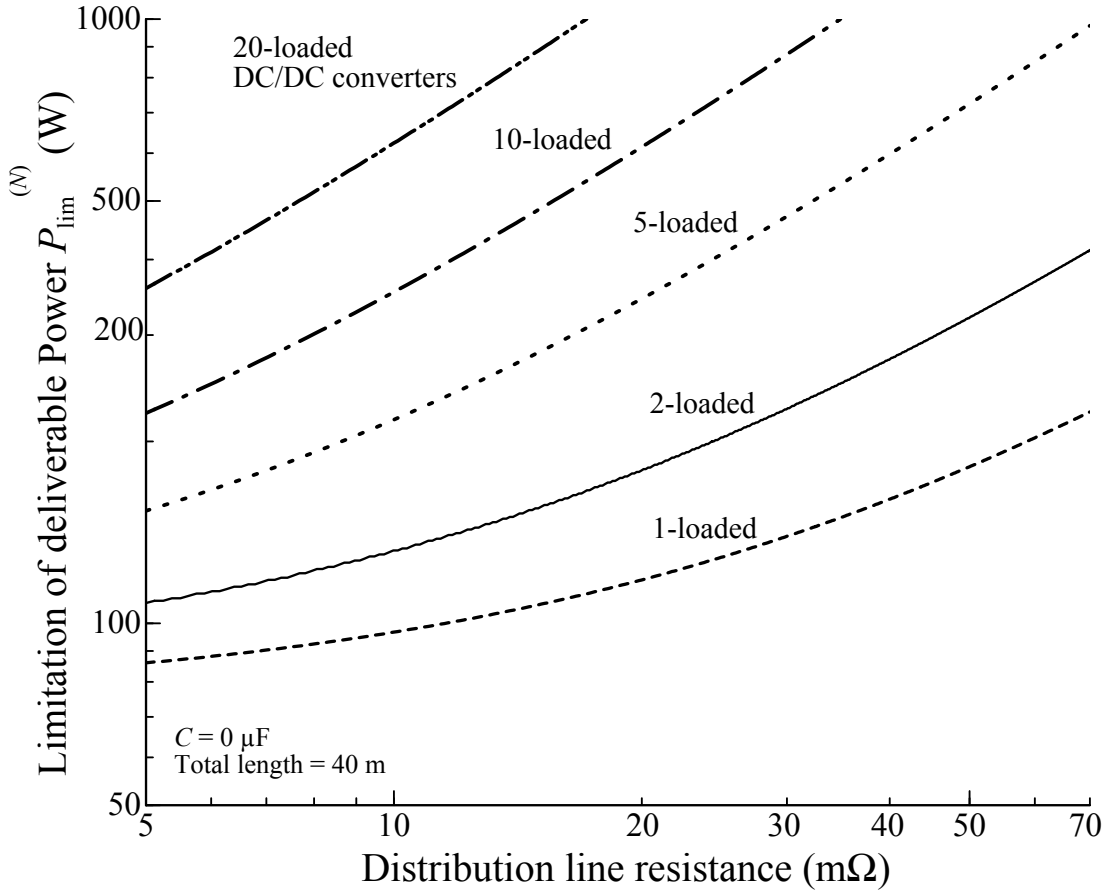

Figure 5.9: *Limitation of deliverable power of $N-$loads.*

As stated earlier, single DC/DC converter used in the calculation has the capability for receiving the power P_0 up to 120 W. When 'N' loads are connected at the receiving ends, they have a total capability of receiving $P_0^{(N)} = NP_0$. From $P_{\text{lim}}^{(N)}$ shown in Figure 5.9, we calculated the ratio of $P_{\text{lim}}^{(N)}$ to $P_0^{(N)}$, in order to determine how much power could be delivered to the load from its power capability. Figure 5.10 presents the calculated $P_{\text{lim}}^{(N)}/P_0^{(N)}$ as a function of R. Results reveal that larger number of loads causes a reduction in the ratio of $P_{\text{lim}}^{(N)}/P_0^{(N)}$. For instance, in the case of 5-loads, it is found that the upper limitation of the deliverable power $P_{\text{lim}}^{(5)}$ is only 58% of $P_0^{(5)}$ at $R = 20$ mΩ. However, in the case of 1-loaded DC/DC converter, the delivered power is increased to 98% of P_0 at the same R. These results indicate that the increasing rate of $P_{\text{lim}}^{(\text{N})}$ is less than the increasing rate of $P_0^{(\text{N})}$, due to the resistance effect. From the obtained results, it is clear that the number of loads remarkably affects the deliverable power in low-voltage DC distribution system.

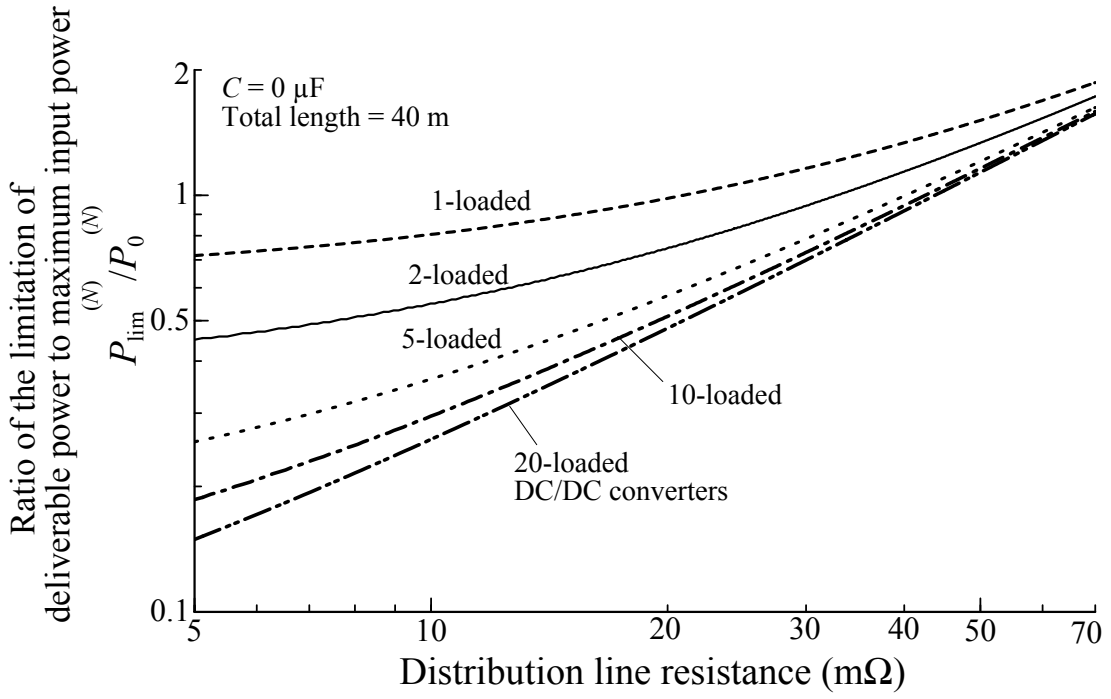

Figure 5.10: *Ratio of the limitation of $N-$loads to the maximum allowable input power.*

5.4.3 Minimum capacitance required at the receiving end

By the same method mentioned in Chapter 4, the minimum capacitance required to increase $P_{\text{lim}}^{(N)}$ to $P_0^{(N)}$ is calculated as presented in Figure 5.11. For example, at $R = 16$ mΩ, a capacitor 67 μF is sufficient to deliver $P_0^{(1)}$ for 1-loaded DC/DC converter. However, to deliver $P_0^{(10)}$ of 10-loads a capacitor of 982 μF is needed.

Larger number of loads requires a higher capacitance at the receiving end of the DC distribution system to deliver the maximum allowable input power of the connected loads.

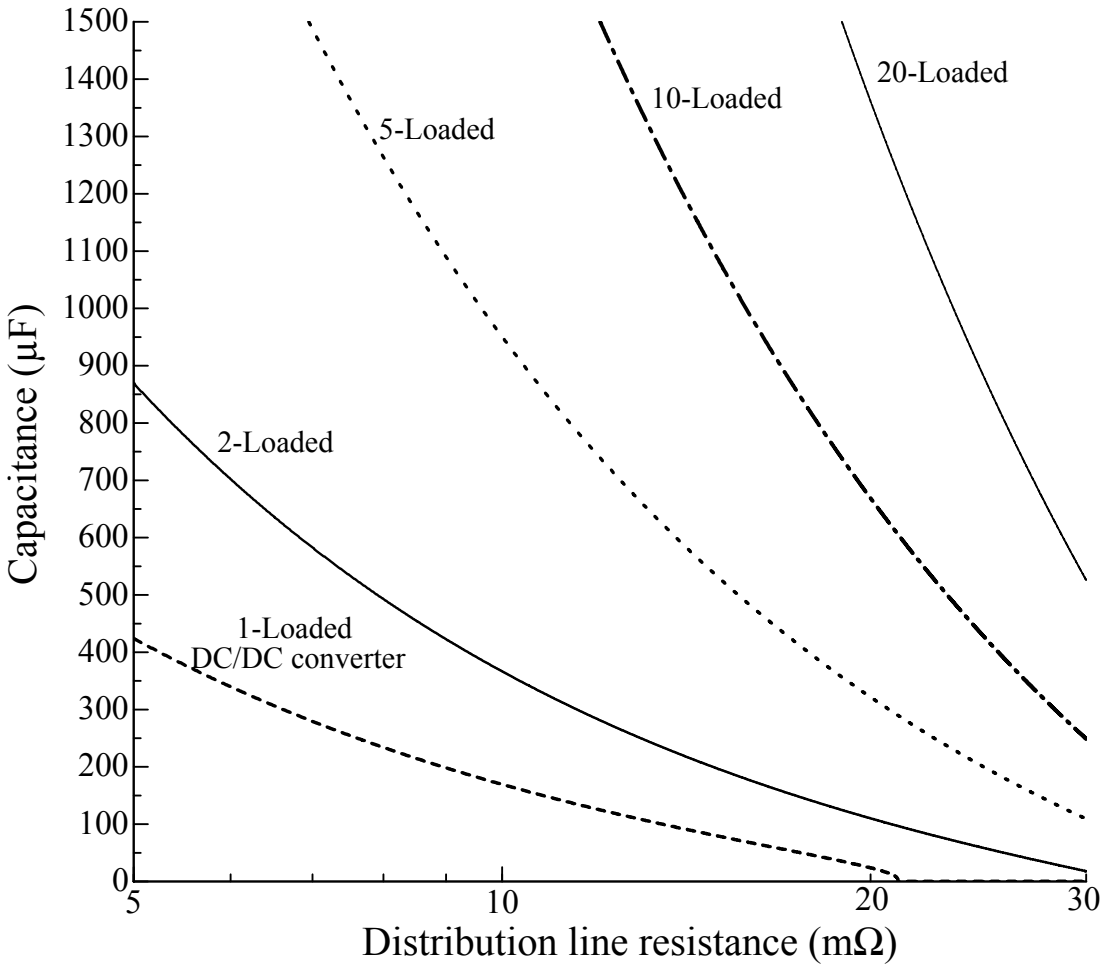

Figure 5.11: *Minimum capacitance for delivering the maximum power consumption of several loaded DC/DC converters.*

5.5 Limitation of deliverable power for several loads consuming different powers

In the previous section, $P_{\lim}^{(N)}$ was calculated based on the derived equivalent circuit of $N-$loads. However, this equivalent circuit is valid under the conditions that the $N-$loads were similar in type and consume the same power P. In this section, the limitation of deliverable power $P_{\lim}^{(N)}$ for $N-$loads consuming different powers is evaluated.

5.5.1 Calculation conditions and evaluation procedures

Let us consider that the circuit shown in Figure 5.7 has only $2-$loads connected to the DC voltage source via a distribution line as shown in Figure 5.12. The model parameters of load-1 are $\alpha_1, R_{\mathrm{in},1}, L_{\mathrm{in},1}$ and $C_{\mathrm{in},1}$, and for load-2, the parameters are $\alpha_2, R_{\mathrm{in},2}, L_{\mathrm{in},2}$ and $C_{\mathrm{in},2}$. The total consumed load powers is P_{t}, corresponding to load powers P_1 and P_2 for load-1 and load-2, respectively. These powers are related to P_{t} by a share parameter η as follows:

$$P_1 = \eta P_{\mathrm{t}}, P_2 = (1-\eta)P_{\mathrm{t}}.$$

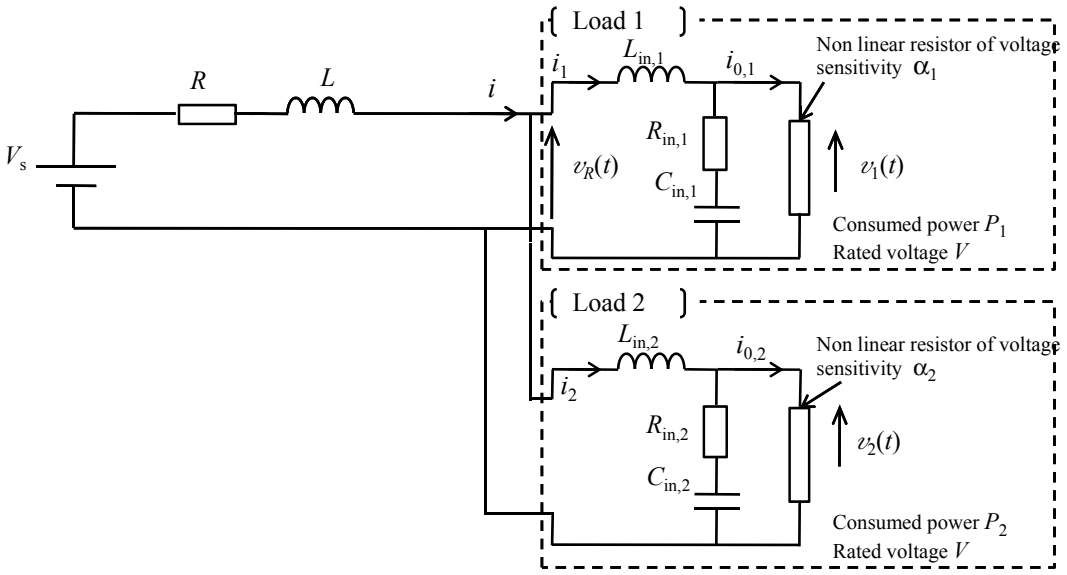

Figure 5.12: *The basic circuit of DC distribution system with 2 DC loads.*

In this situation, the parameters K_1 and K_2 are:

$$K_1 = (\alpha - 1)\frac{\eta P_{\rm t}}{V^2}, \quad K_2 = (\alpha - 1)\frac{(1-\eta)P_{\rm t}}{V^2}. \tag{5.31}$$

Based on these properties, the transfer function $G(s)$ relating the voltage at the receiving end $\Delta v_{\rm R}$ to the sending end voltage $\Delta v_{\rm s}$ is derived. The characteristic equation $X(s)$ is expressed in the case of $C = 0$ as follows:

$$X(s) = a_4 s^4 + a_3 s^3 + a_2 s^2 + a_1 s + a_0. \tag{5.32}$$

The coefficients a_4, a_3, a_2, a_1 and a_0 are defied as:

$$a_4 = 1 + L(\frac{1}{L_{\rm in,1}} + \frac{1}{L_{\rm in,2}}) \tag{5.33}$$

$$a_3 = L(\frac{A_1}{L_{\rm in,2}} + \frac{A_2}{L_{\rm in,1}} + K_1 B_1 + K_2 B_2) + A_1 + A_2 \tag{5.34}$$

$$\begin{aligned} a_2 &= R(B_1 K_1 + B_2 K_2 + \frac{A_1}{L_{\rm in,2}} + \frac{A_2}{L_{\rm in,1}}) + L(\frac{B_1}{L_{\rm in,2}} + \frac{B_2}{L_{\rm in,1}} + K_1 B_1 A_2 + K_2 B_2 A_1) \\ &+ B_1 + B_2 + A_1 A_2 \end{aligned} \tag{5.35}$$

$$\begin{aligned} a_1 &= R(\frac{B_1}{L_{\rm in,2}} + \frac{B_2}{L_{\rm in,1}}) + A_1 B_2 (1 + R K_2) + A_2 B_1 (1 + R K_1) \\ &+ B_1 B_2 L (K_1 + K_2) \end{aligned} \tag{5.36}$$

$$a_0 = B_1 B_2 (1 + R(K_1 + K_2)) \tag{5.37}$$

where

$$A_1 = \frac{R_{\rm in,1} C_{\rm in,1} + L_{\rm in,1} K_1}{L_{\rm in,1} C_{\rm in,1} (1 + K_1 R_{\rm in,1})} \tag{5.38}$$

$$A_2 = \frac{R_{\rm in,2} C_{\rm in,2} + L_{\rm in,2} K_2}{L_{\rm in,2} C_{\rm in,2} (1 + K_2 R_{\rm in,2})} \tag{5.39}$$

$$B_1 = \frac{1}{L_{\rm in,1} C_{\rm in,1} (1 + K_1 R_{\rm in,1})} \tag{5.40}$$

$$B_2 = \frac{1}{L_{\rm in,2} C_{\rm in,2} (1 + K_2 R_{\rm in,2})} \tag{5.41}$$

These coefficients are used in calculating the limitation of deliverable power for any 2-loads. However, in order to investigate the effect of various power shares between loads, we consider that the 2-loads are similar in type. Thus, the 2-loads have the same model parameters $\alpha_1 = \alpha_2 = \alpha$, $R_{\rm in,1} = R_{\rm in,2} = R_{\rm in}$, $L_{\rm in,1} = L_{\rm in,2} = L_{\rm in}$ and $C_{\rm in,1} = C_{\rm in,2} = C_{\rm in}$. For this condition the coefficients a_4, a_3, a_2, a_1 and a_0 will be expressed as:

$$a_4 = 1 + \frac{2L}{L_{\text{in}}} \tag{5.42}$$

$$\begin{aligned} a_3 = {} & \frac{(K_1+K_2)(2LL_{\text{in}} + L_{\text{in}}^2 + R_{\text{in}}^2 L_{\text{in}} C_{\text{in}})}{L_{\text{in}}^2 C_{\text{in}}(1 + R_{\text{in}}(K_1+K_2) + R_{\text{in}}^2 K_1 K_2)} + \frac{2R}{L_{\text{in}}} \\ & + \frac{R_{\text{in}}^2 L C_{\text{in}}(K_1+K_2) + 2R_{\text{in}} C_{\text{in}}(L_{\text{in}}+L)}{L_{\text{in}}^2 C_{\text{in}}(1 + R_{\text{in}}(K_1+K_2) + R_{\text{in}}^2 K_1 K_2)} \\ & + \frac{(2R_{\text{in}} L_{\text{in}}^2 + 4LL_{\text{in}} R_{\text{in}}) K_1 K_2}{L_{\text{in}}^2 C_{\text{in}}(1 + R_{\text{in},1}(K_1+K_2) + R_{\text{in}}^2 K_1 K_2)} \end{aligned} \tag{5.43}$$

$$\begin{aligned} a_2 = {} & \frac{(K_1+K_2)(RR_{\text{in}}^2 C_{\text{in}}^2 + 2LC_{\text{in}} R_{\text{in}})}{L_{\text{in}}^2 C_{\text{in}}^2(1 + R_{\text{in}}(K_1+K_2) + R_{\text{in}}^2 K_1 K_2)} \\ & + \frac{(K_1+K_2)(R_{\text{in}}+R) 2L_{\text{in}} C_{\text{in}}}{L_{\text{in}}^2 C_{\text{in}}^2(1 + R_{\text{in}}(K_1+K_2) + R_{\text{in}}^2 K_1 K_2)} \\ & + \frac{2RC_{\text{in}}^2 R_{\text{in}} + R_{\text{in}}^2 C_{\text{in}}^2 + 2C_{\text{in}}(L+L_{\text{in}})}{L_{\text{in}}^2 C_{\text{in}}^2(1 + R_{\text{in}}(K_1+K_2) + R_{\text{in}}^2 K_1 K_2)} \\ & + \frac{K_1 K_2(4RR_{\text{in}} L_{\text{in}} C_{\text{in}} + L_{\text{in}}(2L+L_{\text{in}})}{L_{\text{in}}^2 C_{\text{in}}^2(1 + R_{\text{in}}(K_1+K_2) + R_{\text{in}}^2 K_1 K_2)} \end{aligned} \tag{5.44}$$

$$\begin{aligned} a_1 = {} & \frac{(K_1+K_2)(L + L_{\text{in}} + 2R_{\text{in}} C_{\text{in}} R)}{L_{\text{in}}^2 C_{\text{in}}^2(1 + R_{\text{in}}(K_1+K_2) + R_{\text{in}}^2 K_1 K_2)} \\ & + \frac{2L_{\text{in}} RK_1 K_2 + 2C_{\text{in}}(R+R_{\text{in}})}{L_{\text{in}}^2 C_{\text{in}}^2(1 + R_{\text{in}}(K_1+K_2) + R_{\text{in}}^2 K_1 K_2)} \end{aligned} \tag{5.45}$$

$$a_0 = \frac{R(K_1+K_2)+1}{L_{\text{in}}^2 C_{\text{in}}^2(1 + R_{\text{in}}(K_1+K_2) + R_{\text{in}}^2 K_1 K_2)}. \tag{5.46}$$

Application of Hurwitz criterion to these coefficients provides the stability conditions needed in calculating $P_{\text{lim}}^{(2)}$ as shown:

$$a_4 > 0, \;\; a_3 > 0, \;\; a_2 > 0, \;\; a_1 > 0, \;\; a_0 > 0, \tag{5.47}$$

$$H_1 = a_3 \quad > 0, \tag{5.48}$$

$$H_2 = a_3 a_2 - a_4 a_1 \quad > 0, \tag{5.49}$$

$$H_3 = a_1 a_2 a_3 - a_3 a_3 a_0 - a_4 a_1 a_1 \quad > 0 \tag{5.50}$$

and

$$H_4 = a_0 H_3 \quad > 0. \tag{5.51}$$

Based on these stability conditions, $P_{\text{lim}}^{(2)}$ was calculated for η = 5, 10, 20, 30, 40 and 50% as a function of distribution line resistance R. Distribution line length of 40 m having inductance per meter l of 0.3 μH/m was used.

Figure 5.13 shows the $P_{\text{lim}}^{(2)}$ as a function of R for various values of η. It is found that $P_{\text{lim}}^{(2)}$ is the same for all values of η. Therefore, the equivalent circuit of $N-$loads presented in section 5.4 becomes valid for several similar loads consuming different powers.

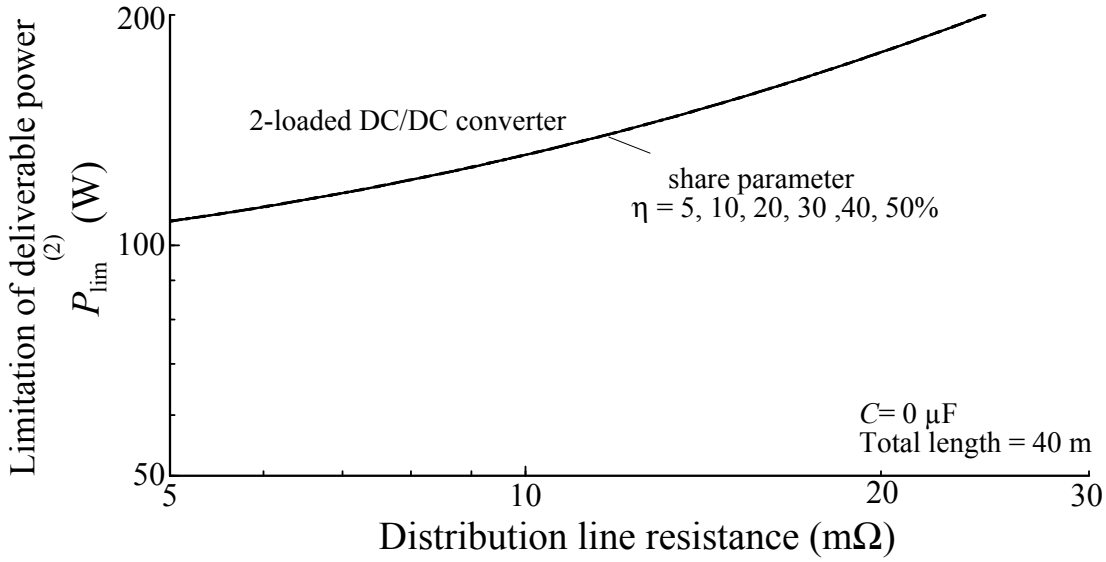

Figure 5.13: *Limitation of deliverable power for 2−loads with various power shares.*

5.6 Conclusion

In this chapter, the influence of load parameters on the upper limitation of deliverable power, P_{lim}, was studied. First, the effect of considering the transient unit was investigated. The results showed that the transient unit should be taken into consideration in order to evaluate the deliverable power capability of the DC system correctly. This is because there was a big difference in P_{lim} when it was calculated with and without considering the transient unit. Then, the effect of the DC model parameters, R_{in}, L_{in} and C_{in}, was evaluated. The dominant parameter of the transient unit that affects the deliverable power was the capacitance. Larger capacitance caused higher deliverable power.

Also, the limitation of deliverable power for several loads connected to the DC distribution system was calculated. With larger number of loads, P_{lim} increased. However, the increasing rate of P_{lim} was less than the increasing rate of the maximum allowable input power of the loads. Accordingly, the minimum capacitance required to deliver the maximum allowable input power became higher for larger number of loads.

Bibliography

[1] D. L. Logue, and P. T. Krein, "Preventing instability in DC distribution systems by using power buffering," *IEEE Power Electronics Specialists Conference, PESC 2001*, vol. 1, pp. 33-37, June 2001.

[2] J. G. Ciezki and R. W. Ashton, "Selection and stability issues associated with a navy shipboard DC zonal electric distribution system," *IEEE Transactions Power Delivery*, vol. 15, no. 2, pp. 665-669, April 2000.

[3] S. Luo and I. Batarseh, "A review of distributed power systems part I: DC distributed power system," *IEEE Aerospace and Electronic Systems Magazine*, vol. 20, no. 8, part 2, pp. 5-16, August 2005.

[4] A. Emadi, "Modeling of power electronic loads in AC distribution systems using the generalized state-space averaging method," *IEEE Transactions Industrial Electronics*, vol. 51, no. 5, pp. 992-1000, October 2004.

Chapter 6
Conclusion and Future Work

6.1 Conclusion

DC distribution system has been proposed as a prospective way to replace the conventional AC distribution system as a result of fast growth of renewable energy sources with inherently DC output or coupled with AC/DC interface. This made it important to understand the deliverable power capability in DC distribution systems. From this viewpoint, this thesis aimed to reveal derivable power characteristics in low-voltage DC distribution systems based on voltage stability.

First, a DC load model was proposed as a preliminary stage for the analysis of voltage stability and deliverable power characteristics. This model was constructed from a steady state unit and a transient unit. The steady state unit simulated the consumed load power under a steady state. This unit was defined by a non-linear resistor with voltage sensitivity parameter α. The voltage sensitivity parameter α was calculated for different loads from steady state measurements of the load powers at various applied voltages. In the transient unit, the load behavior under a transient state was represented by R_{in}, L_{in}, and C_{in} circuit. The magnitude of these components was obtained from the numerical solution of the circuit equations until the calculated load current and consumed load power agree with the measured ones. Experimental measurements had verified the validity of this load model for several DC loads such as a loaded DC/DC converter and a personal computer.

Then, the developed DC load model was used in studying the deliverable power characteristics in low-voltage DC distribution system. It was found that, the voltage instability phenomenon limited the deliverable power to the electrical loads with the voltage sensitivity parameter less than 1. Hurwitz criterion was used in determining the stability conditions. The maximum value of deliverable power necessary to satisfy stability conditions was obtained. This power

was regarded as upper limitation P_{lim} of deliverable power. The theoretical calculation showed that P_{lim} depended on distribution line parameters, load parameters and the operating voltage.

Next, the influence of distribution line parameters on deliverable power was studied. These parameters were line cross-section, inductance per meter and line length. With decreasing the line cross-section, the line resistance became larger. Larger line resistance could damp the oscillations following a disturbance, and hence, higher deliverable power could be obtained. However, larger line resistance caused the higher voltage drop makes a necessity to compromise between both effects in designing a DC distribution system. With increasing the line inductance per meter, P_{lim} decreased drastically. This was attributed to the property of the constant flux linkage provided by the inductance. Increasing the line length resulted in a decrease in P_{lim}, where the destabilizing effect produced by increasing the inductance was more dominant than the stabilizing effect produced by increasing the resistance.

After clarifying the influence of distribution line parameters on deliverable power, the improving of deliverable power characteristics was investigated by adding a capacitor at the load terminals. Adding a capacitor at the load terminals could increase P_{lim}. The minimum capacitance required to deliver the maximum load power was found to depend extremely on the line inductance per meter. In order to validate the obtained theoretical calculations of P_{lim}, an experimental setup was built. For the different line parameters, the experimental measurements were in good agreement with the theoretical calculations. Also, the voltage waveforms under stable and unstable operation could be obtained.

Finally, the influence of load parameters on deliverable power was studied. The importance of considering the transient unit in evaluating the deliverable power characteristics was confirmed. Then, the influence of the DC model parameters, R_{in}, L_{in} and C_{in}, was evaluated. The dominant parameter of the transient unit that affected the deliverable power was the capacitance. Larger capacitance caused higher deliverable power. Also, the limitation of deliverable power for several loads connected to the DC distribution system was calculated. With larger number of loads, P_{lim} increased. However, the increasing rate of P_{lim} was less than the increasing rate of the maximum allowable input power of the loads. With different power shares between loads, there was no effect on deliverable power characteristics.

6.2 Future work

This thesis investigated extensively the deliverable power characteristics for low-voltage DC distribution system. However, the following investigations will be needed in the future.

1. In DC distribution systems, there are different values of voltage level. So, it is important to evaluate the effect of voltage level on deliverable power characteristics. Especially, the stability conditions obtained in this thesis would be dependent on voltage level.

2. In this study, it was assumed that the voltage source is an ideal one. However, it will be interesting to consider actual renewable energy sources with DC output, such as photovoltaic and fuel cells, in studying deliverable power characteristics.

3. Finally, it is important to consider the limitation of deliverable power $N-$loads of different types.

List of Publications Related to the Thesis

Chapter	Title	Journal & Date	Authors
2	Formulated Representation for Upper Limitation of Deliverable Power in Low-Voltage DC Distribution System	IEEJ Transactions on Power and Energy, Vol.131-B, No.4, (2011) To be published	Y. Yokomizu, D. M. Yehia, D. Iioka and T. Matsumura
3	A Novel Approach to Deliverable Power in Low-Voltage DC Distribution System on Basis of Voltage Stability	IEEJ Transactions on Electrical and Electronic Engineering, Vol. 8, No.5, (2011) To be published	D. M. Yehia, Y. Yokomizu, D. Iioka, R. Watanabe and T. Matsumura
4	A Novel Approach to Deliverable Power in Low-Voltage DC Distribution System on Basis of Voltage Stability	IEEJ Transactions on Electrical and Electronic Engineering, Vol. 8, No.5, (2011) To be published	D. M. Yehia, Y. Yokomizu, D. Iioka, R. Watanabe and T. Matsumura
	Deliverable-Power Dependence on Distribution-Line Resistance and Number of Loads in Low-Voltage DC Distribution System	IEEJ Transactions on Electrical and Electronic Engineering Vol. 9, No.1, (2012) To be published	D. M. Yehia, Y. Yokomizu, D. Iioka and T. Matsumura
5	Formulated Representation for Upper Limitation of Deliverable Power in Low-Voltage DC Distribution System	IEEJ Transactions on Power and Energy, Vol.131-B, No.4, (2011) To be published	Y. Yokomizu, D. M. Yehia, D. Iioka and T. Matsumura
	Deliverable-Power Dependence on Distribution-Line Resistance and Number of Loads in Low-Voltage DC Distribution System	IEEJ Transactions on Electrical and Electronic Engineering Vol. 9, No.1, (2012) To be published	D. M. Yehia, Y. Yokomizu, D. Iioka and T. Matsumura

Acknowledgements

First, I would like to deeply thank my supervisor Prof. Toshiro MATSUMURA for his guidance and feedback on my research work. His valuable comments and ideas helped me to improve my research results. He also provided me helpful and useful assistance during my study years in Nagoya University.

I would like to thank Prof. Dr. Naoki HAYAKAWA for taking the time and effort to review my thesis.

I would also like to thank Assoc. Prof. Yasunobu YOKOMIZU for the valuable time and efforts he spent giving advices and discussing my research results. Based on his insightful discussions, my research could be directed into the correct way. Also, I would like to thank him for taking the time and effort to review my thesis.

In addition, I would like to thank Prof. Dr. Katsuhiro ICHIYANAGI of Aichi Institute of Technology for taking the time and effort to review my thesis.

My thanks are extended to Dr. Daisuke IIOKA. His assistance and support during my first days in Nagoya University was very helpful for me.

Moreover, I am thankful to all members of Matsumura Laboratory for their support, help and cooperation throughout my Ph.D. study.

I also wish to express my gratitude to the Egyptian Embassy in Tokyo, Culture Education and Science Bureau for facilitating the renewal of my vacation during my stay in Japan.

Finally, I would like to express my ultimate gratitude to my husband Diaa for his unconditional support and continuous encouragement. I hope he forgive me for my shortage in my duties during my study. Additionally, I deeply thank my parents for their faith in me. Also, I thank my brother and sister for providing me unending encouragement and support. Importantly, I dedicate this thesis to my loving daughter Mariam and my son Ahmed.